

**Zentrum für Humangenetik
Philipps-Universität Marburg**

Director: Prof. Dr. rer. nat. Karl-Heinz Grzeschik
Working group: Prof. Dr. med. Manuela C. Koch

Gene Mapping in Syndactyly Families

Inaugural thesis for the degree of a
Doctor in Human Biology (Dr. rer. physiol.)

presented to the Fachbereich Humamedizin der
Philipps-Universität Marburg, Germany



by

Sajid Perwaiz Malik
from DG Khan, Pakistan

Marburg, February 2005

Angenommen vom Fachbereich Humanmedizin
der Philipps-Universität Marburg am

Gedruckt mit Genehmigung des Fachbereichs

Dekan: Prof. Dr. med. Bernhard Maisch

Referent: Prof. Dr. med. Manuela C. Koch

Correferent: Prof. Dr.

CONTENTS

1	INTRODUCTION	1
1.1	Classification of syndactylies	1
1.1.1	Syndactyly Type I (SD1; MIM 185900)	4
1.1.2	Syndactyly Type II, Synpolydactyly (SPD; MIM 186000)	4
1.1.3	Syndactyly Type III (MIM 186100)	5
1.1.4	Syndactyly Type IV, Haas Type Syndactyly (MIM 186200)	5
1.1.5	Syndactyly Type V (MIM 186300)	5
1.1.6	Syndactyly Type VI, Mitten syndactyly	6
1.1.7	Syndactyly Type VII, Cenani-Lenz Syndactyly (MIM 212780)	6
1.1.8	Syndactyly Type VIII	6
1.2	Animal models for syndactyly	7
1.2.1	Synpolydactyly homologue (<i>spdh</i>) and <i>Hoxd13</i>	7
1.2.2	Syndactyly 1, <i>Sndy1</i> (<i>Sndy1^{Jrr}/Sndy1⁺</i>)	7
1.3	Limb development	8
1.3.1	Anteroposterior axis and digit morphogenesis	10
1.3.2	Separation and spacing of digits	11
1.4	Objectives of the study	13
2	FAMILIES AND PROBANDS	14
2.1	Family 1	15
2.1.1	Clinical report	16
2.1.1.1	Propositus (V-9)	16
2.1.1.2	Sister (V-7) of the propositus	16
2.1.1.3	Relatives	17
2.2	Family 2	19
2.2.1	Clinical report	21
2.2.1.1	Propositus (V-7)	21
2.2.1.2	Brother (V-3) of the propositus	21
2.2.1.3	Other relatives	22
2.3	Family 3	23
2.3.1	Clinical report	25
2.3.1.1	Propositus (IV-41)	25
2.3.1.1.1	Hands	25
2.3.1.1.2	Feet	25
2.3.1.2	Relative V-24	27
2.3.1.2.1	Hands	27
2.3.1.2.2	Feet	27
3	MATERIALS AND METHODS	28
3.1	Materials	28
3.1.1	Devices and accessories	28
3.1.2	Chemicals	29
3.2	Buffers and standard solutions	30

3.2.1	Enzymes	30
3.2.2	DNA size standards	30
3.2.3	Reaction kits	30
3.2.4	PCR reagents	31
3.2.5	Loading dye	31
3.2.6	Oligonucleotides	31
3.2.6.1	Primers for sequencing	32
3.3	Softwares and databanks	33
3.3.1	Softwares	33
3.3.2	Databanks	34
3.4	Methods	35
3.4.1	Blood sampling	35
3.4.2	Genomic DNA extraction	35
3.4.3	Polymerase chain reaction (PCR)	36
3.4.4	Horizontal gel electrophoresis	36
3.4.5	Genotyping	36
3.4.6	Linkage analysis	37
3.4.7	Mutation screening	38
3.4.7.1	Primer designing	38
3.4.7.2	Single strand conformational analysis (SSCA)	38
3.4.7.3	Silver staining	38
3.4.7.4	DNA sequencing	39
3.4.7.5	PCR purification	39
3.4.7.6	Sequencing PCR reactions	39
3.4.7.7	Sequencing PCR purification	40
3.4.7.8	Resuspension of samples and electrophoresis	41
3.4.7.9	Sequence data analysis	41
3.5	Classification protocol for syndactylies	42
4	RESULTS	43
4.1	Proposed syndactyly classification	43
4.2	Family 1	50
4.2.1	Autosomal recessive mesoaxial synostotic syndactyly with phalangeal reduction (MSSD)	50
4.2.2	Exclusion of loci for syndactyly type I, II and III	51
4.2.3	Genome-wide search, fine mapping and locus identification on chromosome 17p13.3	52
4.2.4	Mutation screening	55
4.2.4.1	<i>ROX</i>	55
4.2.4.2	<i>CT120</i>	55
4.2.4.3	<i>LOST1</i>	55
4.3	Family 2	57
4.3.1	Family with autosomal dominant zygodactyly	57
4.3.2	Exclusion of candidate locus SD1 on chromosome 2q34-q36	58
4.3.3	Genome-wide search	59
4.3.4	Fine mapping and locus identification on chromosome 3p21.31	59
4.4	Family 3	64
4.4.1	Family with autosomal dominant syndactyly type II	64

4.4.2	Exclusion of candidate genes <i>HOXD13</i> on chromosome 2q31 and <i>FBLN1</i> on chromosome 22q13.31	65
4.4.3	Genome-wide search	66
4.4.4	Fine mapping and locus identification on chromosome 2q34-q36	67
4.4.5	Fine mapping and locus identification on chromosomes 14q12	69
5	DISCUSSION	73
5.1	Genetic mapping in Pakistani families	73
5.2	Phenotyping and diagnosis	73
5.2.1	Protocol for the syndactyly classification	74
5.3	Inheritance of limb malformations	75
5.4	Collection of biological material	76
5.5	Approach to a genome screen	77
5.6	Genotyping	78
5.7	Data management	79
5.8	Linkage analysis	81
5.8.1	Two-point LOD score analysis	81
5.8.2	Haplotyping	82
5.8.3	Multipoint analysis	82
5.9	Family 1: Autosomal recessive mesoaxial synostotic syndactyly with phalangeal reduction (MSSD) maps to chromosome 17p13.3	83
5.10	Family 2: Zygodactyly maps to chromosome 3p21.31	88
5.11	Family 3: Synpolydactyly (SPD) maps to chromosome 14q12	92
5.12	Outlook	95
5.13	Summary	97
6	ABBREVIATIONS	99
7	REFERENCES	101
8	PUBLICATIONS	107
8.1	Original work	107
8.2	Posters	107
8.3	Seminars	107
9	ACADEMIC TEACHERS	108
10	ACKNOWLEDGEMENTS	109
11	DECLARATION	110
12	CURRICULUM VITAE	111

1 Introduction

Non-syndromic syndactyly is a common, heterogeneous hereditary condition of webbed fingers and/or toes. The malformation can be unilateral or bilateral, and the fusion within the web may be cutaneous or bony. The phenotype varies in families, and intra-familial variability is quite common. The majority of syndactylies show autosomal dominant mode of inheritance, with variable expression and incomplete penetrance. Cenani-Lenz syndactyly is the only type which is autosomal recessively inherited (Cenani and Lenz 1967). The frequency of syndactyly varies in populations and a prevalence of 3 per 10,000 births has been suggested in a Latin-American study (Castilla et al. 1980).

1.1 Classification of syndactylies

Roblot (1906) grouped syndactylies into syndromic and non-syndromic entities. But it was Julia Bell (1953), who pioneered a more sophisticated classification of non-syndromic syndactylies by reviewing 63 families with autosomal dominant inheritance. She separated different variants according to the involvement of hands and/or feet. Since some families had hands and feet involvement, she introduced subgroups, which made the classification difficult to use. Therefore, Temtamy and McKusick (1978) established a new classification based on clinical features and inheritance. They identified five types (I-V) on the basis of the anatomic location of the web and the combinations of involved fingers and/or toes within the web. Although some phenotypic overlap between the various types was observed, each type had its distinguishing features. All variants were reported to exhibit autosomal dominant inheritance with variable expression and incomplete penetrance. Kindreds with obvious autosomal recessive syndactylies were not part of this classification. Goldstein et al. (1994) extended the Temtamy and McKusick classification to eight types. They added an autosomal recessive entity, the Cenani-Lenz syndactyly as type VII (Cenani and Lenz 1967).

The advances in the understanding of molecular embryology of the limb bud prompted Winter and Tickle (1993) to propose a new classification of limb defects. They separated various syndactyly types based on normal or abnormal patterning of the limb.

But this classification was not practical as syndactylies with various pattern defects were observed in the same families (Akarsu et al. 1995; Sayli et al. 1995).

In this thesis I use the classification system proposed by Temtamy and McKusick (1978) and extended by Goldstein et al. (1994). A survey of all syndactyl types is presented in Table 1-1.

Table 1-1: Syndactyly classification based on Temtamy and McKusick (1978) with the extension by Goldstein et al. (1994).

Type	Description	Key features	Inheritance	Locus	Reference
I	Zygodactyly, SD1	Webbing of 3 rd and 4 th fingers and/or 2 nd or 3 rd toes	AD	2q34-q36	Bosse et al. (2000)
II	Synpolydactyly, SPD	Webbing of 3 rd and 4 th fingers, duplication of fingers in the web, webbing of 4-5-6 toes	AD	2q31, (<i>HOXD13</i>)	Muragaki et al. (1996)
III	Ring and little finger syndactyly, ODD*	Webbing of 4 th and 5 th fingers	AD	6q22-q23, (<i>GJAI</i>)	Paznekas et al. (2003)
IV	Complete syndactyly	Syndactyly of all digits 1-2-3-4-5	AD		Haas (1940)
V	Postaxial syndactyly with metacarpal synostosis	Fusion of 4 th and 5 th metacarpals, soft tissue syndactyly of toes	AD		Robinow et al. (1982)
VI	Mitten syndactyly	Unilateral syndactyly of digits 2—5 in hands and feet	AD		Temtamy and McKusick (1978)
VII	Cenani-Lenz type	Gross metacarpals and carpals fusion, radio-ulnar synostosis, spoon-shaped hand	AR		Cenani and Lenz (1967)
VIII	Metacarpal 4—5 fusion		AD, X-R		Lerch (1948)

* oculodentodigital dysplasia

1.1.1 Syndactyly Type I (SD1; MIM 185900)

Syndactyly type I is characterized by complete or partial webbing between the 3rd and 4th fingers and/or 2nd and 3rd toes. In some cases the webbing between fingers is associated with fusion of the distal phalanges. This syndactyly is the most common type of syndactyly which accounts for the majority of isolated syndactylies (Castilla et al. 1980). Type I syndactyly segregates as an autosomal dominant trait, and the occurrence of skipped generations indicates that penetrance is <100% (Montagu 1953). The gene for type I syndactyly has been localized in a large German family to chromosome 2q34-q36 (Bosse et al. 2000). The clinical spectrum of digital malformation in the German family reached from skin fusion between 2nd and 3rd toes to complete webbing between the 2nd to 5th fingers and 1st to 5th toes. Ghadami et al. (2001) reported an Iranian family which was also linked to the same locus on chromosome 2q34-q36.

1.1.2 Syndactyly Type II, Synpolydactyly (SPD; MIM 186000)

Synpolydactyly is characterized as a cutaneous or bony fusion between the middle and ring fingers associated with complete or partial duplication of the ring finger in the web. Duplication of fifth toe in the feet is a usual finding (Temtamy and McKusick 1978). The more extreme phenotype shows complete soft tissue syndactyly involving both hands and feet. In the hands there is polydactyly of the preaxial, mesoaxial, and postaxial digits, loss of the normal tubular shape of the carpal, metacarpal, and phalangeal bones (Akarsu et al. 1995)

Synpolydactyly shows an autosomal dominant mode of inheritance with variable expressivity and an estimated penetrance of 96% (Sayli et al. 1995). First linkage was reported to chromosome 2q31 in a large Turkish family (Sarfarazi et al. 1995). Polyalanine tract expansion mutations in the homeobox containing gene *HOXD13* have been described for SPD (Muragaki et al. 1996). Later studies showed that there is a correlation between the size of expansion in the polyalanine tract and the severity of SPD (Goodman et al. 1997). A complex type of synpolydactyly was observed in a patient with chromosomal translocation, t(12;22), disrupting the fibulin-1 gene (*FBLNI*) on chromosome 22q13.3 (Debeer et al. 2002).

1.1.3 Syndactyly Type III (MIM 186100)

In this syndactyly type there is a complete and bilateral syndactyly between the 4th and 5th fingers. Usually it is soft tissue syndactyly but occasionally the distal phalanges are fused. The 5th finger is short with an absent or rudimentary middle phalanx. The feet are not affected. Type III syndactyly has been reported as a part of oculodentodigital dysplasia (ODD; MIM 16420). The family reported by Johnston and Kirby (1955) was one of the largest fully described pedigrees, involving 7 males and 7 females in a pattern compatible with autosomal dominant inheritance. Bony fusion was observed at the terminal phalanx of the fused phalanges. Brueton et al. (1990) described a family with type III syndactyly and a facial phenotype resembling that of oculodentodigital dysplasia (ODD) but without any of the other characteristic ocular and dental features of ODD. Gladwin et al. (1997) localized the gene for ODD on chromosome 6q22-q24. They proposed that isolated type III syndactyly may be encoded by the same gene as ODD syndrome. Paznekas et al. (2003) found mutations in *GJA1* gene which encodes for the gap junction protein alpha 1 (connexin 43).

1.1.4 Syndactyly Type IV, Haas Type Syndactyly (MIM 186200)

Syndactyly type IV is characterized by complete fusion of all fingers in both hands (Haas et al. 1940). Flexion of the fingers gives the hands a cup-shaped form (Gillesen-Kaesbach and Majewski et al. 1991). There is usually an association of polydactyly, with 6 metacarpals and 6 digits. When feet are involved, they usually show complete fusion of all toes. Haas type syndactyly is a rare phenotype, and there are only four reports available in the literature. The most likely mode of inheritance is autosomal dominant with variable expressivity.

1.1.5 Syndactyly Type V (MIM 186300)

Syndactyly type V is a postaxial syndactyly which is associated with 4th and 5th metacarpal and metatarsal fusion. Soft tissue syndactyly usually affects the 3rd and 4th fingers and the 2nd and 3rd toes. Robinow et al. (1982) reported syndactyly type V in a mother and 3 of her 4 children. All had fusion of metacarpals 4 and 5. None had metatarsal fusion although other anomalies of the feet were present. It is a rare autosomal dominant type with only two reports published so far (Temtam and McKusick 1978; Robinow et al. 1982).

1.1.6 Syndactyly Type VI, Mitten syndactyly

Mitten syndactyly is characterized by a webbing of digits 2—5 in both hands and feet. It can be mistaken for congenital ring constrictions (amniotic bands). Only one family has been described in the literature. The inheritance was autosomal dominant with variable expression and incomplete penetrance (Temtamy and McKusick 1978). No MIM number has yet been allocated to this phenotype.

1.1.7 Syndactyly Type VII, Cenani-Lenz Syndactyly (MIM 212780)

Cenani-Lenz syndactyly is characterized by complete syndactyly of hands and feet, abnormal phalanges, carpal and metacarpal fusion, giving the hand a spoon-like appearance. Occasional mesomelic shortening of arm, radio-ulnar and metacarpal synostosis, as well as disorganized phalanges have been observed. Feet are only mildly affected (Cenani and Lenz 1967). More than fifteen cases have been described in the literature. Cenani-Lenz is the only type known to be segregating as an autosomal recessive entity. No linkage has been reported for Cenani-Lenz syndactyly.

1.1.8 Syndactyly Type VIII

Syndactyly type VIII shows unilateral or bilateral fusion of metacarpal 4th and 5th. The 5th metacarpal is usually hypoplastic and the 5th ray is consequently short. There is, however, great variability in expression, so the degree of fusion may range from minimal to complete and the external aspect of the hand may vary. For the isolated forms an autosomal dominant inheritance was suggested, while the familial cases segregate as X-linked recessive (Lerch 1948; Lonardo et al. 2004). No MIM number has yet been allocated to this phenotype.

1.2 Animal models for syndactyly

1.2.1 Synpolydactyly homologue (*spdh*) and *Hoxd13*

Johnson et al. (1998) described a spontaneous mouse mutant which provided an accurate model for human synpolydactyly. The new mutation, named synpolydactyly homolog (*Spdh*), has a 21-bp in-frame duplication within the polyalanine-encoding region of the 5-prime end of the *Hoxd13* coding sequence. The duplication expands the stretch of alanines from 15 to 22. The same type of expansion has been found in human synpolydactyly (Goodman et al. 1997). Homozygote mice exhibit severe malformations of both fore limbs and hind limbs, including polydactyly, syndactyly, and brachydactyly. *Spdh* probably acts as a dominant-negative or a gain-of-function mutation. Further research to examine the interactions with other *HOX* genes and their protein products during limb development is therefore needed. In 2002 an allelic variant for *Spdh* was described with a same phenotype with an autosomal recessive inheritance (Albrecht et al. 2002).

1.2.2 Syndactyly 1, *Sndy1* (*Sndy1^{Jrt}/Sndy1⁺*)

Rossant (2004) described a syndactylous mouse, *Sndy1*. These chemically induced heterozygous mutant mice (*Sndy1^{Jrt}/Sndy1⁺*) usually exhibit simple complete and/or incomplete syndactyly of digits 2nd and 3rd on one or both of hind limbs. Occasionally digits 1st and 2nd or 3rd and 4th are fused on the hind limbs. However, no involvement of the fore limbs has been detected. Syndactyly 1 maps on mouse chromosome 6 (37.2 cM), and the homologous region in humans is on chromosome 3p25.1. This mouse phenotype is very close to the human syndactyly type I, which maps on chromosome 2q34-q36 (Bosse et al. 2000).

1.3 Limb development

The vertebrate limb is a widely used experimental model for analysing cell-cell signalling and spatiotemporal patterns of gene expression during patterning of embryonic fields and organogenesis. Studying limb development has a number of advantages. In particular, (i) limbs develop externally and are readily accessible in model animals for analysis; (ii) limbs consist of various well-defined segments and are characterized by clear anatomical polarity; (iii) limbs can be experimentally manipulated (both surgically and genetically) without influencing the viability of the embryo, and yet many of the emerging principles can be applied to understand earlier developmental events, such as specifying the main body axes; finally (iv) in humans, developmental malformations of limbs do not interfere with reproductive fitness. In addition, the analysis and comparison of limb development in diverse species has provided much insight into the evolutionary mechanisms through which exchanges in developmental pathways have led to the extraordinary diversity of limbs (Schwabe et al. 1998; Grzeschik 2002).

Much of our understanding of limb development is coming from study of mice. The limb bud first appears as a small protrusion from the flank of the embryo with the establishment of a special group of cells termed the “limb field”. Limb morphogenesis occurs along three axes, which become gradually fixed. During outgrowth the bud elongates along the proximo-distal axis (Pr-D, shoulder-to-finger-tips), flattens along the dorsal-ventral axis (D-V, back-of-hand-to-palm), and develops an asymmetric pattern of cartilage condensations along the anterior-posterior axis (A-P, thumb-to-little-digit) (Figure 1-1). The growth and patterning along these three axes depend on the establishment and maintenance of three distinct signalling regions within the limb bud: (i) the apical ectodermal ridge (AER), a group of columnar cells at the distal edge of the bud at the dorsal-ventral boundary; (ii) the nonridge ectoderm of the bud; and (iii) the zone of polarizing activity (ZPA), a region of specialized mesenchymal cells beneath the posterior boundary of the bud (Figure 1-1) (Niswander 2003).

Some of the molecules produced by these signalling centers and the responding mesenchymal cells have been identified. *HoxA* and *HoxD* genes express in an overlapping fashion in the limb bud, and the cells at different positions express different combinations of *Hox* genes (Figure 1-2). Fibroblast growth factors (FGFs) produced by AER cells are required for outgrowth as well as continued production of Sonic

hedgehog (*Shh*), which is produced in the ZPA (Sun et al. 2000). The expression of FGFs in the AER is in turn up-regulated by *Shh* through *Gremlin*, which suppresses FGF inhibition by *Bmp-2* (Litington 2002). *Shh*, FGFs, and their downstream effectors regulate limb outgrowth and coordinate the patterns of gene expression, in particular the *Hox* family (Tickle 2000; Niswander et al. 1994). This morphogenetic landscape of signals is “interpreted” by a population of proliferating, undifferentiated cells just below the AER.

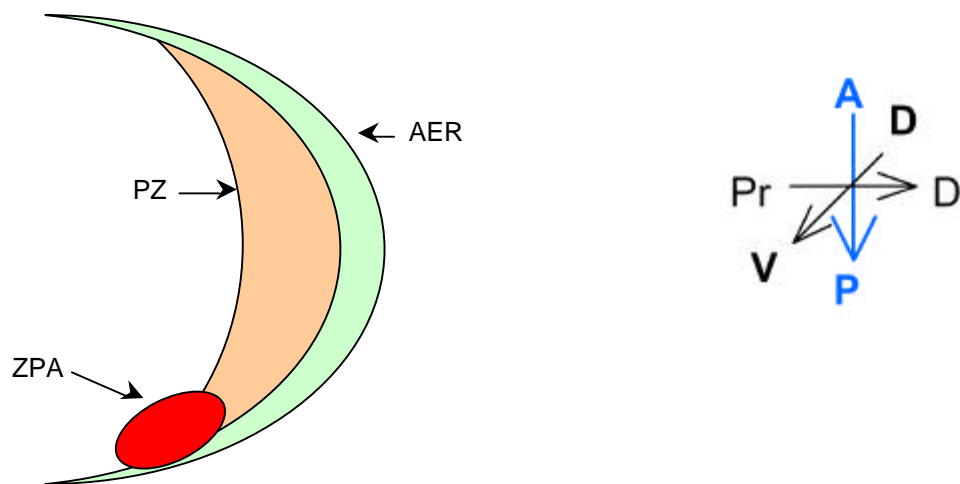


Figure 1-1: Growing limb bud with signal centres.

The limb morphogenesis occurs in three axes of development: Pr-D (proximal-distal), D-V (dorsal-ventral), A-P (anterior-posterior).
(**AER**, apical ectodermal ridge; **PZ**, progress zone (mesodermal); **ZPA**, zone of polarizing activity).

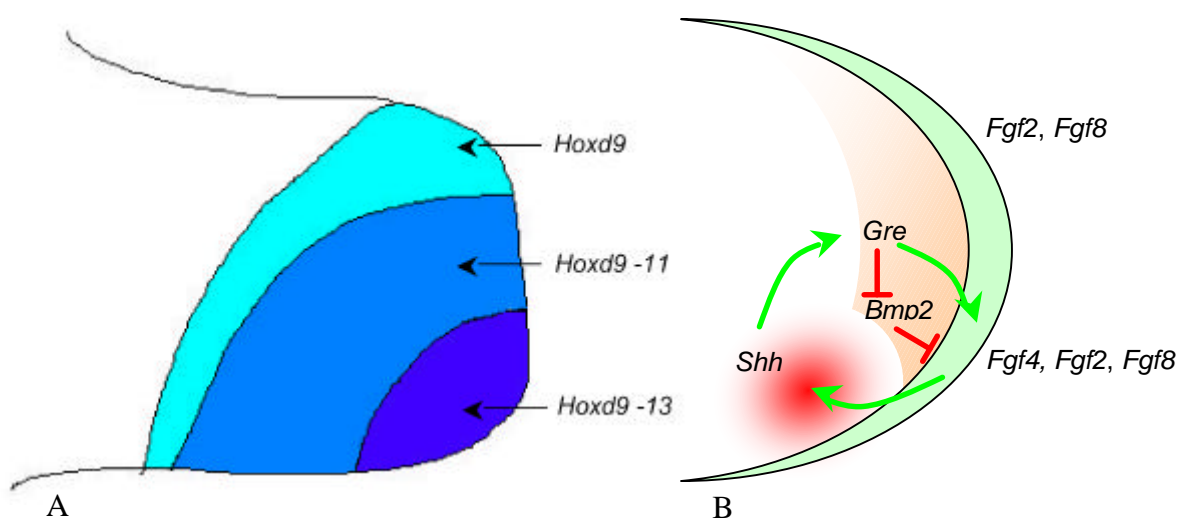


Figure 1-2: A: Overlapping patterns of expression of *Hoxd* genes in the posterior limb bud.

B: Signalling molecules involved in A-P limb patterning.

(*Shh*, Sonic Hedgehog; *Gre*, Gremlin; *Bmp2*, Bone morphogenetic protein 2; *Fgf-2,-4,-8*, Fibroblast growth factors).

1.3.1 Anteroposterior axis and digit morphogenesis

The digit number and identity (thumb vs. little finger/big toe vs. little toe) is regulated by signalling from ZPA (i.e. *Shh*) (Riddle et al. 1993). Digit identity depends on distance from the polarizing region: the most posterior digit forms next to the polarizing region, the most anterior furthest away. Digit number is related to the width of the bud, and this depends on the length of the AER (Brickell and Tickle 1989). The development of a proper hand plate with a series of digits and progressive posteriorization of digit identity depends on *Shh*.

Reciprocal antagonism of *Gli3* and *dHand* prepatterns the limb bud mesenchyme before activation of *Shh* signalling (Figure 1-3). *dHAND* is required to activate *Shh* expression by polarizing region cells. *Shh* signalling inhibits the processing of *Gli3*, which acts as transcriptional repressor (Gli3R). *Shh* positively regulates *HoxD* (*5'HOX*) gene and *Gremlin* (*Gre*) expression in distal mesenchyme (Figure 1-3). The *Shh-Fgf* feedback loop between the polarizing region and the AER is established through Gremlin-mediated *Bmp* antagonism (te Welscher et al. 2002).

Each of the digital rays will develop from cells with a particular antero-posterior identity, and this identity should then determine the subsequent morphogenesis of that particular ray (e.g. number, relative length and shape of phalanges). Morphogenesis of rays can be modified by adjacent interdigital mesenchyme, and the rays develop in accordance with the most posterior interdigital cues received.

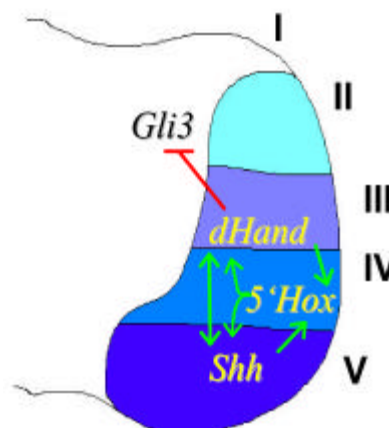


Figure 1-3: Positive feedback loops between *5'Hox* genes, *Shh*, and *dHand*.

This feedback loop triggers the progressive expansion of posterior identity, mostly through the graded impact of the *Shh* product on *Hox* gene expression in the distal bud. I to V indicate presumptive digits, and the graded blue zones represent the *Shh* gradient (adapted from Zakany et al. 2004).

1.3.2 Separation and spacing of digits

Setting up digital versus interdigital areas is the basis for spacing the digits. The initial divergence between digital and interdigital regions in an alternating fashion is achieved by different programmes of cell differentiation (chondrogenesis or apoptosis, respectively). Members of the *Tgf?* superfamily execute two different programmes: (i) *Tgf?s* as chondrogenic signals and, (ii) *Bmps* as apoptotic signals (Figure 1-4) (Ganan 1996; Zuzarte-Luis and Hurlle 2002). Apoptosis helps to sculpt the limb by freeing digits. Interdigital cell death has been shown to occur mainly by caspase-dependent apoptosis (Lindsten et al. 2000). The chromosomal localization of genes involved in human limb development and the known syndactyly loci are shown in Figure 1-5.



Figure 1-4: Apoptosis in mesoderm in developing chick limb bud.

The areas of cell death that have been termed the Interdigital Necrotic Zones (**INZs**) are shown in red (from Zuzarte-Luis and Hurlle 2002).

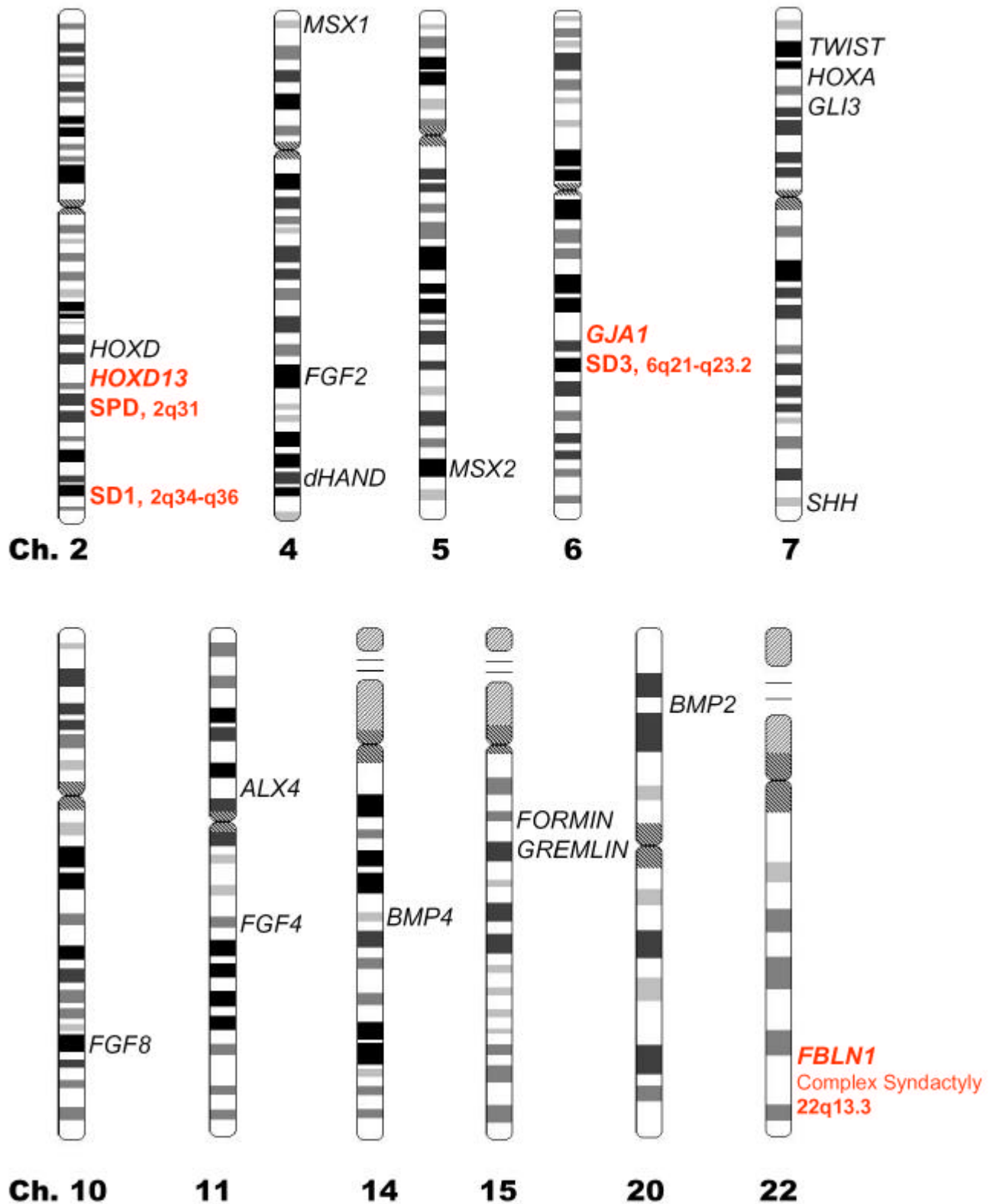


Figure 1-5: Chromosomal localization of human loci involved in limb development (black) and candidate loci for non-syndromic syndactylies (red).

1.4 Objectives of the study

A wide variety of congenital limb abnormalities reflect the complexity and precision of limb development. Identification and characterization of the underlying gene(s) can increase our understanding of normal limb development.

I got the possibility to study three large, inbred Pakistani families with limb defects. I reasoned that these large families may provide an excellent opportunity to localize the limb malformation in the human genome, to identify the underlying gene and hence, to get to know the underlying pathomechanisms of the malformation. Therefore, my aim was:

- ?? to diagnose the hand/foot malformations and to categorize them using the existing classification system;
- ?? to establish whether the limb malformations in these families are syndromic or non-syndromic;
- ?? to find out about the intrafamilial and interfamilial variability of the phenotype (clinical heterogeneity);
- ?? to check the hypothesis whether clinically distinct limb malformations in different families are also genetically heterogeneous;
- ?? to infer the mode of inheritance of the limb phenotype segregating in the three families by constructing the pedigrees;
- ?? to localize the limb malformations within the human genome using a combined strategy of homozygosity mapping, candidate gene approach and genome-wide search;
- ?? to conduct fine mapping in case a locus is identified, and to narrow down the newly established candidate regions;
- ?? having these families linked to a unique locus/loci, the next target should be to identify the underlying gene(s) through mutation screening and finally, to characterize the newly identified gene(s) and protein(s).

2 Families and Probands

Four families with non-syndromic syndactylies were ascertained from various parts of Pakistan (Figure 2-1). During the fieldwork, families were visited at their places of residence, and a detailed pedigree was constructed in each case. Information about intermarriages and deceased subjects was also documented. The information was crosschecked by interviewing different family members. For the clinical study, photographs and radiographs of the affected as well as normal subjects were obtained. Variations in the involvement of one or both hands, upper and lower extremities and bony and soft tissue syndactylies were documented. The malformation in one family showed autosomal recessive mode of inheritance, while in the other three families, the malformation was segregating in an autosomal dominant fashion. For the molecular study, blood samples were drawn from the affected and normal subjects. All material was collected after getting informed consent according to the Helsinki II declaration. Clinical and molecular data of Family 4 were not included in this thesis.

Later in the study the molecular data of a Turkish and a German family was included in the thesis. The results of these families are in press and have been described in the discussion part of the thesis.



Figure 2-1: The places of origin of the four families.

2.1 Family 1

The family originates from the North-Western part of Pakistan. A pedigree of the family was constructed by interviewing the elders of the family (Figure 2-2). The information was cross-checked by interviewing several relatives. Four affected (V-1, V-2, V-7, V-9) and six normal subjects (III-5, III-7, IV-1, IV-6, V-6, V-12) of the family were physically examined. Photographs of three individuals (V-2, V-7, V-9) and X-ray films of two subjects (IV-6, V-9) were obtained.

Six phenotypically normal parents (III-3 and III-4; IV-1 and III-5; IV-5 and IV-6) in three consanguineous loops, had eight affected (five males and three females), and eight normal offspring. All affected subjects have mesoaxial reduction of phalanges of hands and preaxial syndactyly of toes. An autosomal recessive inheritance is most likely (Figure 2-2). Peripheral blood samples from four affected and five normal subjects were obtained.

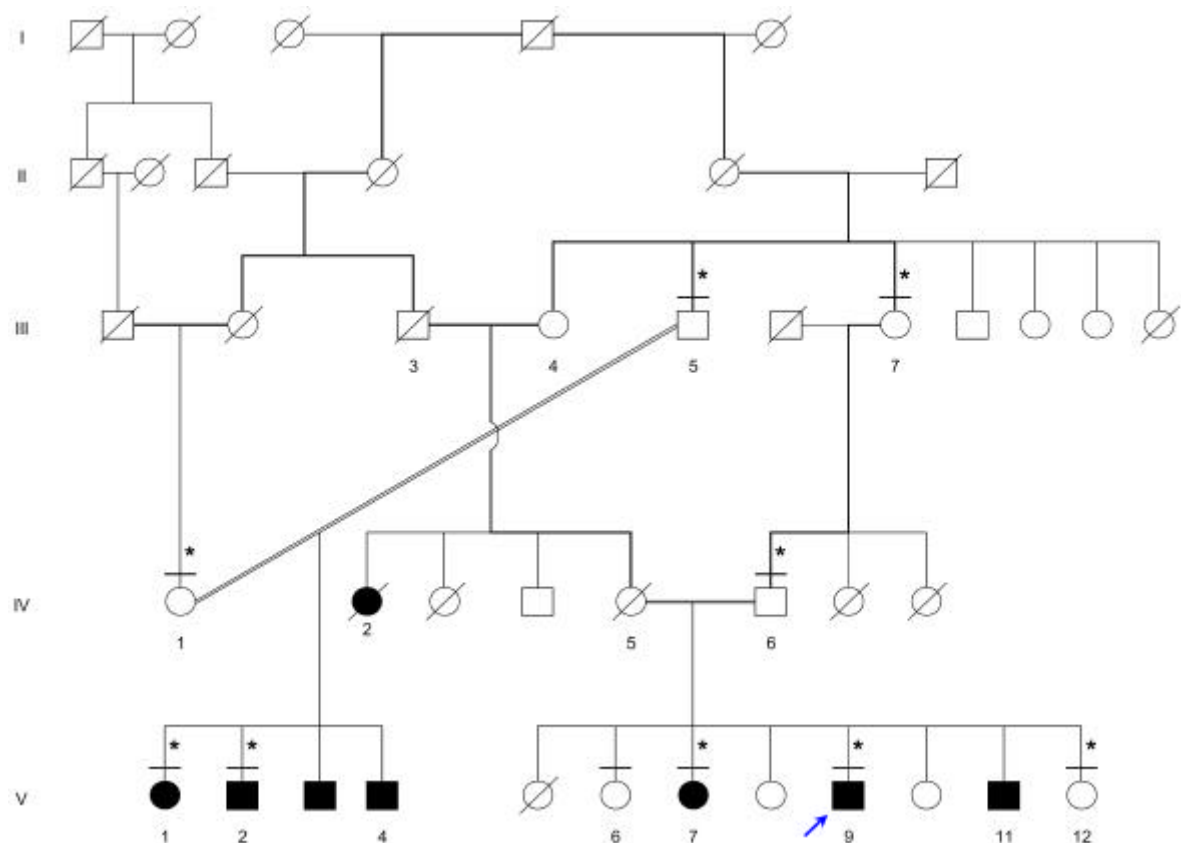


Figure 2-2: Pedigree of Family 1 with autosomal recessive syndactyly.

Solid symbols represent affected subjects, while the open symbols represent normal individuals. Horizontal bars on symbols denote individuals who were physically examined. An asterisk (*) on the symbols indicates the subjects of whom blood was sampled for molecular study.

2.1.1 Clinical report

2.1.1.1 Propositus (V-9)

The propositus (V-9), a 27 year old male, is one of the three affected sibs of related, phenotypically normal parents. The propositus has four 'fingers', which do not hamper in his day-to-day life (Figure 2-3, A). All the digits have lost their shape and identity, except for both thumbs. Radiographs show synostosis of 3rd and 4th metacarpals (Figure 2-3, B). The fused 3rd and 4th metacarpal generate a single, broad and conical proximal phalanx, ending in dysplastic middle and terminal phalanx. In the right hand, the index finger is more like a middle finger, while in left hand the index finger is stumped, bending at 90° on the radial side. The distal head of proximal phalanx of second phalange shows mild hypertrophy, while in the left hand, this proximal phalanx is drastically reduced in to a triangular bone, bearing remnants of middle phalanx on the radial side. In fifth fingers, there is bilateral clinodactyly along with symphalangism of distal phalanx. Distal heads of metacarpals generally show hypoplasia. There is crowding of carpal bones, scaphoid and trapezium showing slight misalignment. Radial and ulnar heads seem to be normal.

In the feet, first three toes are webbed (Figure 2-3, C). Radiological study do not show any bony fusion, yet there is hypoplasia of middle and distal phalanx of all toes (Figure 2-3, D). First metatarsals in both feet appear broad with signs of distortion at the distal heads. There is symphalangism of proximal and distal phalanx of halluces. All the metatarsals generally show hypoplastic distal heads.

2.1.1.2 Sister (V-7) of the propositus

Severe aplasia of digits is observed in the sister of propositus (V-7, age 29 years). In this subject the defect not only affects the mesoaxial fingers but also ranges on either side of the mesoaxial skeletal rays (Figure 2-3, E). The photographs shows that mesoaxial digits 2-3-4 are reduced to one or two dysplastic fingers in the right and left hand, respectively. In the right hand, the thumb seems bifid at the terminal phalanx but this is not confirmed by radiographs. The brother (V-11) of the propositus reportedly has hand involvement similar to V-7, while his feet are said to be normal (no photographs available).

2.1.1.3 Relatives

The relative V-2, a 33 year old male, also shows severe aplasia of digits (Figure 2-3, F). On the right hand, there is hypoplastic thumb, a single phalange representing the 3rd and 4th fingers and clinodactyly of the 5th finger. However, on the left hand, severe reduction of all fingers except the thumb is observed, the fifth finger remains as a peg. His feet are found to be normal on clinical examination. His sister (V-1) and one brother (V-4) have the same phenotype (no photographs available).

Dermatoglyphic changes characteristic of syndactyly are observed in the hands of the examined subjects, showing replacement of triradii by single or bifurcating horizontal or oblique lines (Figure 2-3, F). All affected individuals have normal intelligence and no other associated defects such as craniofacial symptoms.

Six other subjects (III-5, III-7, IV-1, IV-6, V-6, V-12) were examined and found to be phenotypically normal. X-ray films of subject (IV-6) do not show the presence of any type of pathological findings.

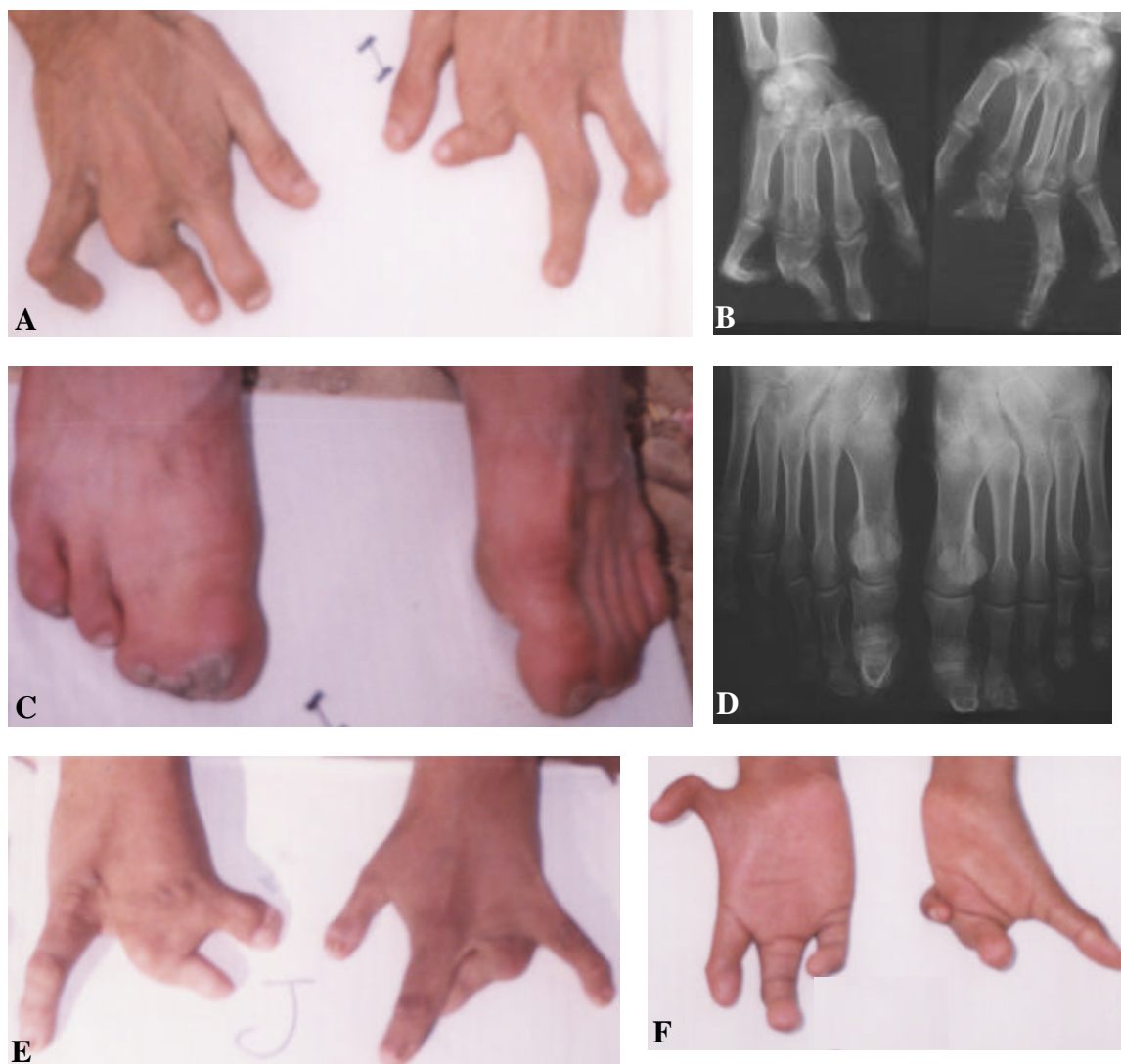


Figure 2-3: Phenotypic appearance of affected subjects in Family 1 with syndactyly.

- A, B and C, D: Hands and feet of the male proband (V-9);
- E: Hands of female subject V-7;
- F: Hands of male subject V-2.

2.2 Family 2

The family originates from DG Khan district of Pakistan. An extended pedigree of the family comprising seven generations was constructed by interviewing the elders of the family (Figure 2-4). The information was crosschecked by interviewing several individuals. Thirteen affected and six normal subjects of the family were physically examined. Photographs and X-ray films of two subjects (V-3 and V-7) were taken.

A total of fifteen subjects (9 males and 6 females) are found to be affected in this inbred family. All the affected subjects have cutaneous webbing of 2nd and 3rd toes only. The phenotypic manifestation is variable throughout the family ranging from mild (unilateral partial fusion) to severe (bilateral complete syndactyly of toes including a fusion of nails). No subject had a syndactyly of hands.

All affected subjects have at least one affected parent, except subjects IV-2 and IV-3. No phenotypic information is available about their deceased parents (III-5 and III-7; Figure 2-4). Therefore, the most obvious mode of inheritance in this family is autosomal dominant.

Blood samples were obtained from seventeen subjects (12 affected and 5 normal) for molecular study.

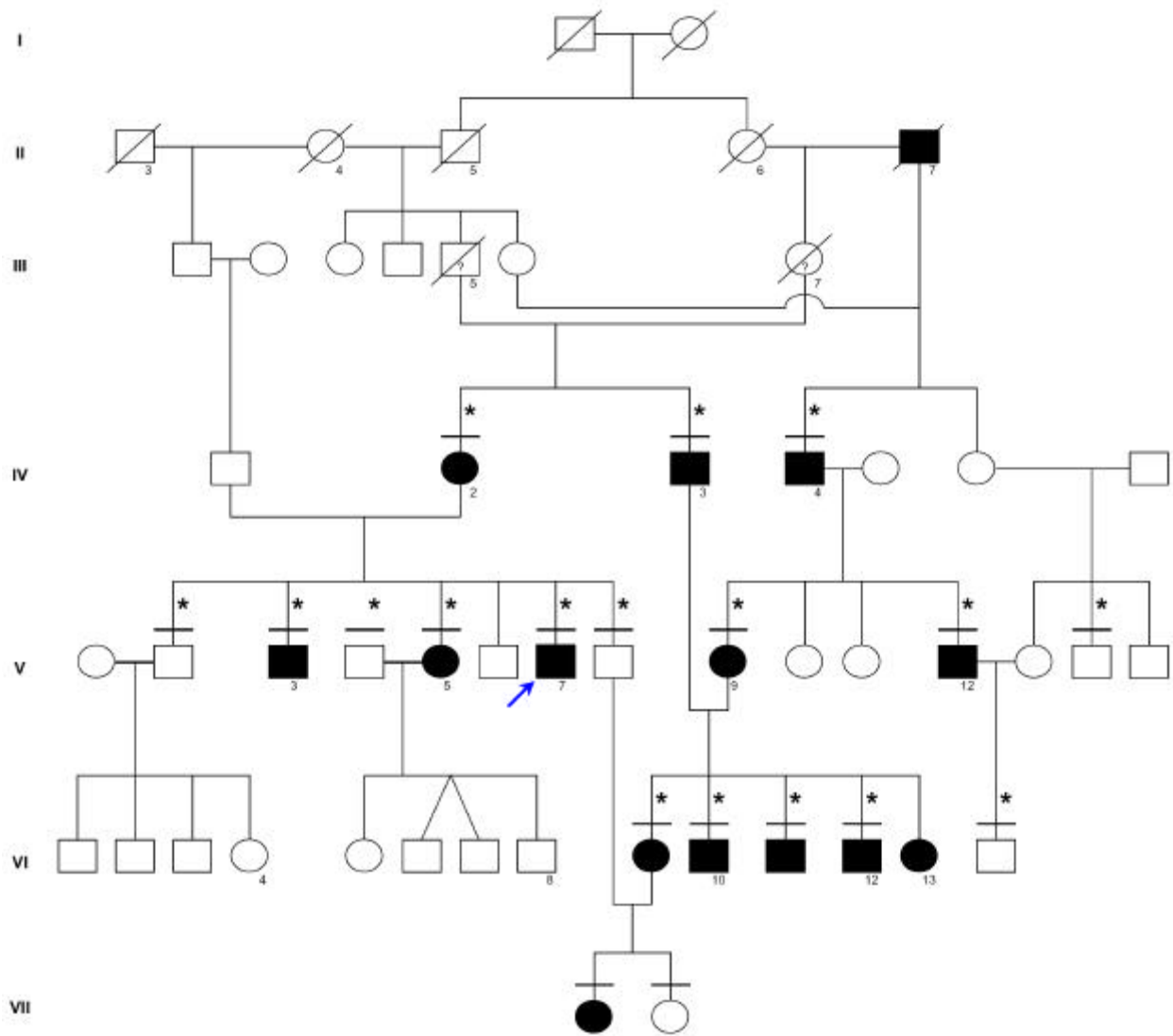


Figure 2-4: Pedigree of Family 2 with autosomal dominant syndactyly.

Solid symbols represent affected subjects, while the open symbols represent normal individuals. Horizontal bars on symbols denote individuals who were physically examined. An asterisk (*) on the symbols indicates the subjects of whom blood was sampled for molecular study.

2.2.1 Clinical report

2.2.1.1 Propositus (V-7)

The propositus (V-7), a 30 year old male, is one of the three affected subjects in a sibship of six individuals. His mother (IV-2) and maternal uncle (IV-3) are also affected. He has bilateral, symmetrical soft tissue syndactyly of 2nd and 3rd toes (Figure 2-5, A). The webbing is complete and results in medial diversion of terminal phalanges of 2nd toes. There is partial fusion of nails at the distal end of the syndactylous toes. Other toes are not involved in the webbing.

The radiographs do not show any bony fusion of the syndactylous toes (Figure 2-5, B). There is however evidence of hypoplastic terminal phalanges of all toes. Both hands were found to be normal with normal dermatoglyphics.

2.2.1.2 Brother (V-3) of the propositus

Contrasting to the propositus, his brother (V-3) shows only partial cutaneous syndactyly of 2nd and 3rd toes. The webbing is bilateral, symmetrical and reaches up to mid-half of the fused toes (Figure 2-5, C). The medial diversion of 2nd toe is not witnessed. There is no involvement of other toes. Both hands are normal.

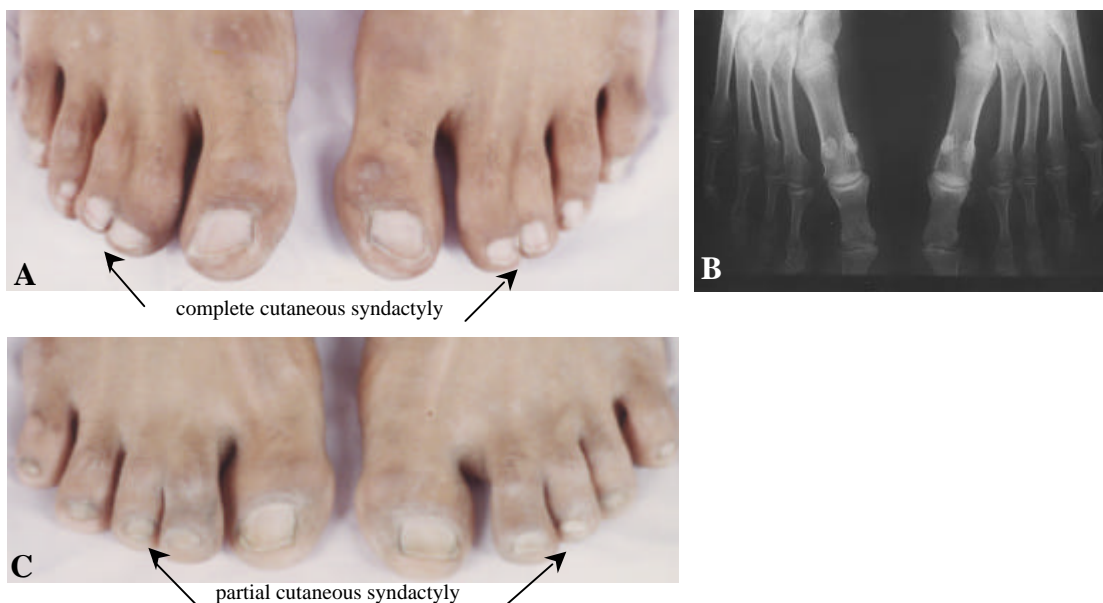


Figure 2-5: Phenotypic appearance of affected subjects in Family 2 with syndactyly.

A and B: Feet of subject V-7, showing complete cutaneous syndactyly of 2nd and 3rd toes.
 C: Feet of subject V-3, with partial cutaneous syndactyly of 2nd and 3rd toes.

2.2.1.3 Other relatives

Bilateral complete syndactyly of 2nd and 3rd toes is also observed in subjects IV-3, VI-9 and VI-10. The subject V-5 has complete 2nd and 3rd toe webbing in her right foot but only partial fusion in the left foot (no photographs available). In individual IV-2, there is bilateral partial syndactyly reaching up to mid-half of the respective toes. Both hands are normal.

Subjects IV-4, VI-13, V-9, V-12 and VII-1 have partial syndactyly of 2nd and 3rd toes in one of the two feet and only a minor impression of webbing in the second foot. Both hands are normal in all these subjects (no photographs available).

2.3 Family 3

The family was ascertained from a remote area of Larkana district, Southern Pakistan. This large family is allocated in three closely situated villages. An extended pedigree was constructed which comprises 124 individuals (Figure 2-6). The information was crosschecked by interviewing several relatives. Eighteen subjects were physically examined. For the clinical study, photographs and X-rays films of two affected subjects (IV-41 and V-24) were obtained.

A total of fifty subjects (24 males and 26 females) are found to be affected segregating in five generations. Syndactyly is bilateral and symmetrical in most patients, affecting both hands and feet. All affected subjects have at least one affected parent, except one instance. Parents of subjects III-14 and III-18 are deceased (II-7 and II-8), and the elders of the family could not recall their phenotype (Figure 2-6). The most likely mode of inheritance is autosomal dominant. Blood samples were obtained from fifteen individuals (13 affected and 2 normal) for molecular study.

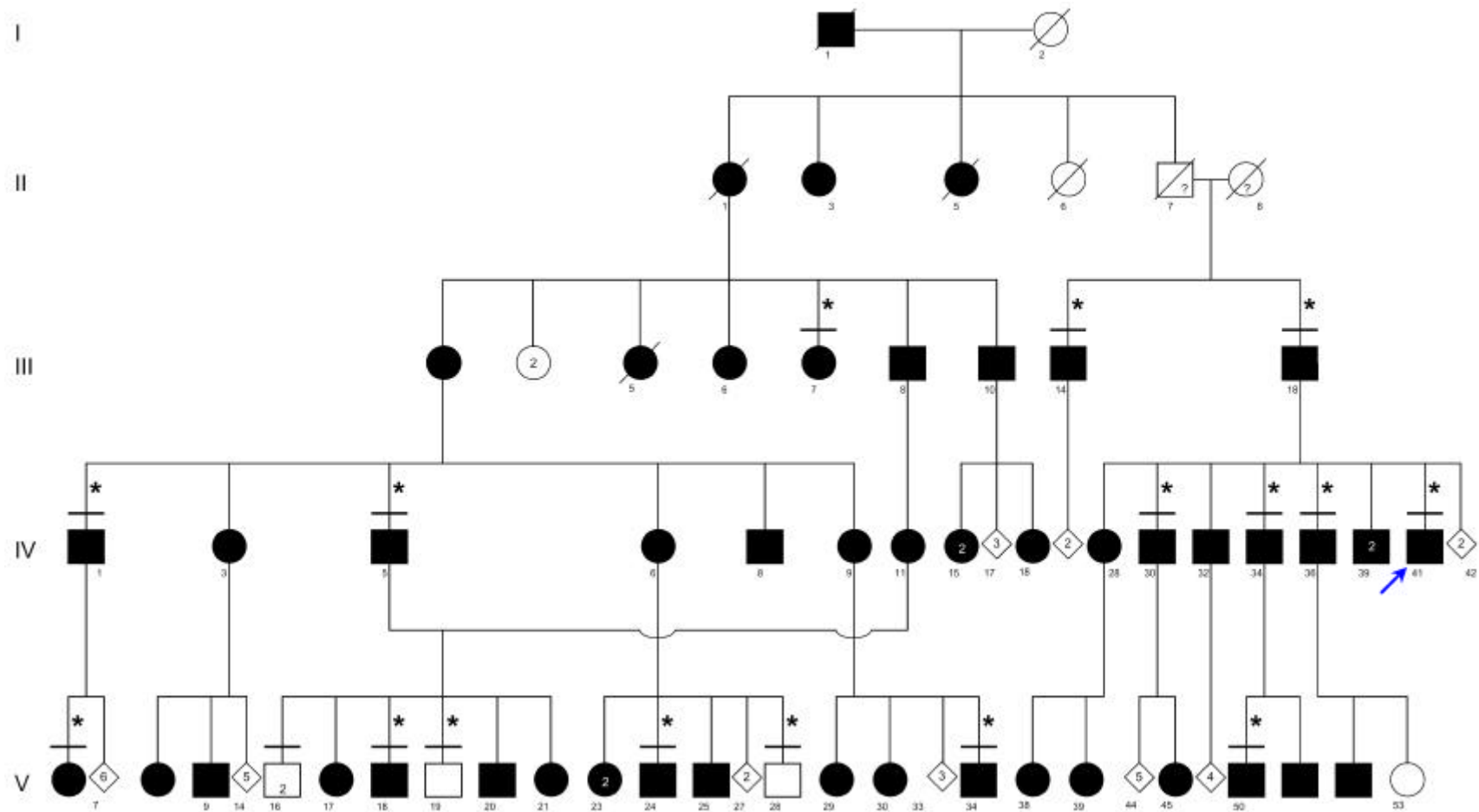


Figure 2-6: A shortened pedigree of Family 3 with autosomal dominant syndactyly.

Solid symbols represent affected subjects, while the open symbols represent normal individuals. Horizontal bars on symbols denote individuals who were physically examined. An asterisk (*) on the symbols indicates the subjects of whom blood was sampled for molecular study.

2.3.1 Clinical report

2.3.1.1 Propositus (IV-41)

2.3.1.1.1 Hands

The propositus has a total of “four” fingers in both hands (Figure 2-7, A). The thumbs are small and low-set with weak terminal phalanx. Both index fingers have camptodactyly with tapering ends. The flexion movement of these fingers is limited. The 3rd and 4th fingers show complete syndactyly, which gives an impression of bony fusion (Figure 2-7, A). The 3rd finger overrides the 4th finger, both ending in a single bony mass. At the terminus, the nails are fused. Fifth fingers in both hands show clinodactyly and symphalangism.

The radiographs show hypoplastic terminal phalanx of both thumbs (Figure 2-7, B). Symphalangism of first and second phalanges of index fingers is evident, which explains the limited movement of these fingers. There is osseous fusion of 3rd and 4th fingers at their tips. The terminal phalanges of both fingers lose their shape and fuse in a knotty structure. The first and second phalanges of 4th fingers are dysmorphic and dysplastic. There is symphalangism of all phalanges of 5th fingers with mid-phalangeal hypoplasia, giving all fingers a clinodactylous shape (Figure 2-7, B).

Metacarpals are club shaped with hypoplastic distal heads. Carpal bones show crowding and misalignment. Trapezium and trapezoid fuse into each other. Similarly, capitate and hamate are located close to each other. Carpal bones are generally hypoplastic and dysmorphic. Distal heads of radius and ulna are normal.

2.3.1.1.2 Feet

There is bilateral synpolydactyly of 5th toes (Figure 2-7, C). The cutaneous webbing extends from 4th to 6th toes. The nails of syndactylous toes are not fused. The radiographs reveal the duplication of terminal phalanges of 5th toes, but no additional metacarpal is observed. The terminal phalanges of all toes are hypoplastic, a feature which is more pronounced in the left foot. There is symphalangism of halluces, bilaterally. The distal heads of all metacarpals show lateral protuberances.

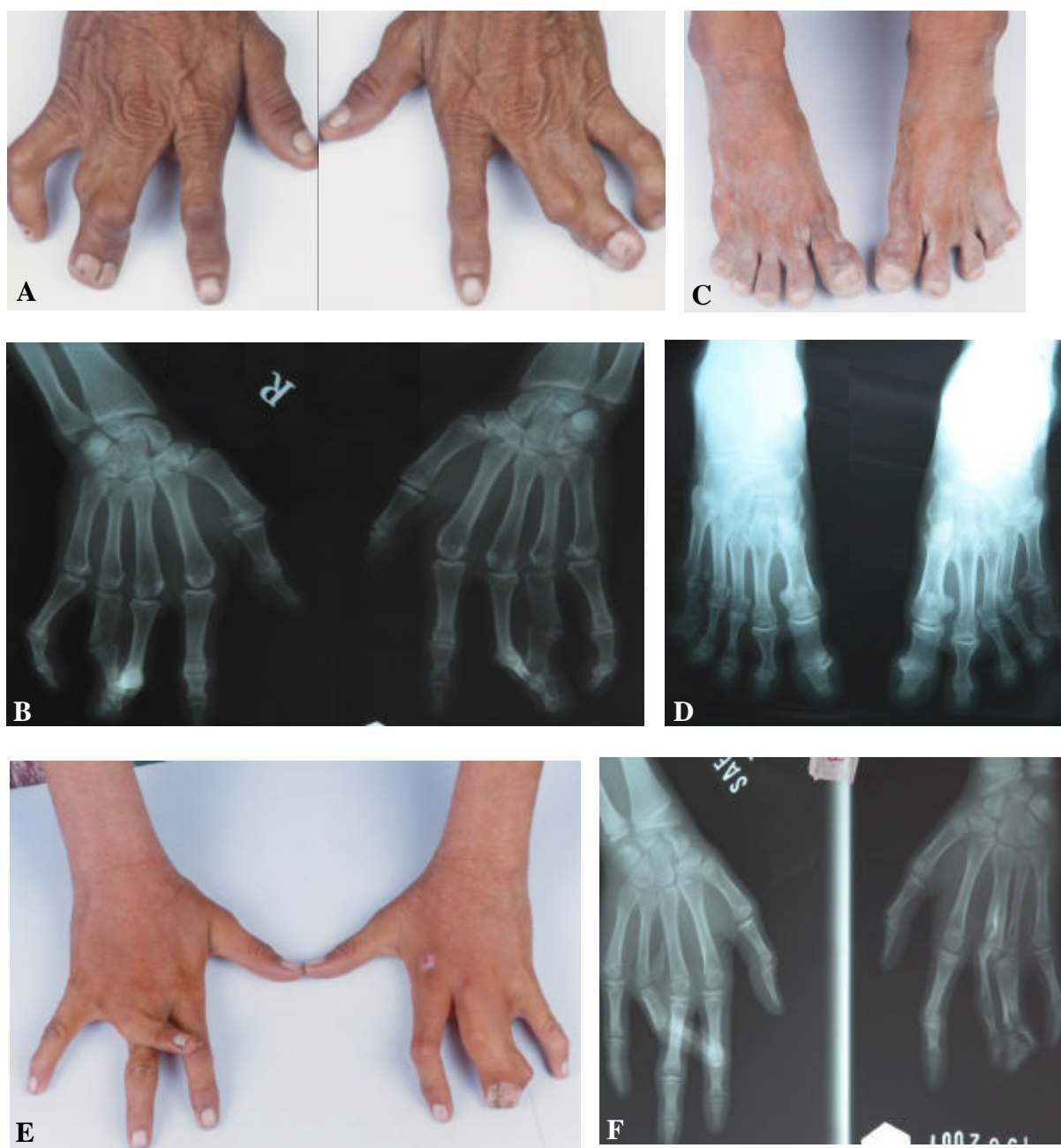


Figure 2-7: Phenotypic appearance of affected subjects in Family 3 with syndactyly.

- A and B: Hands of proband (IV-41) showing complete osseous syndactyly of 3rd and 4th fingers and clinodactyly of 5th finger.
 C and D: Feet of proband (IV-41) with synpolydactyly of 5th toe.
 E and F: Hands of subject V-24.

2.3.1.2 Relative V-24

2.3.1.2.1 Hands

Both thumbs are normal (Figure 2-7, E). The index finger seems normal in the right hand, whereas in the left hand it shows clinodactyly with bending towards the medial axis. In the right hand, the 3rd finger shows swelling and camptodactyly of first phalangeal joint. The 4th finger is bent at 45° towards the radial axis, attaining an odd position over the 3rd finger (Figure 2-7, E). In the left hand, the 3rd and 4th fingers are completely fused, giving an impression of bony fusion. Minor soft tissue syndactyly is observed between 4th and 5th fingers in left hand. The 5th fingers show clinodactyly, bilaterally, which is more pronounced in the left hand.

The radiographs of both thumbs are normal (Figure 2-7, F). In the right hand, there is an incompletely grown bony element between the 3rd and 4th metacarpals. The first phalange of 4th finger is dysplastic which results in the tilting of this finger towards the medial axis.

In the left hand, the index finger shows clino-camptodactyly of first phalangeal joint. The third metacarpal is hypertrophic, whereas the fourth metacarpal is dysplastic. There is osseous fusion at the distal ends of 3rd and 4th metacarpals, which give rises to dysmorphic phalanges, showing osseous fusion. Midphalangeal hypoplasia of fifth fingers is observed in both hands which results in clinodactyly.

All the epiphyseal ends of the long bones show lack of ossification. Metaphyses are hypoplastic showing lack of maturity. Carpal bones are normal whereas the distal heads of radius and ulna have immature epiphyses.

2.3.1.2.2 Feet

The clinical findings in the feet were essentially the same as observed in propositus IV-41.

3 Materials and Methods

3.1 Materials

3.1.1 Devices and accessories

Autoclave	Grössner, Hamburg
ABI Prism 377 DNA-Sequencer	Applied Biosystems, USA
Balance AE 240	Mettler, Giessen, Switzerland
Balance PM 2000	Mettler, Giessen, Switzerland
Centrifuge Sorvall RT 6000B	Du Pont, Dreieich
Cooling centrifuge Sorvall RT 6000	Du Pont, Dreieich
Eppendorf-Centrifuge 5417 C	Eppendorf, Hamburg
Electrophoresis Horizontal tank, A2	Owl Scientific Inc. Wobum, USA
Electrophoresis Hoefer apparatus, SE600	Pharmacia Biotech, San Francisco
Filter Millex-GS 0.22 µm	Millipore, Ireland
Filter Minisart NML 0.45 µM	Sartorius GmbH, Göttingen
Gel Documentation system: E.A.S.Y. RH-3	Herolab, ST. Leon Rot, Wiesloch
GeneAmp PCR System 2400	Applied Biosystems, USA
GeneAmp PCR System 9600	Applied Biosystems, USA
Gradient Cycler	Bio-Rad Laboratories GmbH, München
Microwave Oven	Bosch, Gerlingen-Schillerhöhe
Milli-Q Filtration unit	Spectrum Laboratories
pH-Meter CG 840	Schott, Hofheim a. Ts.
Photometer GeneQuant II, Novospec II	Pharmacia Biotech, Uppsala, Sweden
Pipette Tips Biosphere Quality	Sarstedt, Nümbrecht
Pipette Tips Star Lab (101-1250µl)	Star Lab, Helsinki
Pipettes:	
Eppendorf Pipettes	Eppendorf, Hamburg
Multipette <i>plus</i>	Eppendorf, Hamburg
Multipipette	Dunn Labortechnik und Geräteentwicklung GmbH, Asbach
Hamilton Pipette	Hamilton, Bonaduz, Sweden
Power Supply EPS 500/400	Pharmacia, Uppsala, Sweden

Power Supply LKB ECPS 3000/150	Gibco, BRL, USA
Reaction tubes:	
Falcon Tubes (50 ml)	Falcon, USA
Falcon Tubes (15 ml)	Falcon, USA
Micro Test tubes (1.5 ml)	Eppendorf, Hamburg
MicroTubes (0.5 ml)	Sarstedt, Nümbrecht
Strip tubes	Star Lab, Ahrensburg
Spectrophotometer, Smartspec 3000	Bio-Rad Laboratories GmbH, München
Transilluminator	Ultra-Violet Products
Transilluminator UVT-40 M	Herolab, St. Leon Rot, Wiesloch
Vortex REAX 2000	Heidolph, Hamburg
Waterbath Type 3042	Köttermann, Hänigsen

3.1.2 Chemicals

All chemicals were purchased from the following companies: Sigma (München), Merck (Darmstadt), Roth (Karlsruhe), Riedel-de-Häen (Seelze), Roche Diagnostics (Mannheim), Serva (Heidelberg), FMC Bioproducts (USA).

Electrophoresis Gel for ABI 377 automated sequencer

Long Ranger Gel Solution	BioWhittaker Molecular Applications, USA Carl Roth, Karlsruhe
--------------------------	--

Rotiphorese ® NF-Acrylamide/Bis

Electrophoresis Gel for Single Strand Conformational Analysis (SSCA)

Acrylamid PAGE	12%
Bisacrylamide	0.03%

Triton X-100	Serva, Heidelberg
Tween-20	Sigma, Deisenhofen
DMSO (Dimethylsulfoxide)	Serva Reinbiochemica, Heidelberg
TEMED (Tetramethyldiamide)	Serva Reinbiochemica, Heildelberg

3.2 Buffers and standard solutions

All buffers and solutions were made with Milli-Q water.

DNA Extraction

1x TE-Buffer	10 mM Tris-HCl, pH 7.5 1 mM EDTA
Solution A	0.32 M Sucrose 10 mM Tris, pH 7.5 5 mM MgCl ₂ 1% Triton X-100
Solution B	10 mM Tris, pH 7.5 400 mM NaCl ₂ 2 mM EDTA pH 8.0
Extraction Buffer	20 % SDS
Salting-out Buffer	6 M NaCl ₂

Gel Electrophoresis

5x TBE-Buffer	5 M Tris-HCl, pH 8.3 0.45 M Boric Acid 100 mM EDTA
---------------	--

3.2.1 Enzymes

<i>Taq</i> DNA Polymerase	Qiagen, Heidelberg PeqLab, Erlangen
---------------------------	--

3.2.2 DNA size standards

100 bp DNA ladder	Gibco BRL, Eggenstein
GeneScan-500 TAMRA	Applied Biosystems, Warrington, UK

3.2.3 Reaction kits

Ready-To-Go PCR Beads	Amersham Pharmacia Biotech, Piscataway, USA
QIAquick PCR Purification Kit	Qiagen, Hilden
DYEnamic ET Terminator Cycle Sequencing Kit	Amersham, Buckinghamshire, UK

3.2.4 PCR reagents

10x PCR Buffer	Qiagen, Heidelberg
MgCl ₂ (25 mM)	Qiagen, Heidelberg
DMSO (Dimethylsulfoxide)	Merck, Darmstadt

3.2.5 Loading dye

6x Agarose Gel Loading Dye	2.5 mg/ml Bromophenol blue 150 mg/ml Ficoll 400
Blue Dextran	Applied Biosystems, USA
Formamide Loading Buffer/Dye	38.4 ml formamide 1600 µl 0.5M EDTA 20 mg bromophenol blue 20 mg Xylencyanol

3.2.6 Oligonucleotides

The PCR primers were designed for microsatellite repeat analysis and sequencing by the online program Primer 3 (http://frodo.wi.mit.edu/cgi-bin/primer3/primer3_www.cgi). All synthetic oligonucleotides were supplied by SIGMA-Genosys (UK) and GENSET (France). The optimal annealing temperature was also calculated using the Primer 3 software. The information on microsatellite markers (primer sequences, product length, repeat type, heterozygosity, allelic variants) was obtained from Marshfield Medical Center, Genome Database (GDB) and Centre d'Etude du Polymorphisme Humain (CEPH).

3.2.6.1 Primers for sequencing

Gene	Genebank	Primer Name	Sequence 5' \rightarrow 3'	Product Size
<i>ROX</i>	NM_020310	Ex-01-for	ggc ggg agg cat cgg aag g	390
		Ex-01-rev	gcc agc ccg gcc gct cac	
		Ex-02a-for	ggg tgt cac tga gta ctg act gg	434
		Ex-02a-rev	gca ggc tcc tta atg ctg agt cc	
		Ex-02b-for	cct ggc gcc tcg tca gcc	392
		Ex-02b-rev	ggg cac ctt gtc ttg cac aca g	
		Ex-03/04-for	cag gaa ggc cgt cta atc g	371
		Ex-03/04-rev	gcc cca tac ctg gat gta cc	
		Ex-05-for	ggg gtc ctg ctg tcc ctt ac	331
		Ex-05-rev	cca ggg cca tct ttt cta gc	
		Ex-06a-for	cac aga ggg tga gga caa ca	377
		Ex-06a-rev	cgt ggt tca cag tct gga tg	
		Ex-06b-for	ctc acg ctt cag tca tcc ag	367
		Ex-06b-rev	cca tgg tca cag ggt tga g	
		Ex-06c-for	ctc gca cca gca agt caa c	328
		Ex-06c-rev	gag tct ttg cac ccc ctt c	
<i>CT120</i>	NM_024792	CT-01-for	gcg gag ggt tga aat cgc g	300
		CT-01-rev	ccc ctt ttc cgc cct gg	
		CT-02-for	aat ggc cga tga gcc tcc	306
		CT-02-rev	ttc tga gcg cgt gtg ctg	
		CT-03-for	caa gca cca agc ttg gct gt	330
		CT-03-rev	gac acc cag ctc aac cca g	
		CT-04-for	ccg tca cag tta ccc ttt tc	280
		CT-04-rev	atc aga acc ctc act ctc tc	
		CT-05-for	tta ctg tgg tgg gac ttg gg	430
		CT-05-rev	agg gca caa ttt ggt cca tgg	
<i>LOST1</i>	NM_172367	LT-01-for	agt ctg ggc tgg gga atg	398
		LT-01-rev	taa tct ctg ggg gct tct tg	
		LT-02-for	cct tca agg cca tct ccg ag	371
		LT-02-rev	tct aag agg aag gag gag gcc	
		LT-03-for	act tct ccg ggg aca gcc	449
		LT-03-rev	tat gga ctg gga gga taa ggc	
		LT-04-for	ttc cca agc ctt agc ctt ctc	293
		LT-04-rev	ggt ttc cct ttg agt ctg tgc	

3.3 Softwares and databanks

3.3.1 Softwares

Software	Source
Text Editor	Word 2000, Microsoft
Tables and Data storage	Excel 2000, Microsoft
Graphics	PowerPoint 2000, Microsoft Adobe Acrobat Reader 2000 (5.0) Adobe Photoshop 2000 (6.0)
Pedigree Drawing: Cyrillic version 2.1.3	Cherwell Scientific Publishing 1997 www.cherwell.com
Gel Documentation: EasyWin32	Herolab, ST. Leon Rot, Wiesloch
DNA Fragment Analysis:	
GeneScan version 3.1.2	Applied Biosystems, USA
Genotyper version 2.0	Applied Biosystems, USA
Linkage Analyses:	
MAKEDATA	Dr. Yurii Aulchenko, Rotterdam
MEGA2	Mukhopadhyay et al. (1999)
LINKAGE	
MLINK version 5.1	Lathrop et al. (1984)
FASTLINK version 4.1	Cottingham et al. (1993)
GENEHUNTER version 2.1	Kruglyak et al. (1996)
SIMWALK2 version 2.83	Sobel and Lange (1996)
Primer Designing: Primer 3	http://frodo.wi.mit.edu/cgi-bin/primer3/primer3_www.cgi
Sequence Analysis: Sequencher version 4.2	Gene Codes, Ann Arbor, USA

3.3.2 Databanks

Application	Databank	Internet address
Literature search	PubMed	www.ncbi.nlm.nih.gov/entrez
Genetic disorders catalogue	OMIM (Online Mendelian Inheritance in Man)	http://www.ncbi.nlm.nih.gov/OMIM
Genome resource	NCBI (National Center for Biotechnology Information)	http://www.ncbi.nlm.nih.gov/
Genome data bank	UCSC Genome Bioinformatics	http://genome.ucsc.edu/
Microsatellite resource center	Marshfield Medical Center	http://research.marshfieldclinic.org/genetics/
Microsatellite resource center	GDB (The Genome Database)	http://www.gdb.org/
Microsatellite resource center	CEPH (Centre d'Etude du Polymorphisme Humain)	http://www.cephb.fr/
Microsatellite resource center	CHLC (The Cooperative Human Linkage Center)	http://gai.nci.nih.gov/CHLC/
Linkage resource center	Laboratory of Statistical Genetics, Rockefeller University	http://linkage.rockefeller.edu/
Bioinformatics resource center	HGMP Resource Centre	http://www.hgmp.mrc.ac.uk/
Mouse genome data bank	Mouse Genome Informatics	http://www.informatics.jax.org/

3.4 Methods

3.4.1 Blood sampling

Blood samples were drawn by 10 ml syringes and vacutainer tubes containing EDTA. The blood was stored at 4°C until DNA extraction.

3.4.2 Genomic DNA extraction

Genomic DNA was purified from peripheral blood lymphocytes according to standard salting out SDS-proteinase-K extraction method (Sambrook and Russel 2001).

1. Eight to ten ml blood collected in 50 ml falcon tube.
2. The volume was set to 45 ml by the addition of solution A and was stored on ice for 30 minutes.
3. After chilling, centrifugation was carried out at 5000 rpm for 30 minutes at 4°C to separate white blood cells.
4. The supernatant was discarded and the pellet was resuspended in solution A and centrifuged again.
5. The pellet was resuspended in 3 ml of solution B and incubated overnight at 37°C by adding 100 µl 20 % SDS and 0.5 ml proteinase-K (2 mg/ml).
6. On the following day, the tube was vigorously shaken for 15 seconds after the addition of 1.5 ml saturated solution of sodium chloride (~6M).
7. The tube was centrifuged twice at 5000 rpm to obtain a clean supernatant containing genomic DNA.
8. The clear supernatant was transferred to a new falcon tube, and DNA was precipitated by the addition of two volumes of absolute ethanol.
9. The precipitated DNA was fished out with micropipette tip, washed in 70% ethanol and was placed in a 1.5 ml reaction tube.
10. After evaporation of residual ethanol, DNA was dissolved in an appropriate amount of TE-buffer and stored at 4°C.
11. Genomic DNA was quantified by spectrophotometer at OD₂₆₀, and was diluted to 50 ng/µl for amplification by polymerase chain reaction (PCR).

3.4.3 Polymerase chain reaction (PCR)

Polymerase chain reactions were performed in a total volume of 20 μ l, containing 50 ng of genomic DNA, 2 μ l 10x PCR buffer (Qiagen), 1.8 mM MgCl₂, 5 mM dNTPs, 12.5 ng of each primer and 0.5 U of *Taq* DNA polymerase (Qiagen). The PCR reaction was as follows:

Step	Temperature °C	Duration	Cycles
Denaturation	94	5 min.	1
Denaturation	94	25 sec.	28-35
Annealing	53-63	25 sec.	
Extension	72	30 sec.	
Final Extension	72	10 min.	1

3.4.4 Horizontal gel electrophoresis

The amplification of the genomic region was checked on 1-2% agarose gel, which was prepared by melting 1-2 g. of agarose in 100 ml 1x TBE buffer in a microwave oven for few minutes. Ethidium bromide (final conc. 0.5 μ g/ml) was added to the gel to facilitate visualization of DNA after electrophoresis. PCR reaction products were mixed with Bromophenol blue dye and loaded into the wells. Electrophoresis was performed at 100 Volts for half an hour in 1x TBE buffer. Amplified products were detected by placing the gel on UV transilluminator.

3.4.5 Genotyping

For genomic study of the putative candidate regions, highly polymorphic microsatellite markers were selected from Marshfield Medical Center (<http://research.marshfieldclinic.org/genetics/>). For genome-wide search a panel of 360 autosomal markers was obtained from CHLC screening Set version 6, with an average spacing of ~10 cM and heterozygosity >70%. All markers were 5'-end-labeled with fluorescent dyes: 6-FAM, TET or HEX. A CEPH subject (1347-02) was used as a reference for microsatellite markers.

1.4 μ l of pooled PCR products was mixed with 1.6 μ l loading buffer containing formamide, blue dextran, and GS500XL, the internal lane standard (Applied Biosystems), and analysed on 6% denaturing polyacrylamide gel (Rotiphorese ® NF-

Acrylamide/Bis, Carl Roth, Karlsruhe) in an ABI 377 automated sequencer (Applied Biosystems). Fragment analysis was performed using GeneScan (ver 3.1.2) and Genotyper (ver 2.0) softwares.

3.4.6 Linkage analysis

Pedigree and genotype data were managed and recorded for linkage analysis using Cyrillic 2.1.3 and Excel 2000 (Microsoft). File formatting was done by using MAKEDATA software (Dr. Yurii Aulchenko, Rotterdam) and Mega2 (Mukhopadhyay et al. 1999). Genotype incompatibilities and Mendelian inconsistencies were identified by using PedCheck software version 1.1 (O'Connell and Weeks 1998).

Pedigrees were simulated in order to estimate the potential of finding linkage by using SLINK program of LINKAGE software package version 5.1 (Lathrop et al. 1984). Hundred replicates were used in each simulation. Two-point LOD scores were calculated using the MLINK program of LINKAGE software package version 5.1 (Lathrop et al. 1984) and FASTLINK version 4.1 (Cottingham et al. 1993). Analyses were automated by using linkage support programs (LSP, LCP, MAKEPED, PREPLINK). Multipoint analysis was done with GENEHUNTER version 2.1, and haplotypes were constructed using SIMWALK2 version 2.83 (Kruglyak et al. 1996; Sobel and Lange 1996).

For the Family 1, an autosomal recessive model with a penetrance of 0.999 (phenocopy rate of 0.001 for homozygous normal and heterozygous individuals) and a disease allele frequency of 0.001 was assumed. For Families 2, 3 and 4, an autosomal dominant model with a penetrance of 0.9999 (phenocopy rate of 0.0001 for homozygous normal individuals) and a disease allele frequency of 0.0001 was assumed. The mutation rate was set to zero and equal recombination rates between males and females were assumed. Marker allele frequencies were taken from Marshfield human diversity panel (Asia-Pakistan population, based on approximately 190 individuals) or from CEPH database (<http://www.cephb.fr/>). For fine mapping, the marker allele frequencies were calculated from the family founders or assumed to be equal. Microsatellite marker order and genetic map positions were obtained from Marshfield Medical Center (<http://research.marshfieldclinic.org/genetics/>), deCODE map (Kong et al. 2002) and UCSC Genome Bioinformatics Santa Cruz (<http://genome.ucsc.edu/>). Analyses were

also conducted by using the online facility of GLUE (Genetic Linkage User Environment, UK HGMP Resource Centre; <http://www.rfcgr.mrc.ac.uk/>).

3.4.7 Mutation screening

3.4.7.1 Primer designing

Primers for PCR amplification and subsequent sequencing of the candidate regions were designed by using software at the Primer3 Web site (http://frodo.wi.mit.edu/cgi-bin/primer3/primer3_www.cgi) to flank all the exon–intron boundaries.

3.4.7.2 Single strand conformational analysis (SSCA)

For mutation screening, SSCA was conducted on Hoefer apparatus SE600 (Pharmacia Biotech). 3.5 μ l of PCR products were mixed with equal volume of HPLC-H₂O and 8 μ l of formamide loading buffer and analysed on 12% polyacrylamide non-denaturing, vertical slab gels (size 18cm x 16cm x 0.075cm). Two parallel electrophoresis reactions were performed at 10 and 20°C with a running solution of 0.5x TBE. The gel was run for an initial 10 min. at 200V and subsequently for 90 min. at 600V. Bands were visualised through silver staining. Gels were mounted and stretched on cellophane sheet and dried overnight for permanent storage.

3.4.7.3 Silver staining

All solutions were prepared fresh and staining was performed in a washing tub set on an automated shaker (3 cycles/min). Staining was performed through the following steps:

1. Fixation with 10% glacial acetic acid for 5 min.
2. Oxidation with 1% nitric acid for 10 min.
3. Washing with distilled water, three times.
4. Silver staining with 12 mM AgNO₃ for 20 min.
5. Quick washing, three times.
6. Reduction with 280 mM Na₂CO₃ until the bands are visible.
7. Conservation with 10% glacial acetic acid with 2—3% glycerol.

3.4.7.4 DNA sequencing

In order to screen for mutations in the putative candidate genomic regions, sequencing was conducted through the following steps:

3.4.7.5 PCR purification

The PCR products of the amplified candidate regions were purified by using QIAquick PCR Purification Kit (Qiagen).

1. Added 5 volumes of Buffer PB to 1 volume of the PCR sample and mixed it thoroughly.
2. Placed a QIAquick spin column in a provided 2 ml collection tube.
3. To bind DNA, the sample was applied to the column and centrifuged for 30–60 s.
4. Discarded the flow-through and placed the column back into the same tube.
5. To wash DNA, added 750 μ l Buffer PE to the column and centrifuged for 30–60 s.
6. Discarded the flow-through and placed the column back into the same tube.
7. To dry the sample, centrifuged it for an additional 1 min.
8. Placed the column in a clean 1.5 ml microcentrifuge tube.
9. To elute DNA, added 30-50 μ l Buffer EB (10 mM Tris-Cl, pH 8.5) or HPLC water to the center of the QIAquick membrane and centrifuged the column for 1 min.

Alternatively, for increased DNA concentration, added 30 μ l elution buffer to the center of the QIAquick membrane, allowed the column to stand for 1 min. and then centrifuged.

All centrifugation steps were conducted at 13,000 rpm on a tabletop microcentrifuge (Eppendorf).

3.4.7.6 Sequencing PCR reactions

The sequencing PCR reactions were done by using DYEnamic ET Terminator Cycle Sequencing Kit (Amersham), containing the labeled dNTPs.

The composition of the sequencing PCR reaction was as follows:

Component	Volume (μ l)
Template DNA (40 ng/ μ l)	01
Primer (3.2 pmol)	01
HPLC H ₂ O	04
Sequencing reagent premix (Amersham)	04
Total volume	10

The contents were mixed thoroughly in the reaction tubes by gentle pipetting and centrifuged briefly to bring contents to the bottom of the tubes or wells. Following PCR reaction was conducted:

Step	Temperature °C	Duration	Cycles
Denaturation	95	2 min.	1
Denaturation	95	20 sec.	28
Annealing	53-59	15 sec.	
Extension	61	60 sec.	
Final Extension	72	5 min.	1

3.4.7.7 Sequencing PCR purification

This step is important to ensure very low background noise in the sequencing electrophoresis reaction.

1. 10 μ l of HPLC-H₂O was added to the PCR products to make the total volume of 20 μ l.
2. Added 2 μ l (1/10 volume) of sodium acetate/EDTA buffer to each tube (before adding ethanol).
3. Added 80 μ l of 95% ethanol to each reaction and mixed well using a vortex.
4. Incubated for 20 min. at room temperature.
5. Centrifuged the tubes for 15 min at ~ 14,000 rpm.
6. Removed the supernatant by aspiration from each microcentrifuge tube.
7. Washed the DNA pellets with 300 μ l of 70% ethanol.

8. Centrifuged for 10 min. at ~14,000 rpm.
9. Removed the supernatant quickly by aspiration
10. Air-dried the pellets for 5-10 min.

3.4.7.8 Resuspension of samples and electrophoresis

The purified PCR products were dissolved in 4 μ l formamide loading dye (US79448, Applied Biosystems) for optimal sequencing results and analyzed on 5% denaturing polyacrylamide gel (Rotiphorese ® NF-Acrylamide/Bis, Carl Roth, Karlsruhe) in an ABI 377 automated sequencer (Applied Biosystems).

3.4.7.9 Sequence data analysis

The sequence data was obtained from the ABI 377 automated sequencer (Applied Biosystems) by Sequence Analysis Software ver 3.4.1 (Applied Biosystems) and was analysed by Sequencher software ver 4.2 (Gene Codes).

3.5 Classification protocol for syndactylies

A simple protocol has been designed to facilitate the typing of syndactylies including the eight types established by Temtamy and McKusick (1978) and Goldstein et al. (1994), as well as a ninth type by Malik et al. (2004). Hands with five fingers and feet with five toes are represented by two diagrams with five boxes (Figs. 4-1—3). Shading indicates cutaneous syndactyly of phalanges (e.g. type I), while shading with no separating line indicates bony syndactyly (e.g. type IV). Crosshatching represents metacarpal fusion (e.g. type II). An associated polydactyly is symbolised by adding bars, showing the location of the extra digit (e.g. preaxial, postaxial or mesoaxial polydactyly). Absence of digits is expressed by omitting the box for the corresponding missing digit (e.g. type IX). Fusion of carpal bones and radioulnar synostosis is represented accordingly. For simplicity, two hands and two feet are shown on the same graph.

For a test trial of the protocol a literature search for reports with syndactylies was performed comprising the years 1910-2003. 104 different index cases, with and without other affected family members were ascertained through 60 publications. Seventy-eight cases/families fulfilled the criteria of a good documentation (clinical description, photographs and/or radiograms) and were therefore included in the trial. Families from different publications with an identical or very similar phenotype were grouped into one diagram. For each family the most common phenotype was documented. In a few instances the phenotype within the family was so divergent, that both phenotypic versions (mild and severe), were listed. Families described in more than one publication are listed only once.

4 Results

4.1 Proposed syndactyly classification

To simplify the handling of the classification, syndactylies have been regrouped according to similarities in the phenotype and inheritance into three categories (Figure 4-1, Figure 4-2, Figure 4-3).

Group 1 (Figure 4-1): syndactylies with autosomal dominant inheritance and involvement of phalanges only;

Group 2 (Figure 4-2): syndactylies with autosomal dominant inheritance and malformations of phalanges as well as metacarpal/metatarsal bones;

Group 3 (Figure 4-3): syndactylies with autosomal recessive inheritance, involvement of all bony elements in hands/feet and radial/ulnar fusion, as well as syndactylies with missing fingers.

The first group (Figure 4-1) includes type I, III, IV, and VI featuring various degrees of cutaneous webbing in hands/feet and bony fusion at the phalangeal tips. Metacarpal/metatarsal synostosis is not a feature of this group. Based on the clinical and genetic findings in the Family 2, syndactyly type I has been further divided into four subtypes.

The group is dominated in numbers by type I and III. The two types can easily be discriminated from each other, since type III is part of the oculodentodigital (ODD) syndrome. A constant feature in type I is the mesoaxial involvement with a 3-4 finger and a 2-3 toe syndactyly. The hallmark of type III is the bony 4-5 finger syndactyly, and the graph shows that this is not a feature by other members of the group. There is at least one gene (*GJAI*) identified for ODD.

Type IV has more severe features involving all fingers. If a hexadactyly is present, additional metacarpal bones are also observed, and in these cases discrimination between pre- and postaxial is not possible. An unclassified family of Temtamy and McKusick (1978) was named type VI by Goldstein et al. (1994), and it shows features

similar to type IV. Most cases in this group are autosomal dominantly inherited, but sporadic cases are also described.

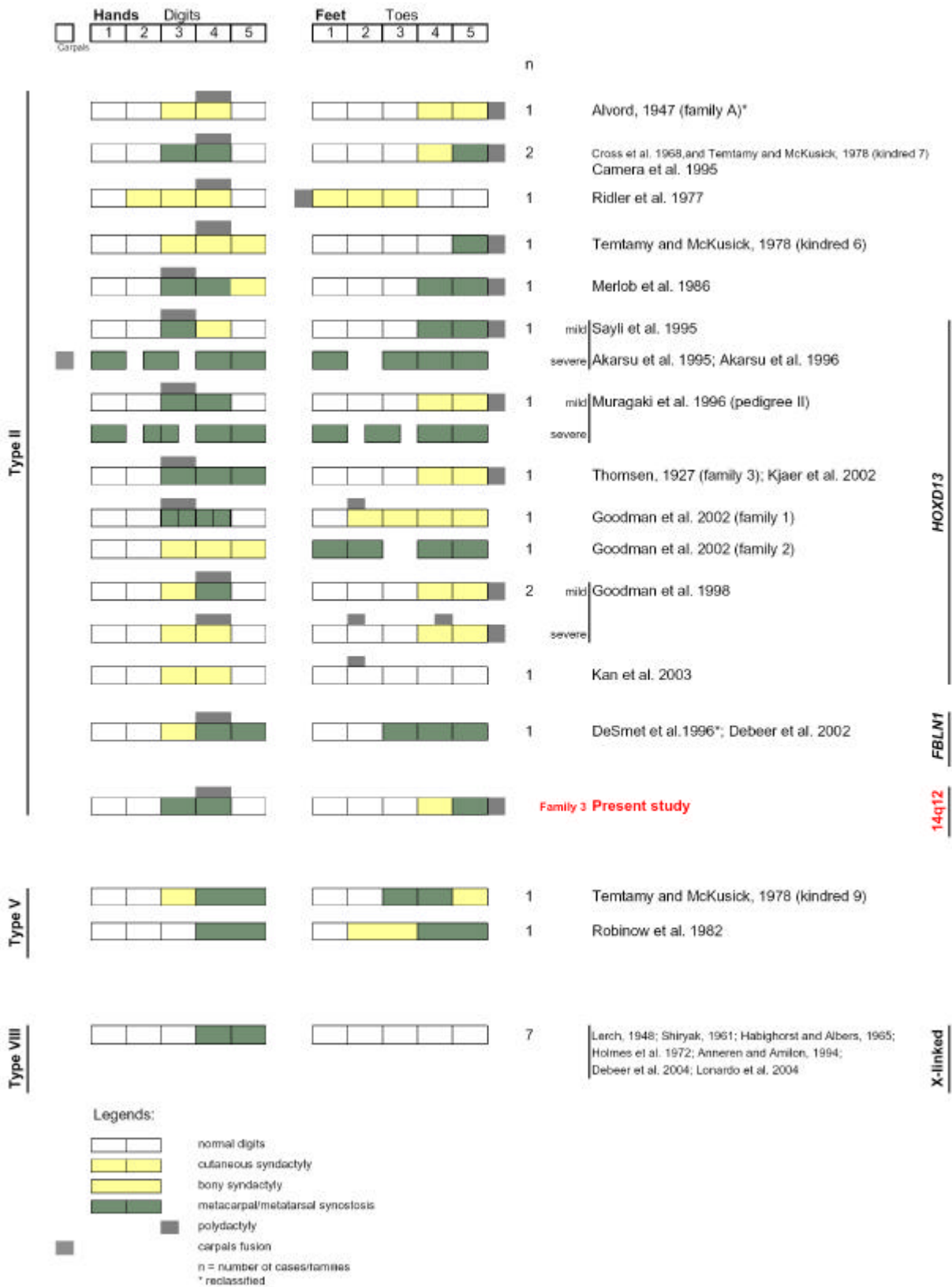


Figure 4-1: Group 1: Syndactylies with involvement of phalanges only.

Group 2 includes syndactylies type II, V and VIII (Figure 4-2). This group is dominated in numbers by the extremely variable type II syndactyly or synpolydactyly. It is easy to see that the hallmark of this type is postaxial synpolydactyly with metacarpal/metatarsal synostosis. There is genetic heterogeneity for this type, and mutations in two genes (*HOXD13*, *FBLN1*) have been reported. The inheritance is autosomal dominant, and the closest phenotype is type V syndactyly, with only two cases in the literature.

A distinct type in this group is type VIII syndactyly with a 4-5 metacarpal fusion and X-linked inheritance. Confusion with other types is not possible.



Figure 4-2: Group 2: Syndactylies involving phalanges and metacarpal/metatarsal synostosis.

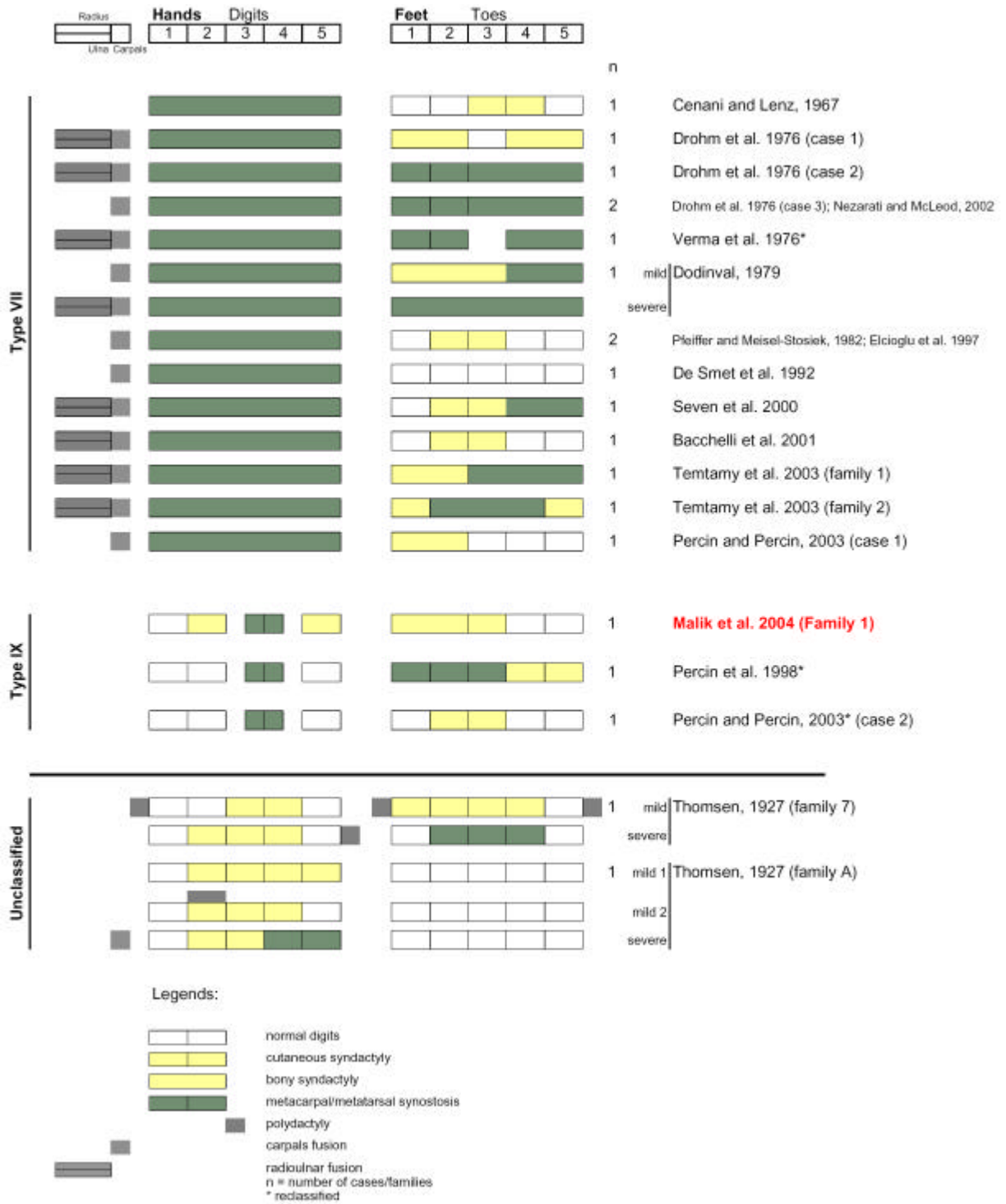
Group 3 (Figure 4-3) is the only one with well-described autosomal recessive phenotypes (types VII, IX). These phenotypes are fairly severe. The Cenani-Lenz type is easy to differentiate from all other syndactylies, since there is additional carpal- and radio/ulnar fusion.

Based on the work described in this thesis I introduced a ninth type (type IX, Malik-Percin type) to the classification, since a Pakistani and a Turkish family have a remarkable phenotypic similarity (Malik et al. 2004; Percin et al. 1998). Both families show metatarsal/metacarpal synostosis and absence of fingers.

I added in Figure 4-3 two unclassified cases described by Thomsen (1927): mild mesoaxial syndactyly with pre- and postaxial polydactyly (family 7); preaxial polydactyly of fingers, postaxial involvement of metacarpal bones and fusion of carpal bones (family A). The combination of clinical features is not in agreement with any of the syndactyly types I—IX.

Applying this classification to published syndactylies, in 71 cases I came to the same conclusion as the original investigators, which proved that my protocol is effective. Cases/families reported by Alvord (1947), De Smeet et al. (1996) (Figure 4-2), Verma et al. (1976), Percin et al. (1998) and Percin and Percin (2003) (Figure 4-3) were reclassified. Two well-documented families reported by Thomsen (1927) (family 7, family A) could not be categorized and are added as a point of interest in Figure 4-3.

This work on the proposed classification of syndactyly is in press (Malik et al. 2005a, Genetic Counseling).



17p13.3

Figure 4-3: Group 3: Severe syndactylies showing autosomal recessive inheritance.

4.2 Family 1

4.2.1 Autosomal recessive mesoaxial synostotic syndactyly with phalangeal reduction (MSSD)

The distinctive phenotype observed in Family 1 has not been witnessed in any syndactyly types established by Temtamy and McKusick (1978) and Goldstein et al. (1994). The cardinal clinical features in Family 1 are mesoaxial reduction of fingers, synostosis of 3rd and 4th metacarpals, clinodactyly of 5th fingers and preaxial webbing of toes. There was a minimal overlap of clinical features with syndactyly type I, II and III, but combination of clinical features and an autosomal recessive mode of inheritance make Family 1 a unique syndactyly type (Figure 4-4; based on METHODS section 3.5).

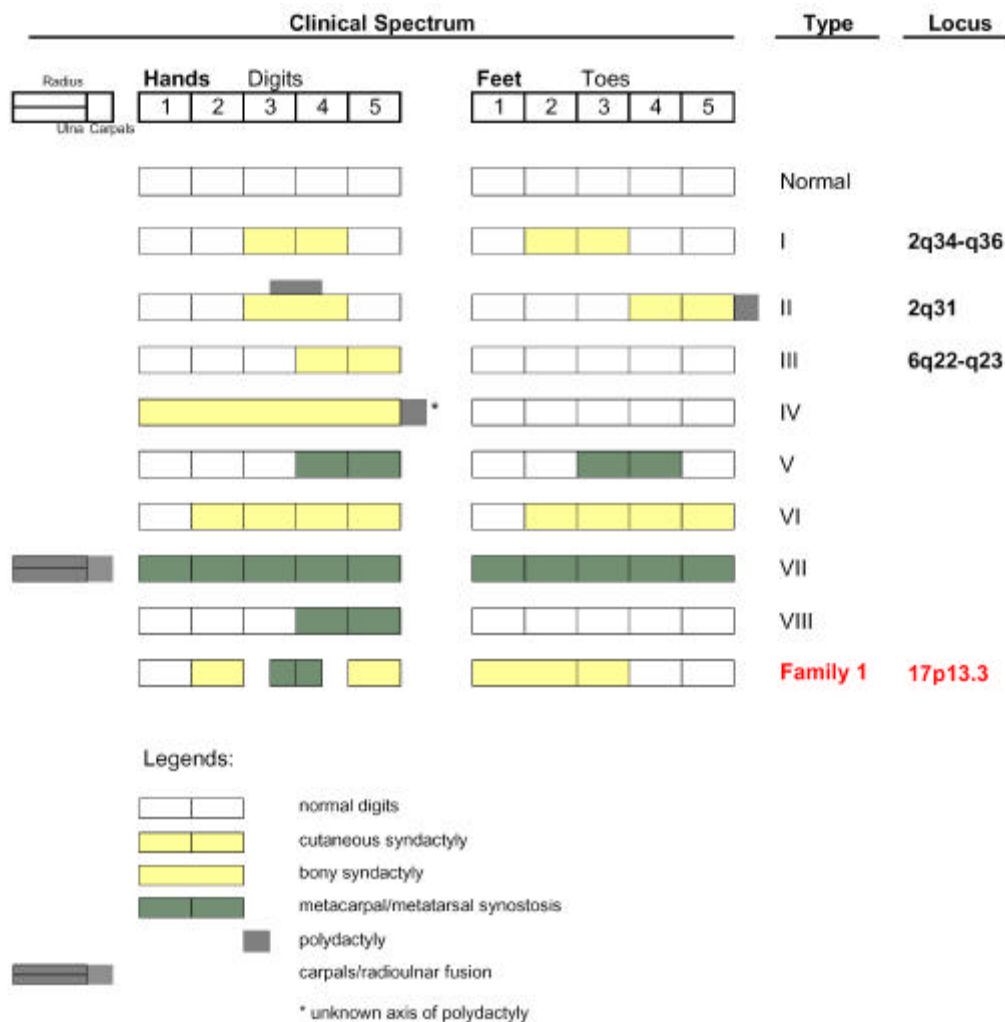


Figure 4-4: A graphical comparison of the phenotype in Family 1 with the phenotypes in other syndactyly types.

4.2.2 Exclusion of loci for syndactyly type I, II and III

Family 1 was evaluated for the possibility that the phenotype is linked to the known loci for syndactyly, namely 2q34-q36 (SD1), 2q31 (SPD) and 6q22-q23 (Bosse et al. 2000; Sarfarazi et al. 1995; Paznekas et al. 2003). Two point linkage analysis yielded significant negative ($\theta = 0.0$) LOD scores at $\theta = 0.0$ for all loci (Table 4-1). Haplotypes constructed for the critical regions do not show homozygosity in the affected individuals. The results excluded all critical regions for syndactylies type I, II and III, flanked by markers D2S1776-D2S1391, D2S434-D2S1279, and D6S474-D6S1003.

Table 4-1: Two-point LOD scores between the phenotype and markers on chromosome 2q and 6q.

Chromosome 2			Recombination fraction (θ)							
Phenotype	Locus	cM	Marker	0.00	0.01	0.05	0.1	0.2	0.3	0.4
SPD	2q12.2	118.16	D2S436	-4.48	-3.68	-1.86	-1.04	-0.38	-0.13	-0.02
		125.18	D2S410	-5.07	-3.55	-2.13	-1.46	-0.78	-0.38	-0.13
	2q21.1	134.45	D2S2215	-0.03	0.21	0.52	0.58	0.49	0.31	0.13
		142.83	D2S114	-0.70	0.14	0.63	0.71	0.61	0.39	0.17
	2q31	173.00	D2S1776	-3.20	-1.99	-0.90	-0.46	-0.13	-0.02	0.00
		186.21	D2S1391	-2.88	-1.77	-0.71	-0.29	-0.01	0.04	0.03
		205.00	D2S1649*	-2.85	-2.09	-1.15	-0.58	-0.13	0.00	0.03
	2q34-q36	215.78	D2S434	-5.90	-3.90	-2.24	-1.45	-0.70	-0.33	-0.12
		227.00	D2S1363	-6.41	-3.17	-1.73	-1.08	-0.51	-0.24	-0.08
		240.79	D2S1279	-6.85	-4.59	-2.33	-1.39	-0.63	-0.32	-0.14
2q37.3	260.63	D2S125	-5.17	-3.39	-2.38	-1.91	-1.11	-0.57	-0.23	
Chromosome 6										
6q11.1		80.45	D6S1053	-7.41	-5.13	-3.43	-2.31	-1.09	-0.50	-0.18
		88.63	D6S1031	-6.89	-4.13	-2.07	-1.20	-0.50	-0.24	-0.11
6q14.3		92.85	D6S1270	-0.47	-0.22	0.09	0.18	0.15	0.06	0.01
		102.81	D6S1056	-6.23	-2.70	-1.32	-0.71	-0.23	-0.05	0.00
6q22-q23	GJA1	118.64	D6S474	-4.20	-3.58	-2.38	-1.61	-0.84	-0.43	-0.17
		128.93	D6S1040	-5.03	-4.11	-3.12	-2.52	-1.48	-0.77	-0.31
6q26		137.74	D6S1009	-6.41	-4.51	-2.48	-1.54	-0.70	-0.30	-0.09
		144.46	D6S1003	-6.37	-4.81	-2.81	-1.80	-0.83	-0.35	-0.10
		159.98	D6S1007	-4.98	-3.35	-2.08	-1.30	-0.55	-0.20	-0.04
		173.31	D6S1277	-0.73	-0.47	-0.10	0.04	0.10	0.08	0.04

* Microsatellite marker not present in Marshfield map

4.2.3 Genome-wide search, fine mapping and locus identification on chromosome 17p13.3

After the exclusion of three loci for syndactyly, a genome-wide search was performed. Only a single autozygous region on 17p13-pter was identified in all four affected individuals (Figure 4-5). No other region was identified with fully informative markers being homozygous in all affected individuals. The subsequent saturation of this region with an extended map of polymorphic microsatellite markers confirmed the presence of a large region of autozygosity in the affected individuals (Figure 4-6, Figure 4-7). The homozygous critical interval spans between markers D17S643 and D17S1828 comprising a region of ~10 cM (Figure 4-6, Figure 4-7). Two-point linkage analysis showed a maximum LOD score (Z_{\max}) of 3.47 for marker D7S1528 at a recombination fraction of zero ($\theta = 0.00$; Table 4-2). Multipoint analysis gave a LOD score of 3.06 (Figure 4-8).

Table 4-2: Two-point LOD scores between the phenotype and the markers on chromosome 17p13.

cM	Marker	Recombination fraction (θ)						
		0.00	0.01	0.05	0.10	0.20	0.30	0.40
0.63	D17S643	-0.05	0.91	1.32	1.27	0.91	0.48	0.17
0.63	D17S849	2.78	2.72	2.45	2.11	1.44	0.80	0.28
0.63	D17S1308	2.38	2.31	2.06	1.74	1.12	0.56	0.15
0.63	D17S926	3.38	3.28	3.00	2.59	1.81	1.03	0.38
3.67	D17S695	3.15	3.08	2.79	2.42	1.67	0.94	0.34
3.96	D17S596	1.65	1.62	1.51	1.35	0.99	0.62	0.28
3.99	D17S1533	2.48	2.41	2.16	1.84	1.20	0.63	0.19
6.60	D17S831	2.01	1.96	1.75	1.49	0.96	0.48	0.13
6.60	D17S1528*	3.47	3.39	3.08	2.69	1.88	1.06	0.39
6.60	D17S1798	1.92	1.90	1.77	1.58	1.14	0.69	0.29
7.19	D17S1583	3.28	3.22	2.91	2.53	1.73	0.97	0.34
10.02	D17S1828	-7.31	-5.53	-3.27	-2.06	-0.93	-0.39	-0.11
10.72	D17S1298	0.84	0.82	0.76	0.67	0.50	0.33	0.16

* The marker that yielded highest LOD score

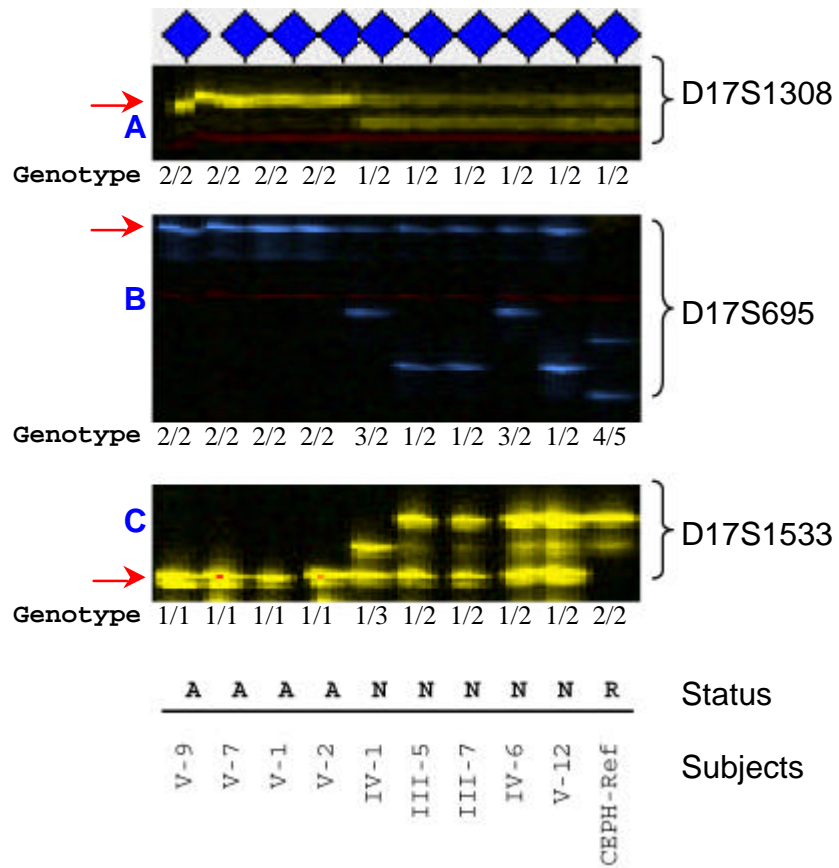


Figure 4-5: Electropherograms (A—C) of three microsatellite markers from chromosome 17p linked to the phenotype.

Red arrows indicate marker alleles homozygous in affected subjects (V-9, V-7, V-1, V-2).

(A = affected; N = normal; R = CEPH reference individual)

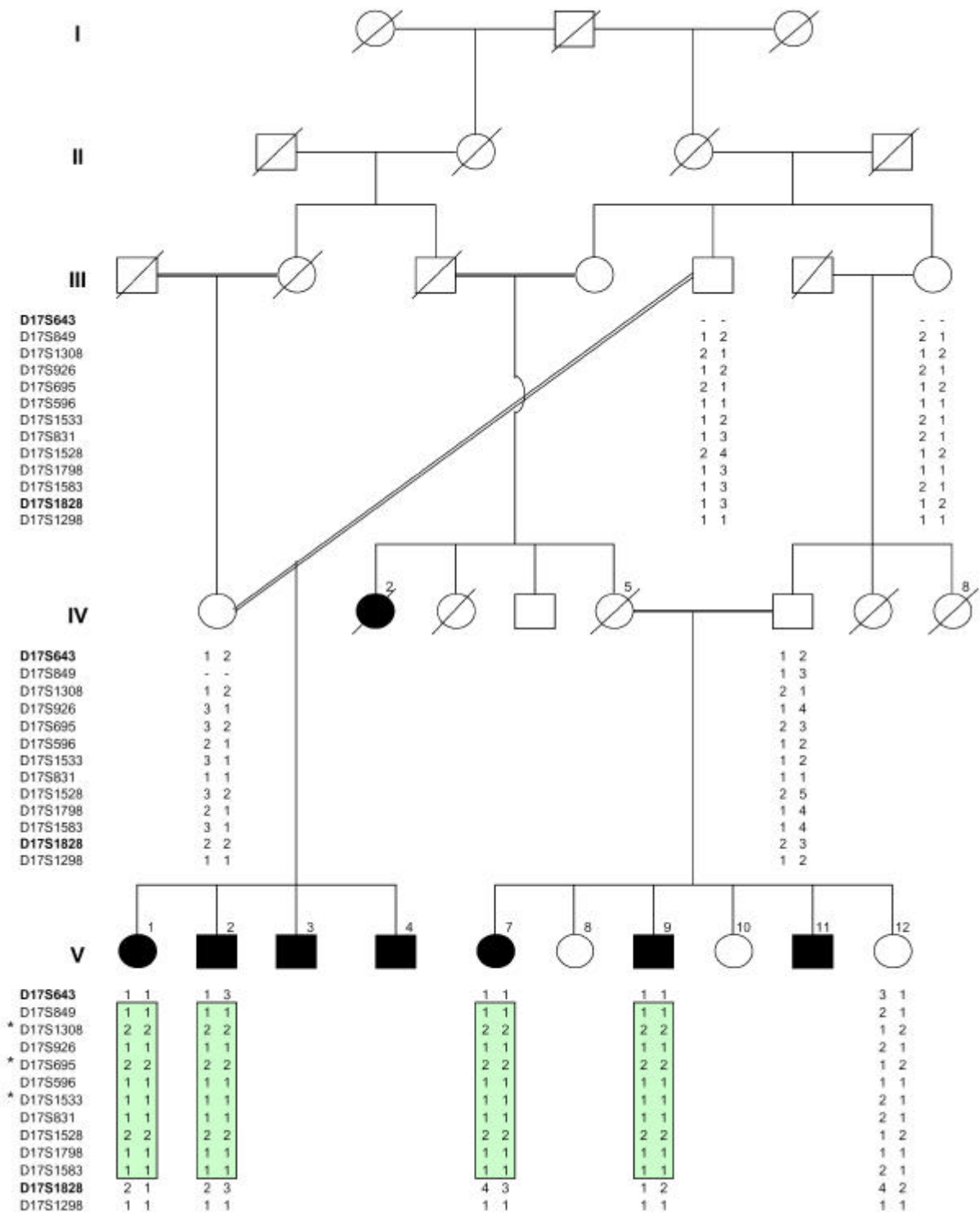


Figure 4-6: Haplotypes of the individuals in Family 1 for thirteen microsatellite markers from chromosome 17p13.

The homozygous region in affected subjects segregating with the phenotype is shown in green. The individual IDs on the pedigree are the same as described in Fig. 2.2. A sign of (-) shows alleles which were not typed due to technical/PCR problems.
 * Typing for these markers is also shown in Figure 4-5.

4.2.4 Mutation screening

During the candidate gene investigations within the critical interval segregating with the syndactyly type IX, the following genes were found to be interesting to screen for mutation:

4.2.4.1 *ROX*

The most likely candidate within the critical interval was *ROX* (NM_020310). *Rox* (MAX binding protein) is involved in transcriptional regulation and mediates cell differentiation and proliferation. MAX binding proteins share a basic helix-loop-helix leucine zipper domains (bHLHZip) and bind DNA at an E box (CANNTG) by forming heterodimers with MAX (Meroni et al. 1997). *ROX* contains six exons, the smallest being 42 bp and the largest 749 bp. Primers were designed to cover all the exons and the flanking sequences of exon-intron boundaries. Sequencing of the coding regions in two affected and one normal subject did not reveal any mutation.

4.2.4.2 *CT120*

CT120 (NM_024792) is a membrane protein expressed in epithelial-like lung adenocarcinoma. It contains five exons (NM_024792). Sequencing of the coding regions in two affected and one normal subject did not reveal any mutation.

4.2.4.3 *LOST1*

LOST1 (NM_172367) contains three exons. Sequencing of the coding regions in two affected and one normal subject did not reveal any mutation.

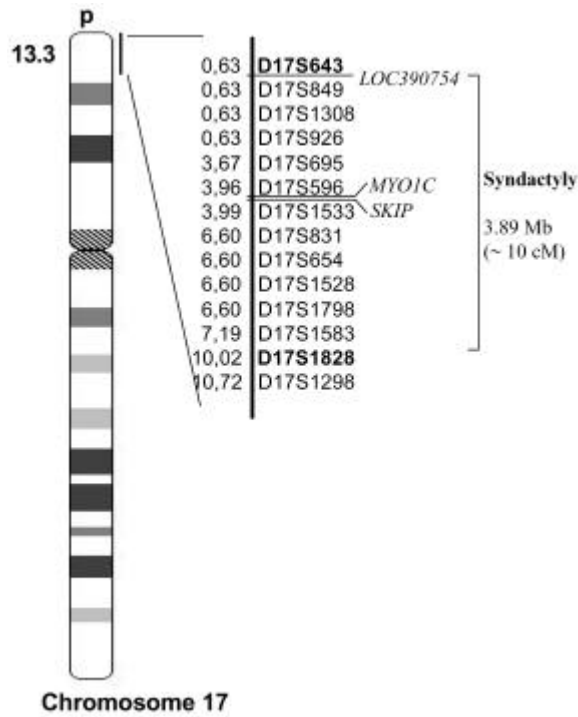


Figure 4-7: Genetic map of chromosome 17 markers used in the saturation mapping.

The marker-map positions (cM) are based on the sex-averaged map from the Center for Medical Genetics, Marshfield Medical Research Foundation or Genome Database (GDB). Markers flanking the syndactyly locus are shown in boldface.

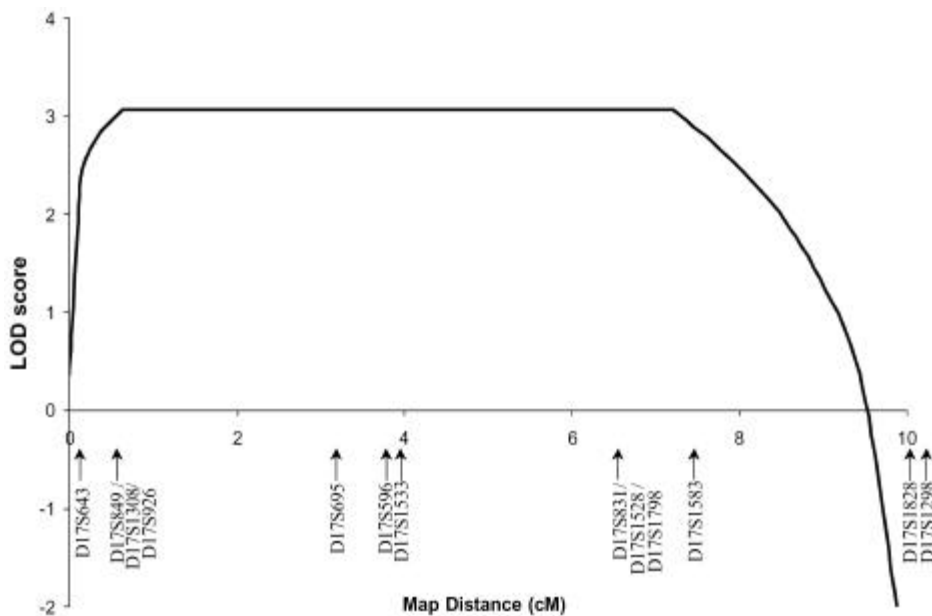


Figure 4-8: Multipoint LOD score analysis for region 17p13.3.

The multipoint linkage analysis localized the locus for syndactyly within an interval of ~7.5 cM between markers D17S849 and D17S1583. Multipoint score throughout this interval was 3.06.

4.3 Family 2

4.3.1 Family with autosomal dominant zygodactyly

Family 2 shows cutaneous fusion of 2nd and 3rd toes without hand malformation. The clinical features are characteristic for zygodactyly (Temtamy and McKusick, 1978). The phenotype in Family 2 is similar to the affected subjects described in a family by Stiles and Hawkins (1946). A comparison of phenotype in Family 2 with other type I syndactyly families is given by a graphical method (Figure 4-9; based on METHODS section 3.5).

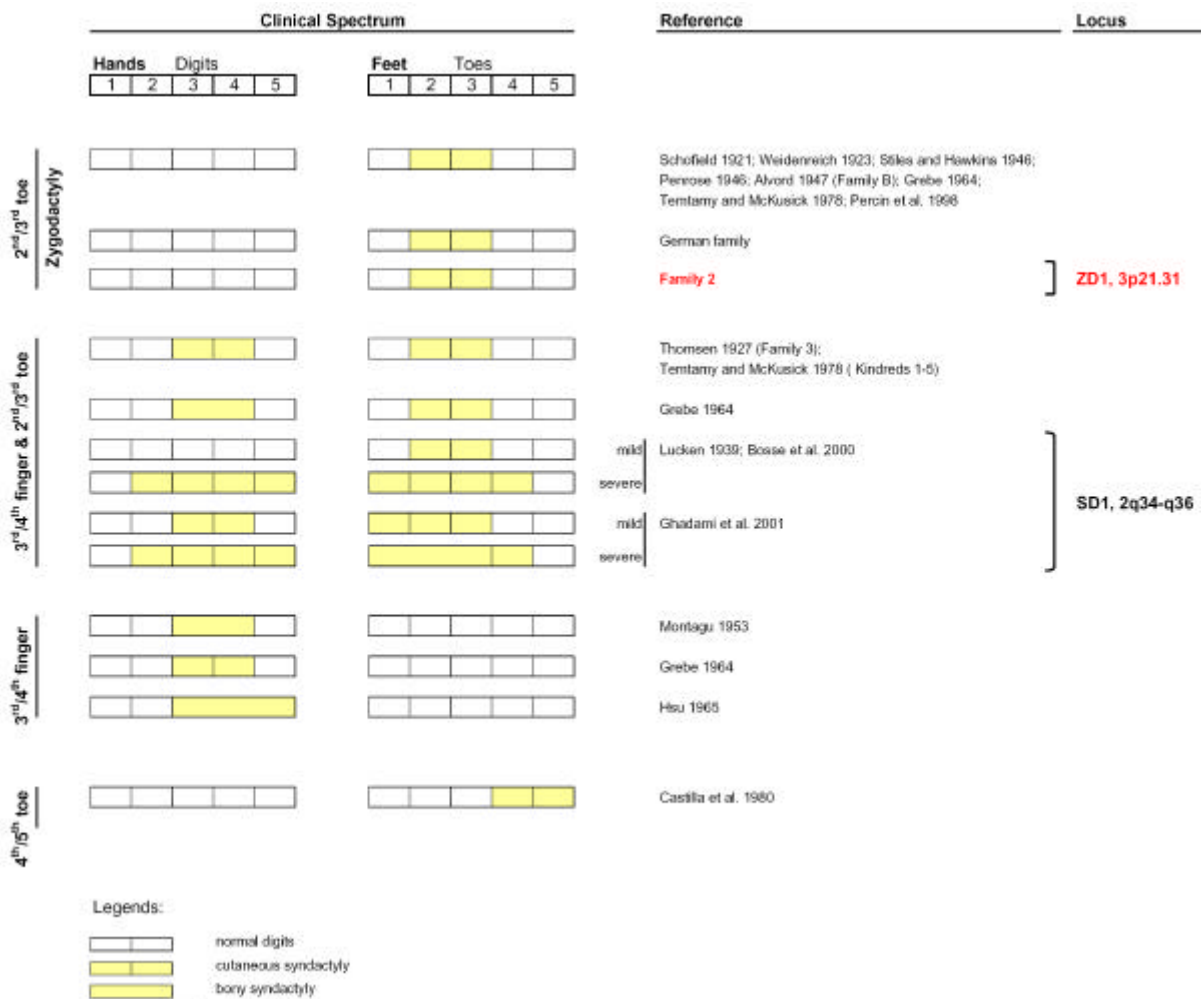


Figure 4-9: A graphical comparison of the phenotype in Family 2 with the phenotypes in other reported type I syndactyly families.

4.3.2 Exclusion of candidate locus SD1 on chromosome 2q34-q36

Since there is a locus for type I syndactyly (SD1) on chromosome 2q34-q36, the malformation in Family 2 was checked for cosegregation with this region (Bosse et al. 2000; Ghadami et al. 2001). A significant negative LOD score (> 2.00 at $\alpha = 0.05$; Table 4-3) at the critical region for SD1 and throughout the long arm of chromosome 2 excluded the possibility of linkage with the malformation in Family 2.

Table 4-3: Two-point LOD scores between the phenotype and markers on chromosome 2q.

Phenotype	Locus	cM	Marker	Recombination fraction (%)						
				0.00	0.01	0.05	0.10	0.20	0.30	0.40
SD1	2q34-q36	118.16	D2S436	-8.60	-3.46	-1.59	-0.87	-0.34	-0.17	-0.09
		125.81	D2S410	-3.70	-1.19	-0.07	0.23	0.31	0.19	0.50
		134.45	D2S2215	-5.19	-1.11	0.06	0.41	0.49	0.33	0.12
		142.83	D2S114	-5.62	-1.57	-0.33	-0.60	0.25	0.20	0.10
		147.40	D2S442	-6.12	-1.79	-0.55	-0.12	0.12	0.13	0.06
		161.81	D2S418	-4.30	-1.07	-0.55	-0.41	-0.24	-0.09	-0.02
		173.00	D2S1776	-4.28	-1.05	-0.41	-0.19	-0.05	-0.02	-0.01
		186.21	D2S1391	-12.71	-6.06	-2.98	-1.71	-0.62	-0.17	0.00
		200.43	D2S1384	-5.14	-2.87	-1.28	-0.62	-0.12	0.03	0.06
		205.00	D2S1649*	-2.09	-1.94	-1.13	-0.68	-0.31	-0.15	-0.05
		210.43	D2S1345	-2.16	-1.12	-0.48	-0.21	0.00	0.06	0.05
		215.78	D2S434	-2.15	-1.12	-0.48	-0.23	-0.04	0.02	0.03
		227.00	D2S1363	-6.85	-2.56	-1.23	-0.70	-0.24	-0.05	0.01
		240.79	D2S1279	-8.92	-2.96	-1.10	-0.42	0.02	0.10	0.05
		250.54	D2S338	-9.18	-3.52	-1.57	-0.82	-0.23	-0.03	0.02
260.63	D2S125	-10.89	-4.80	-2.24	-1.24	-0.43	-0.14	-0.03		

* Microsatellite marker not present in Marshfield map

4.3.3 Genome-wide search

After the exclusion of the known SD1 locus, a genome-wide search was conducted using DNA of 17 subjects of this family. Six chromosomes yielded a LOD score ≥ 1 in the initial genome scan (Table 4-4). However, the only significant evidence of linkage was found at chromosome 3 with marker D3S2409 (two-point LOD score 3.36; $\theta = 0.00$).

Table 4-4: Microsatellite markers which produced a LOD score > 1 in the whole genome scan.

Chromosome	cM	Marker	LOD Score	Theta (?)
3	70.61	D3S2409	3.36	0.00
9	14.23	D9S2169	1.38	0.10
10	93.92	D10S1432	1.20	0.00
	100.92	D10S2327	1.10	0.00
12	160.68	D12S1045	1.10	0.10
15	78.92	D15S653	1.21	0.00
17	74.45	D17S809	1.09	0.10
	93.27	D17S2059	1.10	0.00

4.3.4 Fine mapping and locus identification on chromosome 3p21.31

Saturation mapping by a dense grid of microsatellite markers from chromosome 3p revealed a novel locus segregating with the disease in the Family 2 (Figure 4-10). A maximum two-point LOD score (Z_{max}) 4.18 was obtained with marker D3S3629 ($\theta = 0.00$; Table 4-5). Multipoint LOD score of 3.28 was obtained when analyses were conducted by breaking the pedigree due to computational constraints of software (Figure 4-13). Haplotype analysis disclosed key recombination events between marker Chr3_4919 and D3S2409 in individual IV-2, defining the telomeric boundary of the disease locus. The centromeric limit is determined by a crossover between marker D3S3629 and marker D3S2456, observed in the same subject (Figure 4-11). Therefore, the syndactyly locus lies within the <1 cM region delimited by Chr3_4919 and D3S2456 markers (Figure 4-12). It was observed that subject III-3 harbours no disease haplotype. Therefore it was assumed that this individual has a hand malformation not linked to 3p21.31. Analyses were also repeated by coding subject IV-3 as affected (Table 4-6).

Table 4-5: Two-point LOD scores between the phenotype and markers on chromosome 3p21.31.

CM	Marker	Recombination fraction (?)						
		0.00	0.01	0.05	0.10	0.20	0.30	0.40
61.52	D3S1768	-5.41	0.18	0.74	0.86	0.77	0.51	0.19
67.94	D3S3564	-6.51	-0.31	0.81	1.08	1.02	0.68	0.27
68.47	D3S3647	-5.02	0.45	0.98	0.86	0.52	0.52	0.15
68.48	D3S3597	-5.02	0.46	0.98	1.05	0.86	0.51	0.15
69.19	D3S3582	-6.78	-0.78	0.37	0.72	0.79	0.57	0.25
70.61	D3S3640	-5.02	0.56	0.82	1.10	1.07	0.79	0.43
70.61	D3S3729	1.82	1.79	1.66	1.50	1.16	0.81	0.42
70.61	D3S3560	1.44	1.41	1.32	1.20	0.94	0.66	0.35
70.61	Chr3_4919	-4.02	1.62	2.09	2.08	1.71	1.15	0.50
70.61	D3S2409	3.36	3.24	3.03	2.75	2.11	1.40	0.63
70.61	Chr3_4940	1.89	1.86	1.73	1.56	1.21	0.84	0.44
70.61	D3S3629*	4.18	4.11	3.80	3.44	2.62	1.73	0.78
70.61	D3S2456	-7.49	-1.36	-0.21	0.11	0.14	-0.06	-0.17
70.61	D3S3026	-7.99	-2.81	-1.44	-0.88	-0.39	-0.17	-0.05
71.41	D3S1289	-7.14	-0.94	0.27	0.62	0.71	0.55	0.29
78.64	D3S1766	-5.72	-2.44	-1.10	-0.55	-0.14	-0.04	-0.04

* The marker that yielded highest LOD score

Table 4-6: Revised two-point LOD scores when subject IV-3 was coded as affected.

CM	Marker	Recombination fraction (?)						
		0.00	0.01	0.05	0.10	0.20	0.30	0.40
70.61	Chr3_4919	-3.83	1.37	1.79	1.74	1.34	0.81	0.3
70.61	D3S2409	3.36	3.31	3.01	2.63	1.87	1.11	0.42
70.61	Chr3_4940	-1.13	-0.28	0.26	0.42	0.45	0.35	0.19
70.61	D3S3629	0.31	1.52	1.92	1.88	1.48	0.94	0.39
70.61	D3S2456	-8.51	-3.6	-1.72	-1.02	-0.48	-0.24	-0.08

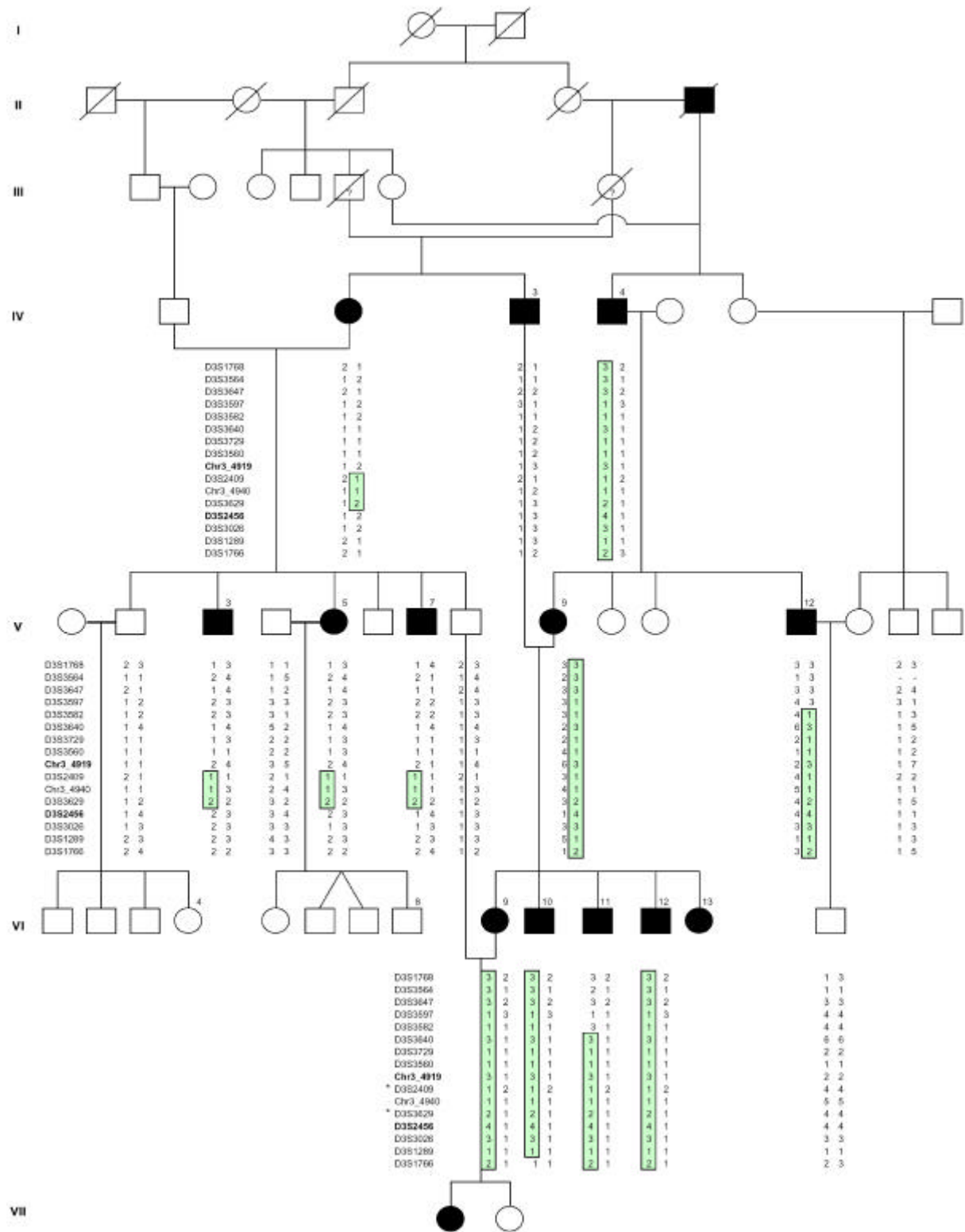


Figure 4-11: Haplotypes of the individuals in Family 2 for sixteen microsatellite markers from chromosome 3p21.31.

The shared haplotype in affected subjects segregating with the phenotype is shown in green. The individual IDs on the pedigree are the same as described in Fig. 2.4. A sign of (-) shows the alleles which were not typed due to technical/PCR problems.

* Typing for these markers is also shown in Figure 4-10.

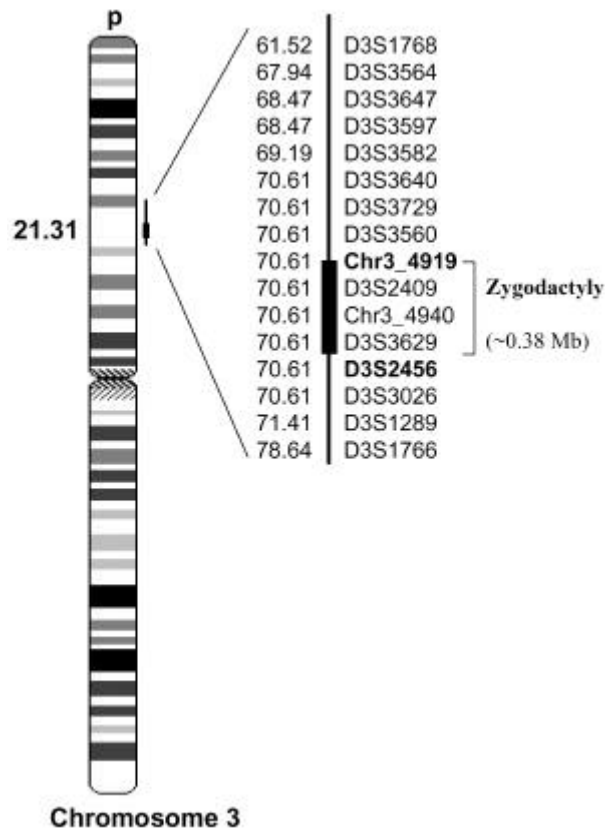


Figure 4-12: Genetic map of chromosome 3 markers used in the saturation mapping.

The marker-map positions (cM) are based on the sex-averaged map from the Center for Medical Genetics, Marshfield Medical Research Foundation or Genome Database (GDB). Markers flanking the syndactyly locus are shown in boldface.

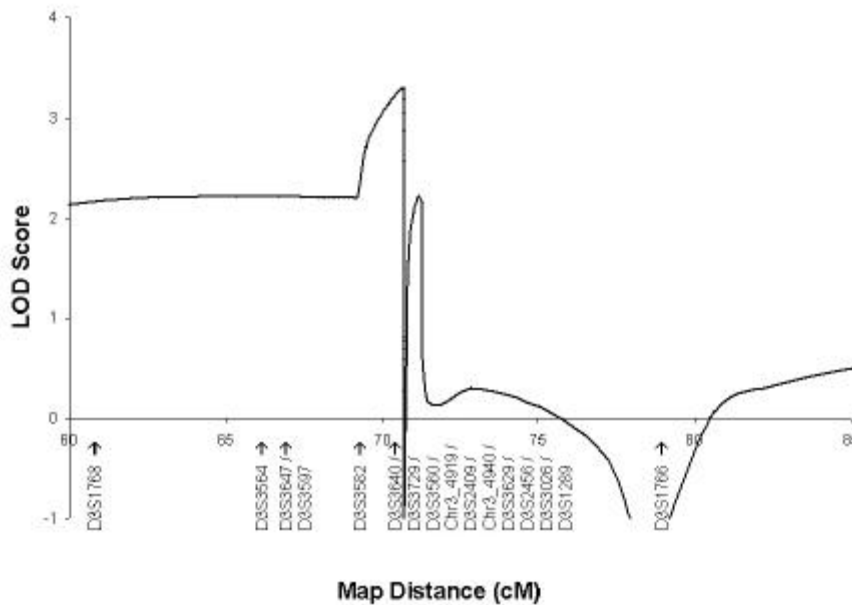


Figure 4-13: Multipoint LOD score analysis for region 3p21.31.

The multipoint linkage analysis localized the locus for zygodactyly between markers D3S3582 and D3S2456 with a LOD score of 3.28.

4.4 Family 3

4.4.1 Family with autosomal dominant syndactyly type II

Family 3 shows osseous fusion of 3rd and 4th fingers and synpolydactyly of toes. These features are characteristic for type II syndactyly or synpolydactyly (SPD) (Temtamy and McKusick 1978). The phenotype in Family 3 is similar to the affected subjects described in families by Cross et al. (1968), Temtamy and McKusick (1978) and Camera et al. (1995). However, no additional fingers were observed in the hands of the affected subjects in Family 3. A comparison of phenotype in Family 3 with other type II syndactyly families is given by a graphical method (Figure 4-14; based on METHODS section 3.5).

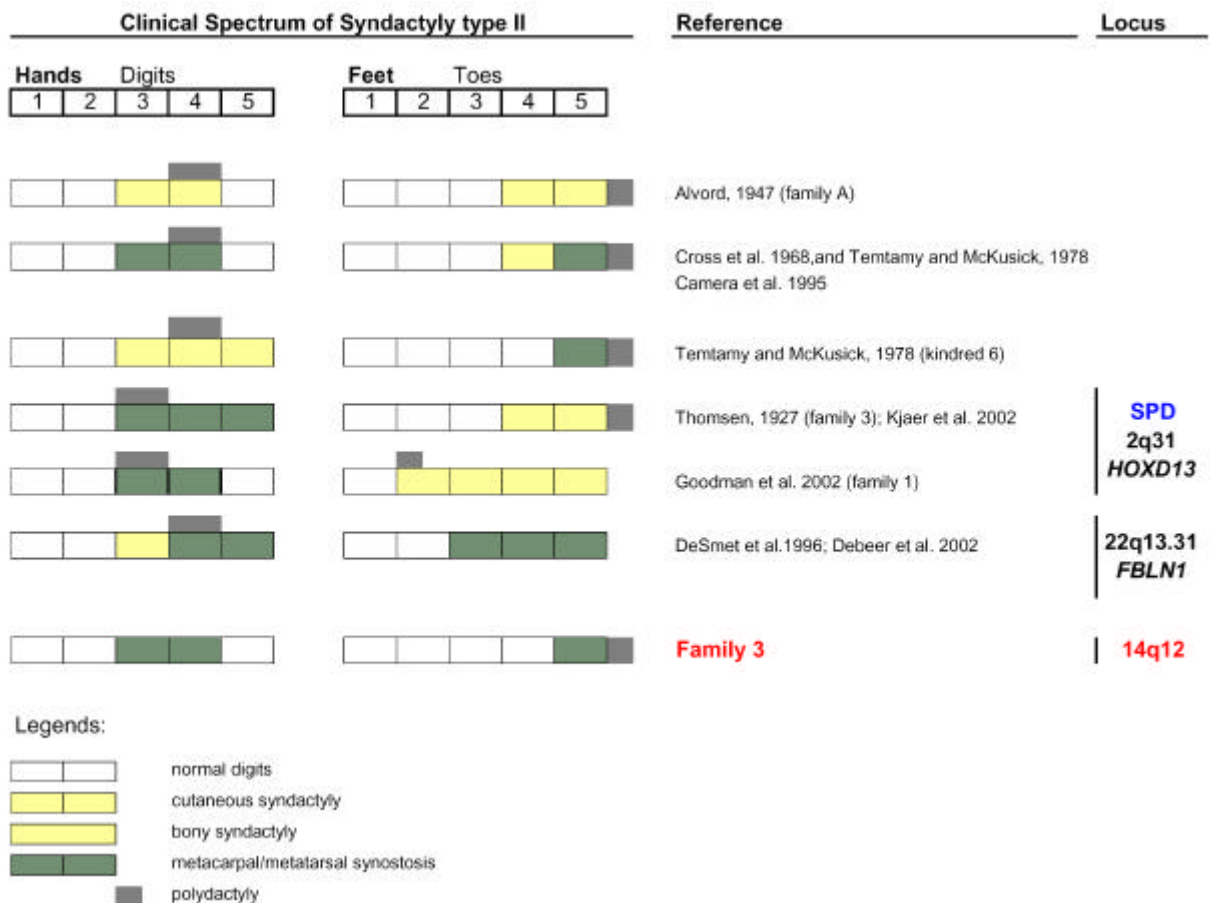


Figure 4-14: A graphical comparison of the phenotype in Family 3 with the phenotypes in other reported type II syndactyly families.

4.4.2 Exclusion of candidate genes *HOXD13* on chromosome 2q31 and *FBLN1* on chromosome 22q13.31

Since homeobox gene *HOXD13* on chromosome 2q31 is known to be mutated in type II syndactyly (SPD; Sarfarazi et al. 1995), the malformation in Family 3 was checked for cosegregation with this region. A significant negative LOD score (≈ -2.00 at $\alpha = 0.05$; Table 4-7) at the critical region for SPD excluded the possibility of linkage with the malformation in Family 3. Likewise, the malformation was also excluded from chromosome 22q13.31 harbouring *FBLN1*. The results showed that there is genetic heterogeneity for type II syndactyly beyond the known loci on chromosome 2q31 and 22q13.31.

Table 4-7: Two-point LOD scores between the phenotype and markers on chromosome 2q and 22q.

Chromosome 2				Recombination fraction (α)						
Phenotype	Locus	cM	Marker	0.00	0.01	0.05	0.10	0.20	0.30	0.40
SPD	<i>HOXD13</i> 2q31	125.81	D2S410	-10.21	-6.16	-3.51	-2.30	-1.16	-0.59	-0.24
		134.45	D2S2215	-12.41	-4.84	-2.31	-1.33	-0.56	-0.23	-0.07
		142.83	D2S114	-13.86	-4.71	-2.13	-1.13	-0.34	-0.06	0.02
		147.40	D2S442	-10.67	-2.43	-0.58	0.06	0.44	0.42	0.23
		149.89	D2S1326	-3.28	0.11	0.63	0.75	0.70	0.50	0.24
		161.81	D2S418	-4.43	-2.09	-0.89	-0.43	-0.09	0.00	0.01
		173.00	D2S1776	-7.30	-3.99	-2.03	-1.26	-0.59	-0.25	-0.06
		186.21	D2S1391	-2.16	-1.14	-0.53	-0.29	-0.11	-0.04	-0.01
		200.43	D2S1384	-4.56	-0.69	-0.07	0.11	0.16	0.09	0.02
		205.00	D2S1649*	1.42	1.40	1.29	1.14	0.83	0.51	0.23
		210.43	D2S1345	-4.04	-1.31	-0.31	0.19	0.25	0.13	0.02
		215.78	D2S434	2.20	2.16	1.98	1.75	1.27	0.79	0.34
		227.00	D2S1363	-10.21	-6.56	-3.30	-1.95	-0.79	-0.29	-0.07
		240.79	D2S206	-1.63	-0.62	-0.07	0.07	0.10	0.05	0.01
		240.79	D2S1279	-12.66	-7.79	-4.06	-2.49	-1.13	-0.52	-0.19
		250.54	D2S338	-12.60	6.58	-3.92	-2.75	-1.46	-0.73	-0.28
260.63	D2S125	-16.97	-8.36	-4.42	-2.81	-1.35	-0.62	-0.21		
Chromosome 22										
		28.57	D22S689	-6.92	-1.66	-0.52	-0.2	-0.11	-0.14	-0.1
	<i>FBLN1</i>	32.39	D22S685	-4.12	-1.08	-0.55	-0.13	0.09	0.08	0.04
	22q13.31	36.22	D22S683	-5.72	-3.27	-1.71	-1.05	-0.45	-0.16	-0.03

* Microsatellite marker not present in Marshfield map

4.4.3 Genome-wide search

After the exclusion of *HOXD13* a genome-wide search was conducted using DNA of 15 available subjects of this family. Five chromosomes yielded a LOD score ≥ 1 in the initial genome scan (Table 4-8). However, suggestive linkage was found for chromosomes 2q and 14q with markers D2S434 and D14S297 (two-point LOD scores ≥ 1.5 ; $\theta = 0.00$).

Table 4-8: Microsatellite markers which produced a LOD score > 1 in the whole genome scan.

Chromosome	cM	Marker	LOD Score	Theta (θ)
2q	205.00	D2S1649	1.42	0.00
	215.78	D2S434	2.20	0.00
10q	173.13	D10S169	1.20	0.00
14q	31.75	D14S297	1.58	0.00
15q	70.73	D15S650	1.27	0.01
22q	4.06	D22S420	1.40	0.00

4.4.4 Fine mapping and locus identification on chromosome 2q34-q36

Chromosomes 2q and 14q were selected for the saturation mapping by a dense grid of microsatellite markers. Saturation mapping on chromosome 2q34-q36 yielded a highest two-point LOD score (Z_{max}) 2.2 with microsatellite marker D2S434 ($\theta = 0.00$; Table 4-9). The LOD score in this genomic region could not be improved by saturation mapping. The haplotype analysis showed that this locus is not in total agreement with the phenotype (Figure 4-15). For instance, the haplotype is similar in the affected subject V-18 and the normal subject V-19 (Figure 4-15). Interestingly, this genomic region harbours a locus for type 1 syndactyly (SD1; 2q34-q36).

Table 4-9: Two-point LOD scores between the phenotype and markers on chromosome 2q34-q36.

cM	Marker	Recombination fraction (θ)						
		0.00	0.01	0.05	0.10	0.20	0.30	0.40
214.71	D2S301	1.05	1.03	0.92	0.79	0.53	0.30	0.11
214.71	D2S164	-3.36	-1.01	0.17	0.53	0.59	0.40	0.17
215.25	D2S1371	1.32	1.31	1.21	1.05	0.71	0.38	0.14
215.78	D2S295	-9.95	-4.78	-2.26	-1.27	-0.50	-0.20	-0.13
215.78	D2S2210	-4.19	-0.48	0.16	0.35	0.36	0.23	0.09
215.78	D2S434*	2.20	2.16	1.98	1.75	1.27	0.79	0.34
215.78	D2S2249	0.78	1.43	1.80	1.76	1.39	0.91	0.41
215.78	D2S173	-2.01	-0.92	-0.33	-0.13	-0.01	0.02	0.02
215.78	D2S2179	-3.22	-1.76	-0.58	-0.14	0.13	0.16	0.10
215.78	D2S104	-2.26	-0.11	0.41	0.51	0.43	0.25	0.08
216.31	D2S433	-1.92	-0.90	-0.33	-0.15	-0.07	-0.06	-0.04
215.78	D2S2244	-0.63	0.35	0.85	0.92	0.75	0.47	0.18
218.45	D2S1242	-4.36	-1.35	-0.22	0.12	0.21	0.12	0.02

* The marker that yielded highest LOD score

4.4.5 Fine mapping and locus identification on chromosomes 14q12

Fine mapping on chromosome 14q revealed a novel locus segregating with the malformation in Family 3 (Figure 4-16). A maximum two-point LOD score (Z_{max}) 3.4 was obtained by marker D14S1034 (Table 4-10). Multipoint LOD score of 3.19 was obtained when analyses were conducted by breaking the pedigree due to computational constraints of software (Figure 4-19). Haplotype analysis disclosed key recombination events between microsatellite markers D14S742 and D14S1280 in subjects IV-1 and IV-5, defining the telomeric boundary of the disease locus (Figure 4-17, Figure 4-18). The centromeric limit is determined by a crossover between microsatellite marker D14S121 and D14S1060, observed in the index subject IV-41. Therefore, the syndactyly locus lies within the ~22.97 cM region flanked by microsatellite markers D14S742 and D14S1060 (Figure 4-18). It was observed that subject V-34 harbours no disease haplotype. Therefore it was assumed to have a malformation not linked to 14q12. Analyses were conducted by coding subject V-34 as normal (Table 4-10).

Table 4-10: Two-point LOD scores between the phenotype and markers on chromosome 14q.

cM	Marker	Recombination fraction (?)						
		0.00	0.01	0.05	0.10	0.20	0.30	0.40
27.01	D14S1431	-5.90	-1.88	-0.11	0.44	0.64	0.49	0.24
28.01	D14S275	-3.03	-1.15	-0.53	-0.34	-0.23	-0.16	-0.08
28.01	D14S615	-5.29	-0.26	0.83	1.08	0.99	0.67	0.32
28.01	D14S608	2.40	2.35	2.15	1.89	1.37	0.86	0.38
28.01	D14S1042	1.96	1.91	1.67	1.39	0.87	0.42	0.11
28.01	D14S262	3.21	3.14	2.85	2.48	1.74	1.04	0.42
31.13	D14S975	1.65	1.60	1.43	1.21	0.78	0.41	0.14
31.75	D14S54	2.41	2.34	2.07	1.74	1.12	0.57	0.15
31.75	D14S1071	2.25	2.22	2.08	1.88	1.40	0.89	0.41
31.75	D14S1040	2.74	2.68	2.41	2.07	1.40	0.78	0.31
31.75	D14S1034*	3.40	3.33	3.04	2.66	1.89	1.12	0.44
31.75	D14S297	1.91	1.87	1.68	1.45	0.99	0.55	0.21
34.43	D14S121	1.47	1.43	1.29	1.11	0.77	0.46	0.20
34.43	D14S1060	-0.20	0.78	1.21	1.21	0.92	0.55	0.22
36.76	D14S741	-2.70	-1.00	0.07	0.38	0.45	0.31	0.15
44.06	D14S306	-9.65	-3.51	-1.62	-0.89	-0.26	-0.02	-0.05

* The marker that yielded highest LOD score

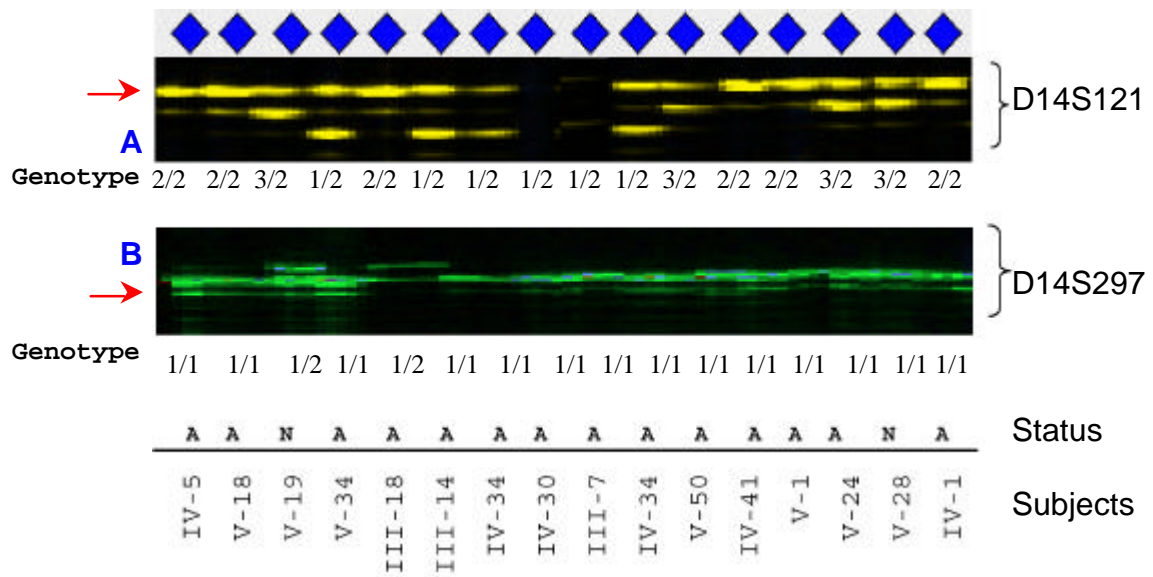


Figure 4-16: Electropherograms (A, B) of two microsatellite markers from chromosome 14q linked to malformation.

Red arrows indicate shared bands observed in all the affected subjects (A). In normal subjects (N) this band represents an allele introduced by married-in individuals. (A = affected; N = normal)

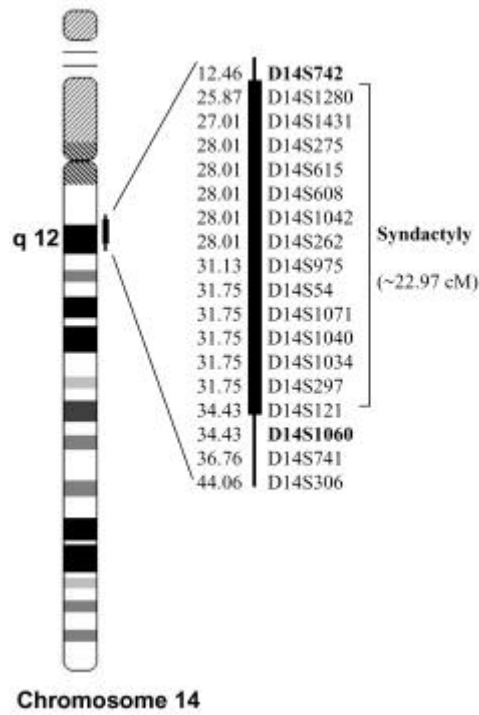


Figure 4-18: Genetic map of chromosome 14 used in the saturation mapping.

The marker-map positions (cM) are based on the sex-averaged map from the Center for Medical Genetics, Marshfield Medical Research Foundation or Genome Database (GDB). Markers flanking the syndactyly locus are shown in boldface.

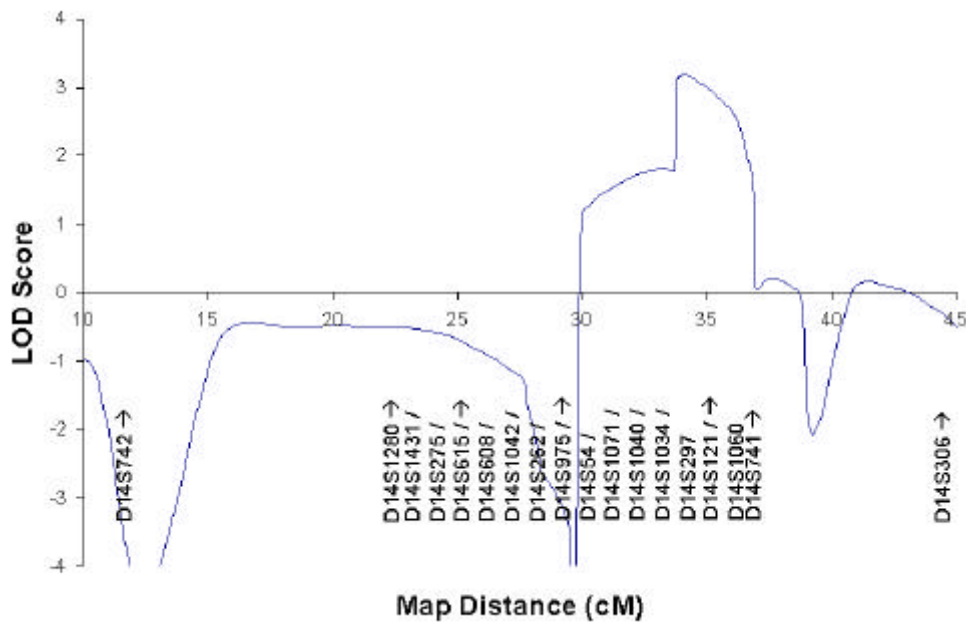


Figure 4-19: Multipoint LOD score analysis for region 14q12.

The multipoint linkage analysis localized the locus for synpolydactyly between markers D14S975 and D14S121 with a LOD score of 3.19.

5 Discussion

5.1 Genetic mapping in Pakistani families

In contrast to the European population the Pakistani population has unique socio-demographic features like stable communities within defined geographic regions, large sibships and a high consanguinity rate. Due to the coexistence of various linguistic and ethnic strata, marriages within families are strongly favored. In geographically remote and inaccessible areas the isolated tribal groups are inclined to marry within the family due to cultural and economic basis (Shami et al. 1989). In an inbred population existing in isolation over many generations without genetic interchange from other subpopulations, rare hereditary diseases and malformations, especially recessive, occasionally become frequent. Therefore, such inbred populations have long been subject of interest for both medical and population genetic studies.

Four large inbred Pakistani families (Fig. 2-1) with unidentified limb malformations and several affected individuals were ascertained by the help of local medical practitioners who approached the colleagues in the Department of Biological Sciences (Quaid-I-Azam University Islamabad) and the Department of Biology (Government College DG Khan). We reasoned that these large families may provide an excellent opportunity to localize the limb malformation in the human genome, to identify the underlying gene and hence, to get to know the underlying pathomechanisms of the malformations. Therefore, these families were visited at their places of residence in order to get permission from the head of the families to conduct a clinical and molecular study. In each family affected and normal subjects were examined to categorize the limb malformation. In order to infer the correct genealogy and the inheritance pattern, an extended pedigree was drawn in each case with the help of the elders of the family. Information was obtained regarding intermarriages, deceased subjects and associated defects.

5.2 Phenotyping and diagnosis

In order to identify the limb phenotypes segregating in the Pakistani families clinical features were documented during the fieldwork. Intrafamilial phenotypic variability was carefully noted. Detailed photographs and X-rays were obtained for the correct diagnosis of the limb malformations. Information was also obtained about the subjects

who had undergone surgical treatment for limb malformation. Since in all four families the hallmark of the malformation was a fusion of fingers and toes without any associated defects, the initial clinical impression was that the malformations could be classified into the non-syndromic syndactylies.

Since it is important in a clinical and molecular study to establish strict diagnostic criteria for the phenotype in question, the phenotype assignment must be done in a rigorously consistent fashion. Especially in a linkage study, even a few misassigned phenotypes may have major negative implications on the analyses, leading to both false positive and/or false negative results. For instance, given the recombination fraction (?) of 0.01 and an estimated misclassification rate of 10%, twice as much data must be sampled to obtain the same power of analysis as would be needed if no misclassification existed (Ott 1992). Therefore, to categorize the syndactylies, a protocol was designed which allows simple and smooth classification of the syndactylies in the Pakistani families. In this thesis, three of the four clinically investigated families are described.

5.2.1 Protocol for the syndactyly classification

In order to use the existing classification of syndactylies but to simplify the clinical typing I have designed a protocol (see section 3.5) using the syndactyly literature from 1910-2003. After an exhaustive review of 60 publications 104 different index cases, with and without other affected family members, were ascertained. Seventy-eight cases were selected for the test trail of this protocol. In 71 cases I came to the same conclusion as the original investigators, which proved that my protocol is effective. Using this protocol the different syndactyly types are simple to understand and their minor differences are easy to record in clinics or visiting the patient and his family at home. It is straightforward to define the phenotype of a family and it takes a small amount of time to categorize the malformation, saving the need to extensively explore the literature beforehand. Scoring can be done at a glance immediately in the counseling session by complementing the diagram with photographs and roentgenograms and the whole clinical spectrum within a family can be typed accordingly. More sophisticated typing might be necessary in a second step. Although the protocol shows both hands and both feet in one graph, in some instances it might be more appropriate to document them separately.

With the help of the protocol, the clinical typing of the Pakistani families with syndactylies was straightforward. The phenotype in family 2 is consistent with type I syndactyly (subtype 1; Fig. 4-9; Malik et al. 2005c). The clinical picture in Family 3 was found to be compatible with type II syndactyly (synpolydactyly; Fig. 4-13). The protocol revealed that the unique autosomal recessive phenotype in Family 1 is not in complete agreement with any of the previously described syndactyly types. Therefore, a ninth type of syndactyly was introduced into the international literature (Fig. 4-4), extending the present systematics of syndactyly. I have proposed to name this novel phenotype **mesoaxial synostotic syndactyly with phalangeal reduction (MSSD, type IX syndactyly, Malik-Percin type)**, and it has been introduced to the international scientific community with this title (Malik et al. 2005b). A more detailed description of the families is given in sections 5.9.

5.3 Inheritance of limb malformations

Clustering of several affected subjects within a family is highly suggestive of a hereditary condition. Hereditary diseases, especially recessive, occasionally become frequent in inbred populations. In the case of syndactyly the diagnosis is made by clinical examination only. The mode of inheritance is easy to infer by drawing the pedigree and observing the transmission to the family members and then deciding whether it is compatible with autosomal dominant or autosomal recessive inheritance. In Family 1 all the affected subjects are the product of consanguineous loops and all parents have normal phenotypic status, thus making an autosomal recessive inheritance the most likely explanation. Occasionally, in highly inbred families the underlying mode of inheritance of the phenotype is difficult to judge. For instance, a homozygous affected individual mates with someone who is heterozygous for the same gene by virtue of descent from a common ancestor, thus giving an impression of an autosomal dominant inheritance. In this case the transmission of an autosomal recessive trait mimicks a dominant pattern and is therefore called pseudodominant inheritance. There was no evidence of pseudodominant transmission of the limb malformations in the described Pakistani families.

Similarly, an autosomal dominant inheritance may be easily overlooked in inbred families and the homozygous status of a dominant gene may remain undetected. Autosomal dominant conditions may show incomplete penetrance, resulting in skipped generations with unaffected, obligate carriers. The transmission of the limb phenotype

in Family 2 and 3 is consistent with autosomal dominant inheritance, since the affected subjects have at least one affected parent and there is equal affected male-to-female ratio. There is no evidence of incomplete penetrance or skipped generations. There are several instances of male-to-male transmission making an autosomal dominant the most likely inheritance pattern. In addition, autosomal dominant conditions depict variability in the degree of phenotypic expression. Family 2 shows type I syndactyly and the phenotype varies from unilateral, minor 2nd and 3rd toe webbing to bilateral complete 2nd and 3rd toe webbing resulting in the fusion of nails. Family 3 depicts type II syndactyly and the phenotype varies from bony fusion of 3rd and 4th fingers to an addition of a mesoaxial bony element within the osseous web. Intrafamilial variability of the phenotype may be due to factors such as epistasis, mosaicism or genetic heterogeneity. In summary, inheritance patterns of rare phenotypes may be difficult to infer in inbred populations and occasionally only the results of molecular haplotype study may give the correct answer. However, in certain instances the findings in molecular haplotyping may lead to confusing results, as discussed in more details for Family 3 (section 5.11).

5.4 Collection of biological material

Before undertaking a linkage study, it is critical to know whether the available pedigree information and the number of individuals is sufficient to allow the detection of the locus underlying the trait of interest. If the family is not large enough then several small families with an identical clinical presentation are recruited for a linkage study, with the assumption that a similar mutated gene is segregating with the malformation in all families. The selection of individuals for genotyping is crucial for a successful linkage study. It depends heavily on the family structure, availability of the subjects and the inheritance pattern of the malformation (i.e. disease model). In case of an autosomal dominant pedigree each informative meiosis leads to an addition of 0.3 in the maximum likelihood of linkage (i.e. LOD score), while for an autosomal recessive pedigree each affected genotyped subject contributes 0.6 in the LOD score. Therefore, minimum of twelve subjects are needed to map a phenotype in a family with an autosomal dominant transmission and six subjects are required to achieve a highly significant evidence of linkage (i.e. LOD score, $Z_{\max} \geq 3.00$) in a family with an autosomal recessive mode of inheritance.

To perform a genome screen, a relatively large and consistent amount of DNA is required. Usually such a supply is obtained through the collection of whole blood in

small amounts (5—10 ml). The villages of the Pakistani families presented in this thesis are situated in remote areas, which are not easily accessible. It was not practical to revisit the family several times especially due to harsh weather conditions and this is why I tried to collect as many blood samples as possible during the initial visit to each family. Another reason for sampling as many individuals as possible was that the laboratory work was intended to be conducted abroad. A large number of samples will assure a successful linkage study and a positive check on the linkage results. All biological material was collected after informed consent by the head of the family according to the Helsinki II declaration.

5.5 Approach to a genome screen

In recent years, there has been success in localizing genes of autosomal dominant and autosomal recessive phenotypes in inbred and isolated populations, since they offer many advantages for genome-wide mapping studies. For the recessive disorders, appearing in inbred sibships, molecular studies using the homozygosity mapping strategy are readily feasible. In this approach, affected individuals can be used for mapping under the assumption that each of them is homozygous for the markers linked to the disease locus.

In Family 1, with an autosomal recessive syndactyly, I have combined the strategy of homozygosity mapping with the candidate gene approach. Previously identified regions for syndactylies on chromosome 2q34-q36, 2q31 and 6q21, were selected to check for homozygosity. After excluding these chromosomal regions, in a second step the phenotype of the family was checked for linkage with candidate genes for limb development (i.e. *SHH*, *GLI3*, *BMP4*, *FORMIN*, *GREMLIN*, *FGF4*). Finally, a genome-wide screening approach was conducted, in which I attempted to cover the entire human genome using markers evenly spaced across the human genetic map.

For Family 2 and 3, consistent with autosomal dominant mode of inheritance, I have conducted the candidate gene approach in order to check whether any of the candidate loci (i.e. chromosome 2q34-q36, 2q31 and 6q21) or genes (i.e. *SHH*, *GLI3*, *BMP4*, *FORMIN*, *GREMLIN*, *FGF4*) segregates with the phenotypes in these families. In autosomal dominant families, I looked for one shared haplotype segregating in all the affected subjects which surrounds the gene in question. The same haplotype should not segregate in any of the normal subjects of the family.

After the initial evidence of linkage emerged in a family, the locus was confirmed by fine mapping. A dense grid of microsatellite markers was used within a specified genomic interval and all family members were typed. Fine mapping finally led to define and pinpoint the disease locus in all three families.

5.6 Genotyping

A conventional genome-wide study involves genotyping with highly polymorphic di-, tri- or tetranucleotide repeat microsatellites markers, which are highly informative, randomly distributed throughout the genome, segregate in Mendelian fashion and are easy to type through PCR. Dinucleotide repeat microsatellite markers, quite often, are difficult to type due to their “smear nature” in the PCR. Therefore, tri- and tetranucleotide repeat markers are generally favored, because they are more reliable, easy to score and, in many cases, show higher heterozygosity and informativeness. For instance, the latest version of the genome screening sets (set # 14) of Marshfield (Center for Medical Genetics, Marshfield, USA), contains 95% tri- and/or tetranucleotide microsatellite repeat markers. For the fine mapping, the selection of microsatellite markers is limited by their availability within the candidate regions. Sometimes, a highly informative microsatellite marker in one population might prove to be homozygous in other population and thus yields no inheritance information. Therefore, in fine mapping an effective strategy is to employ a combination of di-, tri- and tetranucleotide repeat microsatellite markers. For the genotyping of the Pakistani families, I used a panel of 360 markers for the genome-wide screen. During saturation mapping, additional 80 microsatellite markers were employed in various candidate regions, roughly 12 markers for each region.

In this study, the detection and scoring of microsatellite marker alleles was performed on a semi-automated system of ABI 377 automated sequencer (Applied Biosystems). This system uses a separation gel of 2 mm in thickness, which allows to overcome the problems of unsmooth lane running and band-shifts like in the conventional polyacrylamide gels. Fragment analyses were performed by using GeneScan and Genotyper software packages, which is a highly precise and sensitive method. This software is able to discriminate even one base pair differences in fragment sizes, especially in dinucleotide repeat markers, which are hard to analyse in normal polyacrylamide gels. In the conventional polyacrylamide vertical gels with ethidium bromide or silver staining the exact allele sizes cannot be detected because the

fragments are analysed only by visual inspection. In this study, a control individual from the CEPH database (Centre d'Etude du Polymorphisme Humain, France) was always genotyped with each microsatellite marker in order to standardize the allele sizes.

Various research institutes offer commercial genotyping services, ranging from genotyping of candidate regions to genome-wide searches (Microsatellite Center, Berlin; Genotyping Resource Center, Rockefeller University). These services can save time and labour, but on the other hand one does not have the opportunity to learn the methodology. Additionally, these services are expensive. Since I intended to get experience in the laboratory techniques and the hardware and software handling, therefore, I decided to perform each and every single step myself.

5.7 Data management

Data management is vital to the success in genotyping and in the subsequent stages of linkage analysis. It is especially important in the genome-wide screen of large pedigrees, where the number of genotypes required for the analysis will be in hundreds. The task of data management includes the description of the phenotype of each family member and the handling of photographs and X-rays, as well as pedigree information and sometimes further clinical tests. It also includes data storage and backup for subsequent use and effective retrieval. During my study, the field observations were recorded in an electronic word-processing file. The pedigree data and the status information of each individual was managed and recorded using Cyrillic 2.1.3. The genotyping data obtained from the allele-calling procedure of Genotyper software was directly transferred into a spreadsheet for linkage analyses and permanent storage.

To avoid errors and bias of ascertainment myself and a second researcher performed fragment analyses and scoring of the microsatellite markers. The genotyping errors were identified and removed through a multistage approach. Fragment sizes were compared with gels and fluorograms to avoid allele size disparity. This method enables to effectively mitigate the genotyping errors, which emerge during electrophoresis, lane-extraction method of GeneScan software and allele-calling procedure of Genotyper software. Such errors are more common in case of dinucleotide repeat microsatellite markers. Genotypic incompatibilities and Mendelian inconsistencies were identified by

employing PedCheck software (O'Connell and Weeks 1998), and by using the UNKNOWN program of LINKAGE software package (Lathrop et al. 1984).

5.8 Linkage analysis

5.8.1 Two-point LOD score analysis

Linkage refers to the tendency of alleles from two loci to segregate together in a family if they are located physically close to each other on a chromosome. LOD score analysis is a likelihood-based parametric or model based approach to find the evidence for linkage and to estimate the recombination fraction (θ). The LOD score represents \log_{10} of the ratio for two likelihoods, the likelihood of observing a particular configuration of a trait and a marker locus in a family assuming linkage (i.e. $\theta < 0.5$), and the likelihood of observing the same configuration of the two loci within the same family assuming no linkage (i.e. $\theta = 0.5$; Ott 1999). This ratio is referred to as a two-point LOD score (or pair-wise LOD score), since it involves linkage between only two loci (i.e. a disease locus and a marker locus). LOD score analysis is statistically more powerful than any nonparametric method (e.g. association studies). It utilizes every family member's phenotype and genotype information. For the estimation of maximum likelihood (Z_{\max}), LOD scores are calculated and reported at recombination fractions (θ) of 0.00—0.40. In my study, all families were relatively large and inbred with various consanguineous loops, which restricted the straightforward computation of LOD scores. Therefore, inbreeding loops were broken to conduct the two-point analyses. Untyped individuals were removed from the pedigree due to the computational and memory constraints of the linkage softwares (UNKNOWN, MLINK). I have conducted two-point analysis with all the microsatellite markers genotyped in three families. Two-point LOD scores were calculated against all the recombination fractions (θ) from 0.00—0.40.

Maximizing LOD score depends on number of parameters: mode of inheritance, disease allele frequency, family structure, penetrance, phenocopy rate, and marker allele numbers and frequencies. In parametric analysis, misspecifying the disease gene frequency leads to minor penalty in the maximum LOD score (Pal et al. 2001). In my analyses I assumed a disease allele frequency of 0.001 for the autosomal recessive syndactyly family and 0.0001 for autosomal dominant syndactyly family. Microsatellite marker allele frequencies were taken either from Marshfield human diversity panel or assumed to be equal. In fine mapping, the allele frequencies can be calculated from the family founders, especially when no prior estimate of allele frequencies is available and the pedigree is sufficiently large or several families are analysed together. The impact of changing allele frequencies decreases with increasing pedigree size. In this study, the

allele frequencies of the linked alleles were not allowed to be less than 0.1 to avoid overstated evidence of linkage caused by underestimation of marker allele frequencies.

5.8.2 Haplotyping

Haplotype is a linear, ordered arrangement of alleles on a chromosome. Haplotype analysis is a conventional method to identify the disease segregating chromosome in a family. It is useful in identifying the ancestral chromosome and the recombination events which define the candidate interval of the trait. I have performed haplotype analysis with the help of SIMWALK software (Sobel and Lange 1996). Option 46.1 in the batch file was used to obtain vertical haplotypes. Final haplotypes were drawn with the pedigree in Excel (Microsoft 2000) after manual checking.

5.8.3 Multipoint analysis

Multipoint LOD score analysis is an extension of two-point analysis in which linkage of a disease trait is tested not to just one marker, but to an entire map of markers. There are several advantages of multipoint LOD score analysis. First, it provides an opportunity to impute the genotype information at an original uninformative locus via haplotype information. Thus the linkage results are less sensitive to the uninformative or missing genotype at any single marker. In essence, multipoint analysis can extract more of the total inheritance information from the pedigree. Second, it can be very useful to pinpoint a disease gene location in the fine mapping of a Mendelian disorder (Ott 1999). However, if all the meioses are informative in a pedigree then the multipoint analyses cannot yield a higher LOD score.

In my study, the multipoint analyses were not straightforward due to the large family size and large number of markers. Although, there are softwares which allow multipoint computation in large families (e.g. SIMWALK; Sobel and Lange 1996), they do not provide exact estimation of LOD scores. Therefore, I have split the families into reasonable sizes to conduct multipoint computation by GENEHUNTER software (Kruglyak et al. 1996). Breaking the pedigree into pieces and the removal of the founder subjects from the first generation resulted in loss of inheritance information. Consequently the multipoint analyses in Family 1 and 2 showed a decrease in LOD score, in comparison to the two-point analysis (Figure 4-8; Figure 4-13).

5.9 Family 1: Autosomal recessive mesoaxial synostotic syndactyly with phalangeal reduction (MSSD) maps to chromosome 17p13.3

Malik S, Arshad M, Amin-Ud-Din M, Oeffner F, Dempfle A, Haque S, Koch MC, Ahmad W, Grzeschik K-H (2004) A novel type of autosomal recessive syndactyly: clinical and molecular studies in a family of Pakistani origin. *Am J Med Genet* 126A:61-67

Malik S, Percin FE, Ahmad W, Percin S, Akarsu NA, Koch MC, Grzeschik K-H (2005b) Autosomal Recessive Mesoaxial Synostotic Syndactyly with Phalangeal Reduction Maps to Chromosome 17p13.3. *Am J Med Genet* (in press)

The phenotype in Family 1 is not in complete agreement with any of the described eight known syndactylies. All affected subjects are the product of consanguineous loops, making an autosomal recessive inheritance the most likely explanation. The OMIM catalogue [<http://www.ncbi.nlm.nih.gov/Omim/>] documents 109 entries for autosomal recessive syndactylies. All except Cenani-Lenz syndactyly (MIM 212780) are reported to be syndromic conditions. Cenani-Lenz type is a ‘total’ digit syndactyly with extensive metacarpal and carpal fusions, often accompanied by partial or complete radio-ulnar synostosis, culminating in a sort of spoon-like hand. The feet are usually mildly affected (Cenani and Lenz 1967). This makes Family 1 phenotypically distinct from Cenani-Lenz type.

Family 1 shows a distinctive phenotypic manifestation and has minimal overlap of clinical features with syndactylies type I, II, III and V. The defect is predominantly mesoaxial and more severe than syndactylies of type I (SD1). Involvement of the index fingers and first toes in the web is an extremely rare finding in SD1, as pointed out by Bosse et al. (2000). Since the classical feature of type II syndactyly the mesoaxial polydactyly is missing in all 5 affected members, it almost rules out this type. No family member shows any craniofacial symptoms like type III syndactyly, but it overlaps with this condition by showing involvement of mesoaxial skeletal rays. Syndactyly type V is also excluded because of its postaxial involvement of digits and occasional association of brachydactyly and camptodactyly (Temtamy and McKusick 1978; Robinow et al. 1982).

Since minimal overlap with the clinical features of known syndactylies was observed in this family, the phenotypic status might represent an allelic variant of one of the previously described types. Therefore, the phenotype of the family was checked for cosegregation with one of the known loci for syndactylies. Using a panel of highly

polymorphic microsatellite markers, the phenotype was excluded from the critical regions of syndactyly type I (2q34-q36), type II (2q36) and type III (6q22-q23) (Table 4-1). Thus, the clinical impression of the phenotype not fitting into syndactyly type I, II and III has been proven by the exclusion of established candidate gene loci. Genome-wide search with 360 microsatellite markers revealed that the phenotype maps to chromosome 17p. Homozygosity was observed in all the affected subjects for the microsatellite markers selected from chromosome 17p13.3 (Figure 4-6).

A literature search showed that the phenotype of Family 1 resembles three affected subjects in a Turkish family (Percin et al. 1998). Since it is an inbred family and the three affected subjects have normal parents, the most likely mode of inheritance is autosomal recessive. I have included this Turkish family in my study. The field work, the blood collection and the typing of microsatellite markers were performed at the Cumhuriyet University Research Center, Sivas, Turkey. Linkage analysis was done at the Institute of Human Genetics, Philipps University Marburg, Germany. The data of the Turkish family is presented in Figure 5-1 and Table 5-1, in comparison with Family 1. The phenotype of the Turkish family was checked for linkage with the microsatellite markers on chromosome 17p under an autosomal recessive model. Genotyping proved that the three family members (51, 55, 57; Figure 5-1) with a complex hand-foot phenotype, similar to the individuals in Family 1, are homozygous for a cosegregating segment in the critical region on 17p. Two recombination events in individuals 51 and 55 place the disease locus distal to marker D17S831 (Figure 5-1). Thus, in the Turkish family the homozygous region is flanked by markers D17S1866 and D17S831 (Figure 5-1). A maximum two-point LOD score of 1.89 was obtained for marker D17S1533 in the Turkish family ($\alpha = 0.00$; Table 5-1).

When both families (Family 1 and Turkish family) were analysed together, a maximum two-point LOD score (Z_{\max}) of 4.97 was obtained at marker locus D17S695 ($\alpha = 0.00$; Table 5-1). The homozygous region in both families spans between markers D17S643 and D17S831 with a critical interval of 6.6 cM. The identification of a single locus for a complex hand foot malformation in two inbred families with distinct ethnic backgrounds gives evidence for a new form of autosomal recessive syndactyly. I have proposed to name this phenotype **mesoaxial synostotic syndactyly with phalangeal reduction (MSSD)**, respectively type IX syndactyly, Malik-Percin type.

In addition, an autosomal dominant 2nd and 3rd toe webbing without hand malformation is segregating in nine family members of the Turkish family (Percin et al. 1998). This phenotype is a hallmark of type I syndactyly, which has been mapped to the SD1 locus on chromosome 2q34-q36 (Bosse et al. 2000; Ghadami et al. 2001). Therefore, the 2nd and 3rd toe phenotype of the Turkish family was checked for cosegregation with the SD1 locus. The most informative microsatellite marker, D2S2382, excluded the disease phenotype for at least 8.9 cM outside the critical region (exclusion area = 0.089 at $Z_{\max} ? -2$; Table 5-2). The 2nd and 3rd toe webbing was excluded from chromosome 17p13.3 locus under an autosomal dominant model. It is evident that subjects with 2nd and 3rd toe webbing are missing the disease haplotype for 17p (e.g. individual 56; Figure 5-1). Therefore, it is concluded that two different syndactyly types with different inheritance patterns are segregating in the Turkish family: an autosomal recessive type IX syndactyly which localises on chromosome 17p13.3, and an autosomal dominant type I syndactyly, which is neither linked to chromosome 2q34-q36 (SD1) nor to 17p13.3 (MSSD).

The candidate region of homozygosity on 17p contains a number of genes, but none of these have previously been associated with developmental defects in humans or mice (e.g. *YWHAE*, MIM 605066; *SKIP*, MIM 607875; *MYO1C*, MIM 606538). The most likely candidate within the critical interval was *ROX*, which codes for a MAX-binding protein (*ROX*, MIM 603039), which is part of MAX complexes. These complexes are known to be involved in transcriptional regulation, cell differentiation and proliferation. Other candidates were *CT120* and *LOST1*, both close to *ROX*. Mutation screening of these three genes was conducted in two affected individuals (V-9, V-1) and one normal subject (IV-1) of Family 1. No mutation was observed within the coding regions of these three genes.

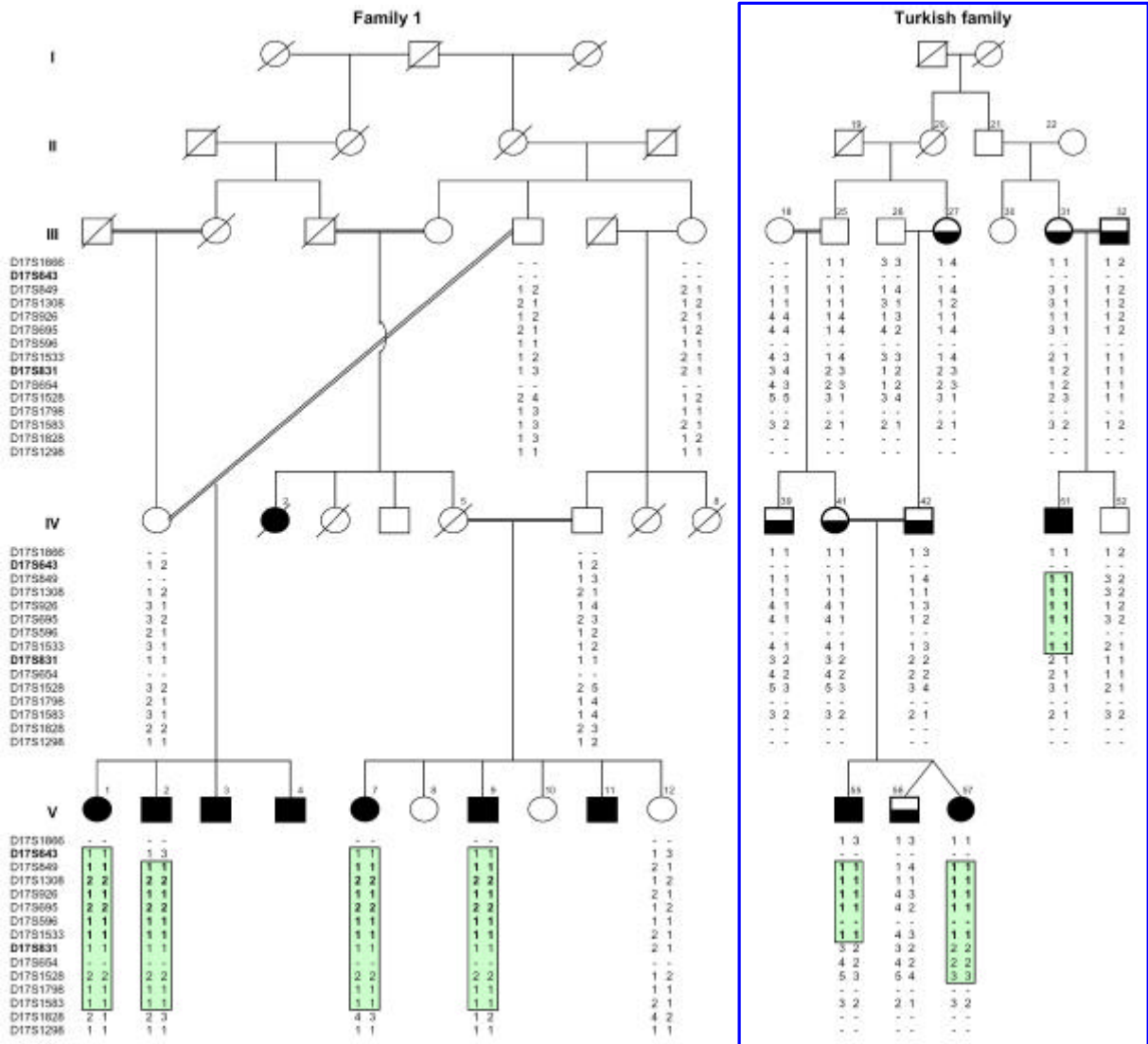


Figure 5-1: Haplotypes for fifteen microsatellite markers from chromosomal region 17p13.3 in Family 1 and the Turkish family.

The homozygous region segregating in both families is shown by allele numbers in boldface. In the Turkish pedigree the solid symbols show subjects with the autosomal recessive phenotype of type IX syndactyly. Half shaded symbols represent subjects with autosomal dominant 2nd and 3rd toe webbing. A sign of (-) shows markers which have not been typed.

Table 5-1: Two-point LOD scores between type IX syndactyly and microsatellite markers on chromosome 17p13.3 in Family 1 and the Turkish family.

Marker	Family 1				Turkish family
	Recombination fraction (?)				
	0.00	0.01	0.05	0.10	0.00
D17S1866	-	-	-	-	-1.06
D17S643	-0.05	0.91	1.32	1.27	-
D17S849	2.78	2.72	2.45	2.11	0.63
D17S1308	2.38	2.31	2.06	1.74	0.19
D17S926	3.38	3.28	3.00	2.59	1.54
D17S695	3.15	3.08	2.79	2.42	1.82
D17S596	1.65	1.62	1.51	1.35	-
D17S1533	2.48	2.41	2.16	1.84	1.89
D17S831	2.01	1.96	1.75	1.49	-0.99
D17S654	-	-	-	-	-0.96
D17S1528	3.47	3.39	3.08	2.69	-0.81
D17S1798	1.92	1.90	1.77	1.58	-
D17S1583	3.28	3.22	2.91	2.53	-0.9
D17S1828	-7.31	-5.53	-3.27	-2.06	-
D17S1298	0.84	0.82	0.76	0.67	-

Table 5-2: Two-point LOD scores between 2nd and 3rd toe syndactyly and the candidate loci on chromosomes 2q34-q36 and 17p13.3 in the Turkish family.

Exclusion area was determined according to the recombination fraction (cM) at which the LOD score was ≤ -2 .

Locus	Marker	CM	Recombination fraction (?)				Exclusion (cM)
			0.00	0.01	0.05	0.10	
Chromosome 2							
2q34-q36	D2S2382	213.49	-4.89	-4.02	-2.34	-1.49	6.03
	D2S301	214.71	-4.07	-2.56	-1.34	-0.81	2.00
	D2S173	215.78	-3.71	-2.59	-1.64	-1.11	3.00
	D2S163	218.45	-4.88	-3.86	-2.23	-1.43	6.03
	D2S344	219.52	-4.77	-3.64	-2.26	-1.14	6.54
Chromosome 17							
17p13.3	D17S695	3.67	-3.87	-1.54	-0.35	0.04	1.00
	D17S1533	3.99	-3.77	-1.45	-0.24	0.15	1.00
	D17S1528	6.60	-3.82	-1.53	-0.34	0.03	1.00

5.10 Family 2: Zygodactyly maps to chromosome 3p21.31

Malik S, Schott J, Ali SW, Oeffner F, Amin-ud-Din M, Ahmad W, Grzeschik K-H, Koch MC (2005c) Evidence for clinical and genetic heterogeneity of syndactyly type I: the phenotype of second and third toe syndactyly maps to chromosome 3p21.31. *Eur J Hum Genet* (submitted)

Based on clinical observation type I syndactyly can be divided into at least four different subtypes. The most frequent subtype, and probably the most prevalent form of all syndactylies, is characterized by bilateral webbing of 2nd and 3rd toe without hand anomalies. The inheritance of the phenotype is autosomal dominant and was originally named zygodactyly (Schofield 1921; Weidenreich 1923; Stiles and Hawkins 1946; Penrose 1946; Alvord 1947; Grebe 1964). Later, it became accepted to use the term zygodactyly as a synonym for type I syndactyly (Tematamy and McKusick 1978; Percin et al. 1998). No locus is known for this subtype.

The second subtype is characterized by bilateral cutaneous 3rd and 4th finger, and 2nd and 3rd toe webbing. More severely affected family members may have additional fingers and toes involved, even with bony impairment (Thomsen 1927; Lucken 1939; Grebe 1964; Tematamy and McKusick 1978; Ghadami et al. 2001). The dominant phenotype was mapped to chromosome 2q34-q36 in a large German family originally described by Lucken in 1939 (Bosse et al. 2000). The gene locus was subsequently confirmed in an Iranian family and was designated as syndactyly type I locus (SD1; Bosse et al. 2000; Ghadami et al. 2001).

The other two subtypes are very rare and no gene loci are known for them. The hallmark of the third subtype is bilateral cutaneous or bony webbing of 3rd to 4th finger and occasionally of 3rd to 5th finger. Feet are not involved and the inheritance is autosomal dominant (Montagu 1953; Grebe 1964; Hsu 1965). The fourth subtype (bilateral cutaneous webbing of 4th and 5th toe) was mentioned in an epidemiological study from Brazil (Castilla et al. 1980). Since neither a detailed clinical description of the phenotype nor the inheritance was given by the authors, the status of subtype four remains uncertain. A phenotypic comparison of the four subtypes is presented in Figure 4-9 as a simplified graph (Malik et al. 2005a).

Apart from clinical evidence that subtype 1 and 2 are two distinct phenotypes, the molecular proof came from a linkage study in a Turkish family with autosomal

dominant zygodactyly, which was excluded from the SD1 locus (section 5.9; Malik et al. 2005b). Additional molecular evidence came from the exclusion of the SD1 locus for the zygodactyly phenotype segregating in Family 2 (Table 4-3). Finally, the zygodactyly phenotype segregating in a German family was also excluded from the SD1 locus (LOD score < -2.00; Table 5-3). The exclusion of the SD1 locus in three ethnically different families with zygodactyly confirmed that there is clinical and genetic heterogeneity for type I syndactyly. These results also established that within type I syndactyly, subtype 1 (i.e. zygodactyly) is a distinct entity from subtype 2 (3rd and 4th finger, and 2nd and 3rd toe webbing).

The genome-wide search in Family 2 revealed that the zygodactyly phenotype is linked to chromosome 3p21.31 (Z_{\max} LOD score = 4.18; Table 4-5). It is the first locus for zygodactyly, and a second locus for type I syndactyly. It was observed that the affected subject (IV-3) in the Family 2 has no disease haplotype (Figure 4-11). Therefore, the zygodactyly phenotype in this subject is not linked to chromosome 3p21.31. Only his wife (V-9) transmits the disease haplotype to four of the affected offsprings (VI-9—12). It is unknown whether the affected subject VI-13 in the same sibship harbors maternal or paternal haplotype, because the individual was not blood sampled for her young age (3 years).

Interestingly, zygodactyly segregating in the German family was excluded from chromosome 3p21.31 (LOD score < -2.00; Table 5-4; Figure 5-2). The exclusion of chromosome 3p21.31 in the German family reinforces the observation that zygodactyly is genetically heterogeneous. These findings have proved that zygodactyly is in itself genetically heterogeneous and has at least two types: one type maps to chromosome 3p21.31, while the other is not linked to chromosome 3p21.31. I therefore, propose to refer to chromosome 3p21.31 locus as ZD1 (i.e. zygodactyly 1). On the account of the high prevalence of zygodactyly in most populations I expect the discovery of several loci. Finally, it would also be interesting to verify whether subtype 3 (i.e. webbing of 3rd and 4th finger without feet malformation) and subtype 4 (i.e. webbing of 4th and 5th toe) are linked either to SD1 (2q34-q36) or ZD1 (3p21.31). Based on my clinical understanding I expect genetic heterogeneity for subtype 3 and 4.

This novel locus brings us a step further towards molecular genetic delineation of this heterogeneous condition. There is no promising limb phenotype or candidate gene

mapped in this region in humans or mice. In zygodactyly the digit number and shape remain unaffected. The defect appears in the final step of separation and spacing of digits. Therefore, in case of zygodactyly I expect an underlying gene involved in the interdigital cell death (Zuzarte-Luis and Hurle 2002).

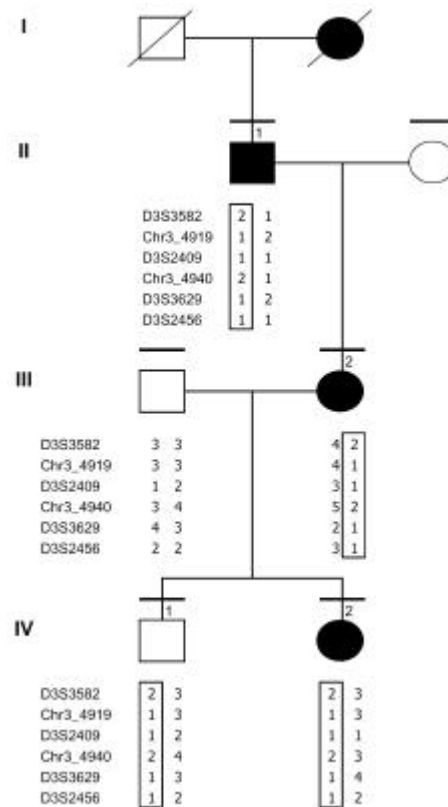


Figure 5-2: Pedigree of the German family with autosomal dominant zygodactyly showing the haplotypes of 6 microsatellite markers on chromosome 3p.

Horizontal bars on symbols denote individuals who were physically examined. The vertical bars indicate the ancestral haplotype, which is transmitted to both grand children.

Table 5-3: Pairwise LOD scores between the zygodactyly phenotype in the German family and the microsatellite markers on chromosome 2q34-q36 (SD1 locus).

cM	Marker	Recombination Fraction (?)						
		0.00	0.01	0.05	0.10	0.20	0.30	0.40
200.43	D2S1384	-2.30	-1.36	-0.71	-0.44	-0.19	-0.07	-0.02
205.00	D2S1649	-2.30	-1.36	-0.71	-0.44	-0.19	-0.07	-0.02
210.43	D2S1345	-2.30	-1.36	-0.71	-0.44	-0.19	-0.07	-0.02
215.78	D2S434	-2.30	-1.36	-0.71	-0.44	-0.19	-0.07	-0.02
227.00	D2S1363	0.30	0.29	0.26	0.21	0.13	0.06	0.02

Table 5-4: Pairwise LOD scores between the zygodactyly phenotype in the German family and the microsatellite markers on chromosome 3p21.31 (ZD1 locus).

cM	Marker	Recombinatin Fraction (?)						
		0.00	0.01	0.05	0.10	0.20	0.30	0.40
69.19	D3S3582	-2.39	-1.36	-0.71	-0.44	-0.19	-0.07	-0.01
70.61	Chr3_4919	0.30	0.29	0.27	0.25	0.20	0.14	0.07
70.61	D3S2409	-2.39	-1.36	-0.71	-0.44	-0.19	-0.07	-0.01
70.61	Chr3_4940	-2.39	-1.36	-0.71	-0.44	-0.19	-0.07	-0.01
70.61	D3S3629	-2.39	-1.36	-0.71	-0.44	-0.19	-0.07	-0.01
70.61	D3S2456	-2.39	-1.36	-0.71	-0.44	-0.19	-0.07	-0.01

5.11 Family 3: Synpolydactyly (SPD) maps to chromosome 14q12

Among all syndactyly types, type II syndactyly or synpolydactyly (SPD) was the first to be localized on chromosome 2q31 (Sarfarazi et al. 1995). Polyalanine expansion mutations in the homeotic gene *HOXD13* were observed in families with SPD (Muragaki et al. 1996; Goodman et al. 1997). Subsequently, a number of reports verified these findings (Table 5-5). Since there is no evidence of change in expansion size within families even over six generations, there is a highly significant increase in penetrance and severity of the phenotype (genetic anticipation) with increasing expansion size. The remarkable correlation between the phenotype and the expansion size suggests that expansion of the polyalanine tract leads to a specific gain of function in the mutant *HOXD13* protein, and has interesting implications for the role of polyalanine tracts in the control of transcription (Goodman et al. 1997).

Table 5-5: Mutational spectrum in the reported families with synpolydactyly (SPD).

Phenotype	Locus	Gene	Mutation	Reference
SPD	2q31	<i>HOXD13</i>	21—30-bp duplications	Muragaki et al. 1996
SPD	2q31	<i>HOXD13</i>	27-bp duplication	Akarsu et al. 1996
SPD	2q31	<i>HOXD13</i>	21—42-bp duplications	Goodman et al. 1997
SPD with novel foot malformation	2q31	<i>HOXD13</i>	Del. 323—336bp exon 1; del 834bp exon 2	Goodman et al. 1998
SPD	2q31	<i>HOXD13</i>	27-bp duplication	Kjaer et al. 2002
Severe digital anomalies	2q31	<i>HOXD13</i>	Missense R31W	Debeer et al. 2002
SPD	2q31	<i>HOXD9-HOXD13, EVX2</i>	117-kb microdeletion	Goodman et al. 2002
3/3'4 synpolydactyly	22q13.3	<i>FBLN1</i>		Debeer et al. 2002

The affected subjects in Family 3 show mesoaxial syndactyly of hands with an additional mesoaxial digital element within the web. Additionally, there is postaxial synpolydactyly of feet. This phenotype is consistent with synpolydactyly (SPD) or syndactyly type II. *HOXD13* gene on chromosome 2q31 was a likely candidate for this

phenotype in Family 3, but the linkage results excluded this gene locus (LOD score < -2 ; Table 4-7). Therefore, a candidate gene approach was conducted, which excluded linkage between the synpolydactyly phenotype and the candidates of limb development (i.e. *SHH*, *GLI3*, *BMP4*, *FORMIN*, *GREMLIN*, *FGF4*). A genome-wide search showed five chromosomes with a LOD score > 1 . Finally, the subsequent fine mapping established two loci with an evidence of linkage. There is one locus on chromosome 14q12 (LOD score Z_{\max} 3.40; Table 4-10) with a disease interval of about 23 cM segregating with the phenotype (Figure 4-17), and possibly, a second locus on chromosome 2q34-q36 (LOD score 2.2; Table 4-9). Interestingly, chromosome 2q34-q36 harbours a candidate locus for type I syndactyly (SD1) which shows quite a different phenotype from the synpolydactyly phenotype segregating in Family 3 (Bosse et al. 2000).

Therefore, the question arises: is there a main locus for the synpolydactyly in Family 3 on chromosome 14q12 and a modifier locus on chromosome 2q34-q36? The most likely candidate locus for the syndactyly phenotype in this family is the 14q12 region, since it depicts a highly significant evidence of linkage with a LOD score of 3.40. This score is supported by fourteen subjects of the family. The affected subject V-34 does not contribute to the score because he does not harbour the 14q12 haplotype (Figure 4-17). The most likely explanation is, that the syndactyly phenotype in this subject is not linked to chromosome 14q12 and it localizes elsewhere. Therefore, this subject represents a phenocopy and gives evidence of further genetic heterogeneity of the phenotype. Since the parents of this subject were not genotyped, an autosomal recessive nature of his phenotype cannot be excluded.

The locus on chromosome 2q34-q36 segregates in one loop of three generations in Family 3 (i.e. descendants of III-14 and III-18; Fig. 4-14), while in other parts of the pedigree the haplotype is segregating in subjects scattered in the pedigree. Therefore the segregation of this locus is not straightforward. Moreover, the suggestive linkage is the result of only one marker (i.e. D2S343, LOD score 2.2; Table 4-9) and might be due to chance alone due to the inbred nature of the pedigree.

To adequately answer the question if there is a main and a modifier locus it is important to revisit the family. Phenotypes of affected and seemingly normal subjects have to be ascertained again together with the haplotype findings. It is also crucial to sample

missing subjects, especially to add more normal individuals of the family and to review the pedigree structure for undetected inbreeding loops. Alternatively, more families with a similar phenotypic presentation might be recruited which could confirm the linkage findings in Family 3.

5.12 Outlook

In this study I have localized syndactyly malformations in three Pakistani families to three different loci. In two families (Family 1, 3), the candidate interval is rather large (~5 and ~23 cM) and contains a number of genes. There are no limb phenotypes or known genes of limb development mapped in these regions or in the homologous regions in mice. Therefore, in these two families the search for the underlying causative genes is not straightforward. An optimal way to proceed might be to sample more affected and normal subjects from these families in order to find recombinants, which may narrow down the candidate intervals. I am also looking for collaborations with international groups interested in limb development, who may have access to families with similar limb phenotypes. New families might have individuals with critical recombination events and therefore might help to refine the disease interval to get closer to the ultimate gene identification. The analysis of the fourth family is under way, and it is expected that for this family yet another locus will be identified.

For the three families I expect the discovery of three unique genes in different molecular cascades, since the syndactyly phenotype in each family is specific. In Families 1 and 3, the malformation appears at the metacarpal level and disrupts the digit number and identity. In mice, the digit number and identity (thumb vs. little finger/big toe vs. little toe) is thought to be regulated by *Shh* from the zone of polarizing activity (ZPA), a region of specialized mesenchymal cells next to the posterior boundary of the bud. Digit identity depends on the distance from the polarizing region: the most posterior digit (i.e. little finger/little toe) forms next to the polarizing region, whereas the most anterior digit (i.e. thumb/big toe) forms furthest away. Digit number is related to the width of the bud, which depends on the length of the apical ectodermal ridge (AER). Few of the *Shh* target genes have been discovered (*Gli3*, *dHand*, *Formin*, *Gremlin* and *Bmps*), and they are expressed in the mesenchyme. Indirect targets of *Shh* include *Fgf4*, *Fgf9* and *Fgf17*, which are expressed in posterior AER. The initial positional information of digit identity is subsequently interpreted and refined by other factors (i.e. *Hox* code) that influence the size and number of digits. In Families 1 and 3, the above named genes have been excluded, which means that there must be unknown factors responsible for digit number and identity during limb development. These unknown factors may be directly or indirectly involved in the *Shh* pathway. Furthermore, in Families 1 and 3 it may well be that two different mutated proteins are somehow connected in a similar

molecular pathway. These proteins may result in diverse phenotypes when mutated alone. On the other hand, mutations in *HOXD13* are implicated in synpolydactyly phenotype. Since the phenotype in Family 3 is very close to the subjects with mutations in *HOXD13* it might well be that the underlying gene in Family 3 is a part of *HOXD13* regulation.

In Family 2 with zygodactyly, I expect the identification of a gene which is responsible for digit separation in the final stages of limb development. The basis for spacing the digits is to establish digital vs. interdigital areas. The initial divergence between digital and interdigital regions in an alternating fashion is achieved by different programmes of cell differentiation. In the digital areas chondrogenesis takes place while the interdigital areas show apoptosis. Members of the TGF β superfamily, along with their receptors, and intracellular transducers control the choice between digital and interdigital fates in the autopod. Apoptosis helps to sculpt the limb by freeing digits. In Family 2, I expect that the underlying gene might be regulating an apoptotic mechanism. Since in a zygodactyly phenotype hands are never involved the candidate gene is expected to show a hind-limb-specific expression pattern.

5.13 Summary

Non-syndromic syndactyly is a common, heterogeneous hereditary condition of webbed fingers and/or toes. It has a prevalence of 3 per 10,000 births. The malformation can be unilateral or bilateral, and the fusion within the web may be cutaneous or bony. Phenotypic variability exists not only between affected individuals, but also within individuals. Nine different types have been described majority of which show autosomal dominant mode of inheritance, except Cenani-Lenz type (type VII) and Malik-Percin syndactyly (type IX) which segregate as autosomal recessive entities. Syndactyly shows failure to achieve a normal limb development, more precisely, the malformation affects the digits number, identity and separation in the last developmental cascades.

In this thesis I report on the clinical and molecular data as well as gene localizations in three large Pakistani families with non-syndromic syndactylies.

- ?? I have categorized these families according to the existing syndactyly classification.
- ?? I have proposed a clinical protocol which helps to use the existing systematics of syndactyly, and on the other hand simplifies the clinical typing of this malformation.
- ?? For the first time I report on a family with a novel autosomal recessive hand/foot malformation with mesoaxial synostotic syndactyly (Family 1). In order to classify this type, I have extended the existing syndactyly systematics and have proposed a new name for this novel syndactyly: mesoaxial synostotic syndactyly with phalangeal reduction (MSSD); type IX syndactyly, Malik-Percin type. This term was introduced into the international literature. Through a genome-wide study with highly polymorphic microsatellite markers and linkage analysis, I have localized this unique autosomal recessive syndactyly phenotype on chromosome 17p13.3 with a disease interval of ~5 cM.
- ?? By my own experience of phenotyping limb defects in different families and by reviewing the international literature I propose that type I syndactyly has at least four subtypes. I have established that zygodactyly in Family 2, the most common subtype, has a locus on chromosome 3p21.31 with a critical interval of

~0.38 Mb. Additionally, I provide molecular evidence of further genetic heterogeneity within zygodactyly. Considering the high prevalence of zygodactyly in all populations I expect, that diverse loci are responsible for the phenotype and therefore I expect more loci.

?? Since *HOXD13* gene has been excluded in Family 3, therefore, I have good evidence that syndactyly type II is genetically heterogeneous. A genome-wide search has depicted that the phenotype in this family is mapped on chromosome 14q12 and might have a modifier locus on chromosome 2q34-q36.

The discovery of three novel loci for syndactylies will significantly help in the clinical and genetic delineation of this complex limb malformation. It will be of tremendous help to the families with limb malformations seeking genetic advice. The ultimate elucidation of the underlying genes might increase our understanding of limb development, especially in the context of getting insight into the developmental cascades of digit number, identity and separation.

6 Abbreviations

AgNO ₃	Silver nitrate
APS	Ammonium peroxodisulfate
ATP	Adenosintriphosphate
bp	base pair
cDNA	complementary DNA
CEPH	Centre d'Etude du Polymorphisme Humain, France
cM	centi Morgan
DMSO	Dimethyl sulfoxide
DNA	Deoxyribonucleic acid
dNTP	Deoxynucleotidetriphosphate
EDTA	Ethylenediaminetetraacetic acid
Fig	Figure
for	forward
g	gram
HCL	Hydrochloric acid
HPLC	High Performance Liquid Chromatography
kb	kilo bases
LOD	Logarithm of Odds
M	Molar
Mb	Mega base pair
MgCl ₂	Magnesium chloride
mRNA	messenger Ribonucleic acid
MSSD	mesoaxial synostotic syndactyly
NaCl	Sodium chloride
Na ₂ CO ₃	Sodium Carbonate
ng	nanogram
OD	Optical density
Oligos	Oligonucleotides
OMIM	Online Mendelian Inheritance in Man (online catalogue)
PCR	Polymerase chain reaction
pmol	picomol

r	reverse
RNA	Ribonucleic acid
SDS	Sodium Dodecyl Sulfate
SSCA	Single-stranded conformational analysis
<i>Taq</i>	Polymerase isolated from <i>Thermus aquaticus</i>
TBE	Tris-Borate-EDTA
TE	Tris-EDTA buffer
TEMED	Tetramethylethylene diamine
Tris	Tri-hydroxymethyl aminomethane
U	Unit
UV	Ultra violet
V	Voltage
ver	version
w/v	weight/volume

7 References

- Akarsu AN, Akhan O, Sayli BS, Sayli U, Baskaya G, Sarfarazi M (1995) A large Turkish kindred with syndactyly type II (synpolydactyly). 2. Homozygous phenotype? *J Med Genet* 32:435-441
- Akarsu AN, Stoilov I, Yilmaz E, Sayli BS, Sarfarazi M (1996) Genomic structure of *HOXD13* gene: a nine polyalanine duplication causes synpolydactyly in two unrelated families. *Hum Mol Genet* 5:945-952
- Albrecht AN, Schwabe GC, Stricker S, Boddreich A, Wanker EE, Mundlos S (2002) The synpolydactyly homolog (spdh) mutation in the mouse -- a defect in patterning and growth of limb cartilage elements. *Mech Dev* 112:53-67
- Alvord RM (1947) Zygodactyly and associated variations in a Utah family. *J Hered* 38:49-53
- Anneren G, Amilon A (1994) X-linked recessive fusion of metacarpals IV and V and hypoplastic metacarpal V. *Am J Med Genet* 52:248-250
- Bacchelli C, Goodman FR, Scambler PJ, Winter RM (2001) Cenani-Lenz syndrome with renal hypoplasia is not linked to *FORMIN* or *GREMLIN*. *Clin Genet* 59:203-205
- Bell J (1953) On syndactylies and its association with polydactyly. In: *The treasury of human inheritance*. Cambridge University Press, pp 33-50
- Bosse K, Betz RC, Lee Y-A, Wienker TF, Reis A, Kleen H, Propping P, Cichon S, Nöthen MM (2000) Localization of a gene for syndactyly type 1 to chromosome 2q34-q36. *Am J Hum Genet* 67:492-497
- Brickell PM, Tickle C (1989) Morphogens in chick limb development. *Bioessays* 11:145-159
- Brueton LA, Huson SM, Farren B, Winter RM (1990) Oculodentodigital dysplasia and type III syndactyly: separate genetic entities or disease spectrum? *J Med Genet* 27:169-175
- Camera G, Camera A, Pozzolo S, Costa M, Mantero R (1995) Synpolydactyly (type II syndactyly) with aplasia/hypoplasia of the middle phalanges of the toes: report on a family with eight affected members in four generations. *Am J Med Genet* 55:244-246
- Castilla EE, Paz JE, Orioli-Parreiras IM (1980) Syndactyly: frequency of specific types. *Am J Med Genet* 5:357-364
- Cenani A, Lenz W (1967) Totale Syndaktylie und totale radioulnare Synostose bei zwei Brüdern. Ein Beitrag zur Genetik der Syndaktylien. *Ztschr Kinderheilk* 101:181-190
- Collette DT (1954) A case of syndactylism of the ring and little finger. *Am J Hum Genet* 6:241:243
- Cottingham RW, Jr., Idury RM, Schäffer AA (1993) Faster sequential genetic linkage computations. *Am J Hum Genet* 53:252-263
- Cross HE, Lerberg DB, McKusick VA (1968) Type II syndactyly. *Am J Hum Genet* 20:368-380

- De Smet L, De Beer P, Fryns JP (1996) Cenani-Lenz syndrome in father and daughter. *Genet Couns* 7:153-157
- De Smet L, Mulier T, Fabry G (1994) Syndactyly of the ring and small finger. *Genet Couns* 5:45-49
- De Smet L, Winnepeninckx B, Fryns JP, Fabry G (1992) Cenani-Lenz type of syndactyly: a complex type of syndactyly with multiple synostoses. *Genet Couns* 3:145-147
- Debeer P, Schoenmakers EF, Twal WO, Argraves WS, De Smet L, Fryns JP, Van De Ven WJ (2002) The fibulin-1 gene (*FBLN1*) is disrupted in a t(12;22) associated with a complex type of synpolydactyly. *J Med Genet* 39:98-104
- Debeer PH, De Smedt M, Fryns JP (2004) Sporadic case of bilateral fusion of metacarpal 4 and 5. *Am J Med Genet* 125A:214-215
- Dodinval P (1979) Oligodactyly and multiple synostoses of the extremities: two cases in sibs. A variant of Cenani-Lenz syndactyly. *Hum Genet* 48:183-189
- Drohms D, Lenz W, Yang TS (1976) Totale Syndaktylie mit mesomeler Armverkürzung, radioulnären und metacarpalen Synostosen und Disorganisation der Phalangen ("Cenani-Syndaktylie"). *Klin Pädiatr* 188:359-365
- Elcioglu N, Atas M, Cenani A (1997) Dermatoglyphics in patients with Cenani-Lenz type syndactyly: studies in a new case. *Am J Med Genet* 70:341-5
- Ganan Y, Macias D, Duterque-Coquillaud M, Ros MA, Hurler JM (1996) Role of TGF beta s and BMPs as signals controlling the position of the digits and the areas of interdigital cell death in the developing chick limb autopod. *Development* 122:2349-2357
- Ghadami M, Majidzadeh-A K, Haerian B-S, Damavandi E, Yamada K, Pasallar P, Najafi MT, Nishimura G, Tomita H-A, Yoshiura K-I, Niikawa N (2001) Confirmation of genetic homogeneity of syndactyly type 1 in an Iranian family. *Am J Med Genet* 104:147-151
- Gillessen-Kaesbach G, Majewski F (1991) Bilateral complete polysyndactyly (type IV Haas). *Am J Med Genet* 38:29-31
- Gladwin A, Donnai D, Metcalfe K, Schrandt-Stumpel C, Brueton L, Verloes A, Aylsworth A, Toriello H, Winter R, Dixon M (1997) Localization of a gene for oculodentodigital syndrome to human chromosome 6q22-q24. *Hum Mol Genet* 6:123-127
- Goldstein DJ, Kambouris M, Ward RE (1994) Familial crossed polysyndactyly. *Am J Med Genet* 50:215-223
- Goodman F, Giovannucci-Uzielli ML, Hall C, Reardon W, Winter R, Scambler P (1998) Deletions in *HOXD13* segregate with an identical, novel foot malformation in two unrelated families. *Am J Hum Genet* 63:992-1000
- Goodman FR, Majewski F, Collins AL, Scambler PJ (2002) A 117-kb microdeletion removing *HOXD9-HOXD13* and *EVX2* causes synpolydactyly. *Am J Hum Genet* 70:547-555
- Goodman FR, Mundlos S, Muragaki Y, Donnai D, Giovannucci-Uzielli ML, Lapi E, Majewski F, McGaughan J, McKeown C, Reardon W, Upton J, Winter RM, Olsen BR, Scambler PJ (1997) Synpolydactyly phenotypes correlate with size of expansions in *HOXD13* polyalanine tract. *Proc Natl Acad Sci USA* 94:7458-7463

- Grebe H (1964) Syndaktylien. In: Humangenetik, Ein kurzes Handbuch in fünf Bänden. Georg Thieme Verlag, Stuttgart, pp 297-304
- Grzeschik KH (2002) Human limb malformations; an approach to the molecular basis of development. *Int J Dev Biol* 46:983-991
- Gutmann DH, Zackai EH, McDonald-McGinn DM, Fischbeck KH, Kamholz J (1991) Oculodentodigital dysplasia syndrome associated with abnormal cerebral white matter. *Am J Med Genet* 41:18-20
- Haas SL (1940) Bilateral complete syndactylism of all fingers. *Am J Surg* 50:363-366
- Habighorst LV, Albers P (1965) Familiaere synostosis metacarpi IV und V. *Z Orthop Ihre Grenzgeb* 100:521-525
- Holmes LB, Wolf E, Miettinen OS (1972) Metacarpal 4-5 fusion with X-linked recessive inheritance. *Am J Hum Genet* 24:562-568
- Hsu CK (1965) Hereditary syndactylia in a Chinese family. *Chin Med J* 84:482-485
- Johnston O, Kirby VV, Jr. (1955) Syndactyly of the ring and little finger. *Am J Hum Genet* 7:80-82
- Kan SH, Johnson D, Giele H, Wilkie AO (2003) An acceptor splice site mutation in *HOXD13* results in variable hand, but consistent foot malformations. *Am J Med Genet* 121A:69-74
- Kjaer KW, Hedeboe J, Bugge M, Hansen C, Friis-Henriksen K, Vestergaard MB, Tommerup N, Opitz JM (2002) *HOXD13* polyalanine tract expansion in classical synpolydactyly type Vordingborg. *Am J Med Genet* 110:116-121
- Kong A, Gudbjartsson DF, Sainz J, Jonsdottir GM, Gudjonsson SA, Richardsson B, Sigurdardottir S, Barnard J, Hallbeck B, Masson G, Shlien A, Palsson ST, Frigge ML, Thorgeirsson TE, Gulcher JR, Stefansson K (2002) A high-resolution recombination map of the human genome. *Nat Genet* 31:241-247
- Kruglyak L, Daly MJ, Reeve-Daly MP, Lander ES (1996) Parametric and nonparametric linkage analysis: a unified multipoint approach. *Am J Hum Genet* 58:1347-1363
- Lathrop GM, Lalouel JM, Julier C, Ott J (1984) Strategies for multilocus linkage analysis in humans. *Proc Natl Acad Sci USA* 81:3443-3446
- Lerch H (1948) Erbliche Synostosen der Ossa metacarpalia IV und V. *Z Orthop* 78:13-16
- Lindsten T, Ross AJ, King A, Zong WX, Rathmell JC, Shiels HA, Ulrich E, Waymire KG, Mahar P, Frauwirth K, Chen Y, Wei M, Eng VM, Adelman DM, Simon MC, Ma A, Golden JA, Evan G, Korsmeyer SJ, MacGregor GR, Thompson CB (2000) The combined functions of proapoptotic Bcl-2 family members bak and bax are essential for normal development of multiple tissues. *Mol Cell* 6:1389-1399
- Litingtung Y, Dahn RD, Li Y, Fallon JF, Chiang C (2002) Shh and Gli3 are dispensable for limb skeleton formation but regulate digit number and identity. *Nature* 418:979-983
- Lonardo F, Della Monica M, Riccardi G, Riccio I, Riccio V, Scarano G (2004) A family with X-linked recessive fusion of metacarpals IV and V. *Am J Med Genet* 124A:407-410
- Lucken KG (1939) Über eine Familie mit Syndaktylie. *Z Konstit -Lehre* 22:152-159

- Malik S, Ahmad W, Grzeschik K-H, Koch MC (2005a) A simple method for characterising syndactyly in clinical practice. *Genet Couns* (in press)
- Malik S, Arshad M, Amin-Ud-Din M, Oeffner F, Dempfle A, Haque S, Koch MC, Ahmad W, Grzeschik KH (2004) A novel type of autosomal recessive syndactyly: clinical and molecular studies in a family of Pakistani origin. *Am J Med Genet* 126A:61-67
- Malik S, Percin FE, Ahmad W, Percin S, Akarsu NA, Koch MC, Grzeschik K-H (2005b) Autosomal Recessive Mesoaxial Synostotic Syndactyly with Phalangeal Reduction Maps to Chromosome 17p13.3. *Am J Med Genet* (in press)
- Malik S, Schott J, Ali SW, Oeffner F, Amin-ud-Din M, Ahmad W, Grzeschik K-H, Koch MC (2005c) Evidence for clinical and genetic heterogeneity in syndactyly type I: the phenotype of second and third toe syndactyly maps to chromosome 3p21.31. *Eur J Hum Genet* (submitted)
- Merlob P, Grunebaum M (1986) Type II syndactyly or synpolydactyly. *J Med Genet* 23:237-241
- Meroni G, Reymond A, Alcalay M, Borsani G, Tanigami A, Tonlorenzi R, Nigro CL, Messali S, Zollo M, Ledbetter DH, Brent R, Ballabio A, Carrozzo R (1997) Rox, a novel bHLHZip protein expressed in quiescent cells that heterodimerizes with Max, binds a non-canonical E box and acts as a transcriptional repressor. *Embo J* 16:2892-2906
- Miyata T (1911) Über einen seltenen Fall von Syndaktylie. *Z Orthop Chir* 29:257-262
- Montagu MF (1953) A pedigree of syndactylism of the middle and ring fingers. *Am J Hum Genet* 5:70-72
- Mukhopadhyay N, Almasy L, Schroeder M, Mulvihill WP, Weeks DE (1999) Mega2. a data-handling program for facilitating genetic linkage and association analyses. *Am J Hum Genet* 65:A436
- Muragaki Y, Mundlos S, Upton J, Olsen BR (1996) Altered growth and branching patterns in synpolydactyly caused by mutations in *HOXD13*. *Science* 272:548-551
- Nezarati MM, McLeod DR (2002) Cenani-Lenz syndrome: report of a new case and review of the literature. *Clin Dysmorphol* 11:215-218
- Niswander L, Jeffrey S, Martin GR, Tickle C (1994) A positive feedback loop coordinates growth and patterning in the vertebrate limb. *Nature* 371:609-612
- O'Connell JR, Weeks DE (1998) PedCheck: a program for identification of genotype incompatibilities in linkage analysis. *Am J Hum Genet* 63:259-266
- Ott J (1992) Strategies for characterizing highly polymorphic markers in human gene mapping. *Am J Hum Genet* 51:283-290
- Pal DK, Durner M, Greenberg DA (2001) Effect of misspecification of gene frequency on the two-point LOD score. *Eur J Hum Genet* 9:855-859
- Paznekas WA, Boyadjiev SA, Shapiro RE, Daniels O, Wollnik B, Keegan CE, Innis JW, Dinulos MB, Christian C, Hannibal MC, Jabs EW (2003) Connexin 43 (*GJA1*) mutations cause the pleiotropic phenotype of oculodentodigital dysplasia. *Am J Hum Genet* 72:408-418
- Penrose LS (1946) Inheritance of zygodactyly. *J Hered* 37:285-287

- Percin EF, Percin S (2003) Two unusual types of syndactyly in the same family; Cenani-Lenz type and "new" type versus severe type I syndactyly? *Genet Couns* 14:313-319
- Percin EF, Percin S, Egilmez H, Sezgin I, Ozbas F, Akarsu AN (1998) Mesoaxial complete syndactyly and synostosis with hypoplastic thumbs: an unusual combination or homozygous expression of syndactyly type I? *J Med Genet* 35:868-874
- Perkoff D (1928) Syndactylism in four generations. *Br Med J* 2:341-342
- Pfeiffer RA, Meisel-Stosiek M (1982) Present nosology of the Cenani-Lenz type of syndactyly. *Clin Genet* 21:74-79
- Riddle RD, Johnson RL, Laufer E, Tabin C (1993) Sonic hedgehog mediates the polarizing activity of the ZPA. *Cell* 75:1401-1416
- Ridler MA, Laxova R, Dewhurst K, Saldana-Garcia P (1977) A family with syndactyly type II (synpolydactyly). *Clin Genet* 12:213-220
- Robinow M, Johnson GF, Broock GJ (1982) Syndactyly type V. *Am J Med Genet* 11:475-482
- Roblot G (1906) *La syndactylie congénitale*. Paris, Maulde, Doumencet Cie
- Rossant J (2004) ENU mutants from the Center of Modeling Human Disease. MGI Direct Data Submission, Accession ID MGI:3032560
- Sambrook J, Russel DW (2001) *Molecular cloning: a laboratory manual*. 3rd Ed. Cold Spring Harbor Laboratory Press, Cold Spring harbor, NY
- Sarfarazi M, Akarsu AN, Sayli BS (1995) Localization of the syndactyly type II (synpolydactyly) locus to 2q31 region and identification of tight linkage to *HOXD8* intragenic marker. *Hum Mol Genet* 4:1453-1458
- Sayli BS, Akarsu AN, Sayli U, Akhan O, Ceylaner S, Sarfarazi M (1995) A large Turkish kindred with syndactyly type II (synpolydactyly). 1. Field investigation, clinical and pedigree data. *J Med Genet* 32:421-434
- Schofield R (1921) Inheritance of webbed toes. *J Hered* 12:400-401
- Schwabe JW, Rodriguez-Esteban C, Izpisua Belmonte JC (1998) Limbs are moving: where are they going? *Trends Genet* 14:229-235
- Seven M, Yuksel A, Ozkilib A, Elcioglu N (2000) A variant of Cenani-Lenz type syndactyly. *Genet Couns* 11:41-47
- Shami SA, Schmitt LH, Bittles AH (1989) Consanguinity related prenatal and postnatal mortality of the populations of seven Pakistani Punjab cities. *J Med Genet* 26:267-271
- Shiryak FM (1961) A case of bilateral congenital bony syndactyly of the IV-V metacarpals. *Arkh Anat* 41:70-71
- Sobel E, Lange K (1996) Descent graphs in pedigree analysis: applications to haplotyping, location scores, and marker-sharing statistics. *Am J Hum Genet* 58:1323-1337
- Stiles KA, Hawkins DA (1946) The inheritance of zygodactyly. *J Hered* 37:16-18

- Sun X, Lewandoski M, Meyers EN, Liu YH, Maxson RE, Jr., Martin GR (2000) Conditional inactivation of *Fgf4* reveals complexity of signalling during limb bud development. *Nat Genet* 25:83-86
- te Welscher P, Zuniga A, Kuijper S, Drenth T, Goedemans HJ, Meijlink F, Zeller R (2002) Progression of vertebrate limb development through SHH-mediated counteraction of GLI3. *Science* 298:827-830
- Temtamy SA, Ismail S, Nemat A (2003) Mild facial dysmorphism and quasidominant inheritance in Cenani-Lenz syndrome. *Clin Dysmorphol* 12:77-83
- Temtamy SA, McKusick VA (1978) Syndactyly. In: *The genetics of hand malformations*. New York, Alan R. Liss, pp 301-322
- Thomsen O (1927) Einige Eigentümlichkeiten der erblichen Poly-und Syndaktylie bei Menschen. *Acta Med Scand* 65:609-644
- Tickle C (2000) Limb development: an international model for vertebrate pattern formation. *Int J Dev Biol* 44:101-108
- Verma IC, Joseph R, Bhargava S, Mehta S (1976) Split-hand and split-foot deformity inherited as an autosomal recessive trait. *Clin Genet* 9:8-14
- Weidenreich F (1923) Die Zygodaktylie und ihre Vererbung. *Z Abst Vererb* 32:304
- Winter RM, Tickle C (1993) Syndactylies and polydactylies: embryological overview and suggested classification. *Eur J Hum Genet* 1:96-104
- Zakany J, Kmita M, Duboule D (2004) A dual role for *Hox* genes in limb anterior-posterior asymmetry. *Science* 304:1669-1672
- Zuzarte-Luis V, Hurler JM (2002) Programmed cell death in the developing limb. *Int J Dev Biol* 46:871-876

8 Publications

8.1 Original work

- Malik S, Arshad M, Amin-Ud-Din M, Oeffner F, Dempfle A, Haque S, Koch MC, Ahmad W, Grzeschik K-H (2004) A novel type of autosomal recessive syndactyly: clinical and molecular studies in a family of Pakistani origin. *Am J Med Genet* 126A:61-67
- Malik S, Ahmad W, Grzeschik K-H, Koch MC (2005a) A simple method for characterising syndactyly in clinical practice. *Genet Couns* (in press)
- Malik S, Percin FE, Ahmad W, Percin S, Akarsu NA, Koch MC, Grzeschik K-H (2005b) Autosomal Recessive Mesoaxial Synostotic Syndactyly with Phalangeal Reduction Maps to Chromosome 17p13.3. *Am J Med Genet* (in press)
- Malik S, Schott J, Ali SW, Oeffner F, Amin-ud-Din M, Ahmad W, Grzeschik K-H, Koch MC (2005c) Evidence for clinical and genetic heterogeneity of syndactyly type I: the phenotype of second and third toe syndactyly maps to chromosome 3p21.31. *Eur J Hum Genet* (submitted)

8.2 Posters

- Malik S, Arshad M, Amin-Ud-Din M, Oeffner F, Dempfle A, Haque S, Koch MC, Ahmad W, Grzeschik K-H (2003) A novel type of autosomal recessive syndactyly: clinical and molecular studies in a family of Pakistani origin. 14th Annual meeting of the German Society of Human Genetics, Marburg Germany (Oct. 01-04, 2003)
- Malik S, Arshad M, Amin-ud-Din M, Haque S, Oeffner F, Bornholdt D, Lerche D, Richardt T, Koch MC, Ahmad W, Grzeschik K-H (2004) Genetic mapping in families with hereditary syndactylies. *Eur J Hum Genet* 12,Supplement 1:112. Annual meeting of European Human Genetics Conference, Munich Germany (June 12-15, 2004)
- Malik S, Percin FE, Ahmad W, Percin S, Akarsu NA, Koch MC, Grzeschik K-H (2005) Autosomal recessive mesoaxial synostotic syndactyly with phalangeal reduction maps to chromosome 17p13.3. 16th Annual meeting of the German Society of Human Genetics, Halle Germany (Mar. 9-12, 2005)
- Malik S, Percin FE, Ahmad W, Percin S, Akarsu NA, Koch MC, Grzeschik K-H (2005) A novel locus for recessive syndactyly maps to chromosome 17p13.3. Annual meeting of European Society of Human Genetics, Prague Czech Republic (May 7-10, 2005)

8.3 Seminars

- Genetic analysis of candidate genes for syndactyly identified in Pakistani families. Progress report at the meeting of the International Graduiertenkolleg GRK767, 9th Nov. 2002, IMT Marburg, Germany
- Genetic mapping in Families with hereditary syndactylies. 2nd Winterschool of the Graduiertenkolleg 767 Marburg/Giessen-Rotterdam. Transcriptional Control of Developmental Processes, 13-18 March 2004, Kleinwalsertal, Austria

9 Academic Teachers

Pakistan

Ahmad, M
Ahmad, W
Ajab
Amin-ud-Din
Ashraf
Fatima
Haque
Hussain
Mirza
Qureshi
Shami

Marburg

Grzeschik
Kämper, J
Kämper, U
Klingenspor
Koch
Kunz

Rotterdam

Aulchenko
Clayton
Cordell
Holmes
Houwing-Duistermaat
Leal
Muller

10 Acknowledgements

This work would not have been possible without the support and encouragement of my teacher Prof. Dr. Karl-Heinz Grzeschik, under whose supervision I chose this topic and began the thesis. The best advisor and teacher I could have wished for, he has always been a continuous source of inspiration for me. Prof. Dr. med. Manuela C. Koch, my advisor throughout the study, has also been abundantly helpful, and has assisted and guided me in numerous ways. Under her kind supervision I have finished my thesis and have conducted the clinical part of my research work.

I am thankful to my supervisor in Pakistan Prof. Dr. Wasim Ahmad and my colleagues for their help during the field work: Muhammad Arshad, Muhammd Amin-ud-Din, Sayedul Haque, Muhammad Wajid, Syed Wajahat Ali, Amir Ali Abbasi.

I am also grateful to Astrid Dempfle (Institut für Medizinische Biometrie und Epidemiologie, Marburg), Dr. Yurii Aulchenko (Erasmus MC, Rotterdam) and Dr. Suzanne M. Leal (Baylor College of Medicine, Houston, Texas), for their help and valuable suggestions in the data analysis.

I am thankful to my colleagues at the Institute of Human Genetics, Philipps University Marburg, Germany, for their cooperation and nice company: Zisis Papanicolaou, Claudia Moch, Shalini Singh, Dorothea Bornholdt, Daniela Lerche, Toni Richardt, Hartmut Engel, Jörg Schott, Dr. Frank Oeffner, Dr. Jürgen Kunz, Dr. Leonora Leveleki, Silke Janitz, Gerti Panzner. Thanks to Steffen Uebe, Benjamin Marquez-Klaka, Harald Balz for their support with the computers.

I am obliged to Drs. Ferda E. Percin, Sitki Percin (Cumhuriyet University, Turkey) and Nurten A. Akarsu (Hecettepe University, Turkey) for their scientific cooperation.

I also wish to thank to the Deutsche Forschungsgemeinschaft and the Graduiertenkolleg (GRK 767) for funding my research project, and the families for their participation in the study.

I cannot end without thanking my family, on whose constant encouragement and love I have relied throughout my time at Philipps University Marburg, Germany. This thesis is dedicated to my parents.

11 Declaration

I hereby declare that I have worked on my thesis "Gene mapping in syndactyly families" independently and without assistance, and the work presented here is original. The thesis has not been submitted in the current or a similar form to any other university.

Parts of the work has been published (chapter 8).

Marburg, February 2005

(Sajid Perwaiz Malik)

12 Curriculum Vitae

Personal Data

Name	Sajid Perwaiz Malik
Address (Pakistan)	Bait-ul-Abdullah, 27/Z Model Town, 32200 DG Khan
Address (Germany)	Geschwister Scholl Str. 1/124, 35037 Marburg
Date of Birth	02-02-1978
Birth Place	DG Khan, Pakistan

School

1982—1991	City High School, DG Khan
1991—1993	Government College, DG Kahn

University

1993—1995	B.Sc (Zool./Bot./Chem.)	Bahauddin Zakaria Universtiy, Multan
1995—1998	M.Sc (Zoology)	Bahauddin Zakaria Universtiy, Multan
1998—2000	M.Phil. (Genetics)	Department of Biological Sciences, Quaid-i-Azam Universtiy, Islamabad Thesis: A study of Pakistani families showing hereditary skeletal dysplasias.
2000—2001	Wildlife consultant	Working with Hagler Bailly Inc. Pakistan in the Brown Bear Project (Deosai National Park, Northern Areas, Pakistan), and Environmental Impact Assessment (EIA)
2001—2002	Lecturer in Zoology	Federal Government College H-9, Ministry of Education, Islamabad
2002—2005	Ph.D. studies (Human Biology)	Institute of Human Genetics, Philipps University Marburg Thesis: Gene mapping in syndactyly families.